Gene flow, morphology, and taxonomic revision of cave-obligate *Hesperochernes* pseudoscorpions

by

Charles Donald Robert Stephen

A dissertation submitted to the Graduate Faculty of
Auburn University
in partial fulfillment of the
requirements for the Degree of
Doctor of Philosophy

Auburn, Alabama
May 7, 2022

Keywords: Arachnida, cave biology, gene flow, geometric morphometrics, taxonomy

Approved by

Jonathan W. Armbruster, Professor and Director of Auburn University Museum of Natural History, Department of Biological Sciences
Jason E. Bond, Professor, Department of Nematology and Entomology, University of California at Davis, and Associate, Department of Biological Sciences,
Kenneth W. Halanych, Professor, University of North Carolina, and Associate, Department of Biological Sciences,
Leslie Goertzen, Professor, Department of Biological Sciences

Abstract

Pseudoscorpions are small predatory arthropods that are found in surface and subterranean habitats. Subterranean habitats such as caves tend to harbor pseudoscorpion species with highly restricted gene flow and high degrees of endemism. Species described in the genus *Hesperochernes* contradict this pattern. To investigate gene flow and taxonomically evaluate cave-obligate species in this genus located in eastern North America, an extensive field sampling effort was made that included four major karst regions, permissions to collect in ten states, included over 100 caves, and spanned a distance of over 1000 km. Molecular data were acquired through DNA extraction followed by reduced representation genomic sampling using the 3RAD variant method of RADseq. Population genetic analyses revealed extensive gene flow across putative biogeographic barriers to a nonvolant cave-restricted arthropod. To demonstrate the efficacy and applicability of 2D geometric morphometrics to study of pseudoscorpion morphology, landmarks were developed and assessed through an examination of sexual dimorphism in adult females and males of the chernetid pseudoscorpion *Hesperochernes mirabilis* collected from a large population found in Oaks Cave, Tennessee. Combining the results of population genetic analyses and the utility of this new 2D geometric morphometrics tool for pseudoscorpions, the three described species were revised and redescribed, with the most senior name, *Hesperochernes mirabilis*, taking precedence over its two new junior synonyms, *Hesperochernes holsingeri* and *Hesperochernes occidentalis*.

Table of Contents

List of Abbreviations

°C	degrees Celsius
3RAD	restriction digest enzyme associated DNA sequencing with three enzymes
AL	Alabama
ANOVA	analysis of variance
ASC	Alabama Supercomputer, Alabama Supercomputer Authority, Huntsville, Alabama
AUMNH	Auburn University Museum of Natural History, Auburn, Alabama
b	basal trichobothrium of the pedipalp movable finger
Co.	county
CSV	comma-separated values text file
CVA	canonical variance analysis
DFA	discriminant function analysis
DNA	deoxyribonucleic acid
esb	external subbasal trichobothrium of the pedipalp chela and fixed finger
est	external subterminal trichobothrium of the pedipalp chela and fixed finger
et	external terminal trichobothrium of the pedipalp chela and fixed finger
EtOH	ethyl alcohol
FMNH	Field Museum of Natural History, Chicago, Illinois
F_{ST}	fixation index
GA	Georgia
GPA	generalized Procrustes analysis
mm	millimeter
PC	principal component

PCA	principal components analysis
RADseq	restriction digest enzyme associated DNA sequencing
sb	subbasal trichobothrium of the pedipalp movable finger
st	subterminal trichobothrium of the pedipalp movable finger
SNP	single nucleotide polymorphism
t	terminal trichobothrium of the pedipalp movable finger
TAG	the cave-rich karst regions of Tennessee, Alabama, and Georgia
TN	Tennessee
UFB	ultrafast bootstrap
VA	Virginia
XML	extensible markup language
ZMB	Museum für Naturkunde, Berlin, Germany

List of Tables

List of Figures

Chapter 1

Long-distance and widespread gene flow in three species of the cave-obligate arachnid *Hesperochernes* (Pseudoscorpiones: Chernetidae)

Authors

Charles D. R. Stephen[1,2,3], James Starrett[4], Jonathan W. Armbruster[1], Matthew L. Niemiller[5], Jason E. Bond[4]

[1] Auburn University, Auburn, Alabama, USA

[2] Corresponding author: cdr.stephen@gmail.com

[3] Missouri State University, Springfield, Missouri, USA

[4] University of California at Davis, Davis, California, USA

[5] University of Alabama in Huntsville, Huntsville, Alabama, USA

Abstract

We present evidence for gene flow across major biogeographic barriers within and between three subterranean species of the pseudoscorpion genus *Hesperochernes*. We use the 3RAD method to generate reduced representation genomic libraries from 132 individuals of three species distributed among 73 caves. Specimens were sampled from four major karst regions in the eastern United States, ranging from west of the Mississippi River in the Ozark Mountains to the Appalachian Mountains of northeastern Virginia. Cryptic speciation was not uncovered; rather, monophyly was not recovered for the three described subterranean species. The evidence for gene flow is remarkable, as it extends over large distances lacking caves or any type of subterranean connection and infers gene flow across major river systems that are putative strong barriers to the dispersal of subterranean-restricted and nonvolant species. This lack of population structure, particularly between caves within the same karst regions, suggests rampant migration of individuals between cave systems. This pattern contrasts with the more typical highly localized endemism of most North American cave pseudoscorpions and other cave-restricted fauna. Minimal genetic structuring does not suggest connectivity through shallow subterranean habitat that may exist

between geographically proximate cave systems. We hypothesize that dispersal may be mediated through volant or nonvolant phoretic hosts, if *Hesperochernes* pseudoscorpions are able to survive briefly outside of the subterranean habitat. Alternatively, should they be capable of surviving immersion in water for long periods of time, transportation through groundwater connections between cave systems and underlying aquifers may be an alternate but considered unlikely mode of dispersal.

Introduction

Caves represent one part of a larger habitat system that extends below the ground surface. The minimum technical criteria for this highly variable geological feature including a cavity in rock being formed by natural processes, having some degree of a dark zone where light cannot penetrate, a surface entry accessible to humans, and a minimum length of passage (usually about 10 m) that is traversable by humans (Palmer, 2007). Caves may extend for tens of kilometers, include multiple levels of passage with multiple entry points, and may connect to wider cave systems extending hundreds of kilometers. Caves may form through dissolution of soluble rock, volcanic action, or fractures generated by tectonic activity (Palmer, 2007). Most biological work in caves has been in those formed through dissolution of limestone. Limestone caves are common in karstic regions, which are characterized by alternating layers of sandstone and limestone of Paleozoic or Mesozoic origin (Palmer, 2007). Water and atmospheric carbon dioxide that forms carbonic acid in solution are the primary drivers of subterranean habitat creation in karst landscapes (Kaye, 1957). Calcium carbonate in limestone is slowly dissolved and redeposited as formations (speleothems) or washed out of caves as water flows across the rock or through cracks of folded layers (Back, 1961; Davies, 1960). These form disconnected solution pools of saturated rock, which in time with constant flow of water result in opening passages that humans can explore, with passage shape and complexity related to water flow dynamics (Davies, 1960; Palmer, 1975). Most passages in eastern North America were likely influenced by Pleistocene drainage patterns and are at least that old, although some may be Cretaceous in age (Barr, 1961). In highly folded karst regions, such as the Appalachian Mountains of eastern North America, caves or upper passage sections in hills and ridges tend to be older than those in the valleys at or below the water table. Vertical passages tend to be the youngest and quickest forming, as rainwater flowing through

cracks in rock follows gravity and widens these cracks into vertical shafts (Pohl, 1955). Vertical passages may connect formerly separated horizontal passages of different ages that were formed from more slowly moving water of groundwater streams (Pohl, 1955).

Caves are by far the most biologically explored subterranean habitat. However, this represents a small fraction of that available to life. Subterranean habitat accessible only to fauna smaller than humans includes fractures between larger rocks (the epikarst), continuous connections of small cavities in loosely deposited rock such as from past rockslides (the *milieu souterrain superficial* or mesovoid shallow substratum), and solid formed passages that are yet too small to fit a human body (Culver & Pipan, 2014; Ortuño et al., 2013; Pipan, López, Oromí, Polak, & Culver, 2010). Groundwater aquifers lie beneath some cave systems and may contain source populations of subterranean aquatic fauna (Reiss et al., 2019). Additionally, the time component is important: lineages extant in caves today may have had surface sister taxa adapted to past cooler climactic periods, which invaded caves following past warming events (Barr, 1960). Altogether, these factors represent pathways to aid reconstruction of biological connectivity between caves. It is likely that some combination of these factors has affected the distributions of the subterranean-adapted fauna in eastern North America: bats, rodents, herpetofauna, fishes, crustaceans, insects, arachnids, flatworms, and nematodes (Bailey, 1940; Barr, 1961; Culver, Kane, & Fong, 1995; Juberthie, Delay, & Bouillon, 1980; Ortuño et al., 2013; Vandel, 1965).

Terrestrial fauna completely adapted to subterranean life are incapable of surviving in surface environments that have strong fluctuations in humidity and temperature, however there are degrees of variation in these adaptations and some may survive brief or extended excursions to surface habitat (Barr, 1961). A complicating factor for terrestrial fauna is that most karst caves include not only dry passage, but also stream passage partly filled with water, and permanently or seasonally flooded (sumped) passage. Many authors, particularly taxonomists describing species, have operated under a working hypothesis that terrestrial fauna (and to an extent, aquatic fauna) are effectively trapped within caves. Under this perspective caves are islands of habitat in a sea of karst (Culver, 1970): species cannot leave to the surface to disperse, and are cut off from other caves when passages connecting caves and other subterranean terrestrial habitat are sumped or destroyed following geologic or human activity.

Although the view of caves as islands is naïve to other geologic connectivity that may exist, nonetheless both aquatic and terrestrial fauna that exclusively inhabit subterranean habitat tend to be regionally endemic and show little gene flow across local geography within bands of locally cave-forming rock. Many species since their original description from a single cave continue to be known from one cave, including after extensive additional sampling efforts in a region (Zigler et al., 2020). This pattern is typical in North American cave fauna, and has been found in eyeless fishes, salamanders, freshwater crustacean crayfish and shrimp, aquatic isopods, spiders, beetles, and millipedes (Barr, 1985; Christman, Culver, Madden, & White, 2005; Coleman & Zigler, 2015; Culver et al., 1995; Harlan & Zigler, 2009; Lewis, 2003, 2009; Loria, Zigler, & Lewis, 2011; Niemiller & Zigler, 2013; Niemiller et al., 2016; Peck, 1989; Snowman, Zigler, & Hedin, 2010), with only genetic lineages of the Southern Cavefish, *Typhlichthys subterraneus*, showing ranges that include multiple cave systems including caves situated in multiple karst regions (Hart et al., 2020; Niemiller et al., 2016). Similar patterns of highly localized endemism in cave fauna have been reported in Brazil, southern Europe, and southeastern Asia (Cardoso, Ferreira, & Souza-Silva, 2021; Sket, 1997; Zhao & Zhang, 2016). Certain bats and birds are volant migrants that use caves in geographically separated regions in different parts of the year. Such species may act as conduits of microbial life (Miller-Butterworth, Vonhof, Rosenstern, Turner, & Russell, 2014). This can be problematic with respect to pathogens such as *Pseudogymnoascus destructans*, the fungus causing White-Nose Syndrome that has devastated North American hibernating bat populations over the last few decades and is likely being spread by migratory bats after its introduction from European caves (Miller-Butterworth et al., 2014; Puechmaille et al., 2011).

Arachnids known from caves in eastern North America include spiders, harvestmen, mites, and pseudoscorpions. The focus of this study is pseudoscorpions. These small (1-12 mm) arachnids include approximately 3800 described species and are predators of small arthropods (M. S. Harvey, 2013). Outside of caves, pseudoscorpions may be found under logs, under bark, and in leaf litter (Chamberlin, 1931). Pseudoscorpions are particularly emblematic of subterranean faunal endemism and range restriction in eastern North America (Engel et al., 2017). This phenomenon of range restriction in cave-obligate pseudoscorpion species is the typical pattern for the diverse assemblage of pseudoscorpions known from caves in this region, with many species described

based on a small number of specimens from a single cave (Engel et al., 2017; Peck, 1989; Zigler et al., 2020).

An exception to the predominant pattern of restricted endemism in cave-obligate pseudoscorpions in eastern North America is in the family Chernetidae, of which only *Hesperochernes* includes subterranean species (Muchmore, 1974): *Hesperochernes mirabilis* (Banks, 1895), *H. occidentalis* (Hoff and Bolsterli, 1964), and *H. holsingeri* (Muchmore, 1994). *Hesperochernes mirabilis* (Fig. 1.1a) was originally described from disjunct type localities in Kentucky and Virginia separated by several hundred kilometers (Banks, 1895). Caves from which type specimens were collected are located in karstic regions with distinct fauna assemblages that rarely mix: Whites Cave, Kentucky, in the Interior Low Plateau karst region, and Gilley Cave, Virginia (see Chapter 3), in the Appalachian karst region (Culver, Master, Christman, & Hobbs, 2000). A thorough review of grey literature and published accounts is provided in Chapter 3. The distribution we report here is approximately bounded in the west by the Mississippi River, in the east by the eastern edge of the Appalachian Mountains, in the south by the Tennessee River, and in the north by the Ohio River. *Hesperochernes holsingeri* (Fig. 1.1b) is only known from its type locality in southern Indiana: a single cave located north of the Ohio River (Muchmore, 1994). Published and grey literature accounts do not suggest a wider distribution. The distribution of *H. occidentalis* (Fig. 1.1c) as published and reported in the grey literature (see Chapter 3) generally limits its range to the Ozarks karst region, situated west of the Mississippi River and east of the Great Plains (Hoff & Bolsterli, 1956). However, this species has also been found in caves located in eastern Texas (Muchmore, 1992). Although some caves do occur in the Great Plains, they are sparse and this region is poorly sampled for cave fauna (Culver et al., 2000). No *Hesperochernes* records are known from caves in the Great Plains.

The nearest known distributions of congeneric *Hesperochernes* to the southeastern USA region include four surface and two subterranean species. The four surface species are *H. tamiae* from northeastern USA and southeastern Canada (Buddle, 2010; Nelson, 1975); *H. canadensis* from southwestern Canada; *H. unicolor* from Texas (Banks, 1908; Muchmore, 1992); and *H. riograndensis* from northern Mexico and southwestern USA in New Mexico and Texas (Muchmore, 1992). The two subterranean species are *H. bradybaughi*, from southwestern USA in

Arizona where it is known from two caves (M. S. Harvey & Wynne, 2014); and *H. vespertilionis*, from caves with bat populations in Dominican Republic on the Greater Antilles island of Hispaniola (Beier, 1976; Perez-Gelabert, 2008).

The principle aim of this study is to investigate the relationships within and between populations of eastern USA *Hesperochernes* cave-obligate species. We set to evaluate whether gene flow is occurring among geographically proximate populations, whether presumed biogeographic barriers to nonvolant cave-obligate species are effective at isolating populations, and whether evidence existed for long-distance gene flow. We sampled extensively through the known and inferred ranges of subterranean *Hesperochernes* species. We included specimens from type localities of each species or as near as possible to a type locality, and from these points radiated outwards to as many caves as we could sample for potential *Hesperochernes* populations in all major karst regions of the eastern USA.

Methods and Results

1. Collection

1.1 Collection from cave localities

Collections were made at type locality caves and in caves throughout all major eastern karst regions for which we could gain access (Fig. 1.2). The primary method of sampling was through visual encounter surveys as detailed in Zigler et al. (2020). All voucher specimens are accessioned into the Auburn University Museum of Natural History (AUMNH). Specimens were collected in the field with a paintbrush live or into 95% EtOH, kept cool, and transported to the lab at AUMNH. Here they were sorted and identified, then transferred to cryotubes into fresh 95% EtOH and stored at -20 °C until DNA extraction. Total coverage of specimens is in Fig. 1.2; total distribution of known subterranean localities of *Hesperochernes* east of the Great Plains in Fig. 1.3. Details for how the distribution map in Fig. 1.3 was created are in Chapter 3.

1.2 Collection from surface localities

In addition to sampling in caves, we sampled from surface localities to test the hypothesis that *Hesperochernes* species are not cave-obligate animals and thus may be found outside of caves. We sampled surface localities for leaf litter while traveling through karst regions and from localities

proximate to cave entrances. Bulk samples of surface leaf litter were collected adjacent to cave entrances and in protected karstic regions across the breadth of the subterranean distribution confirmed here for *Hesperochernes* in southeastern North America from >100 localities. (Fig. 3.2). Leaf litter sampling was done following the recommendations of Hoff (1949). Briefly, we typically processed ca. 10 L of leaf litter material (leaves and soil hummus) through a Winkler sifter to concentrate litter to finer particles, temporarily storing sifted material in a plastic bag, and then manually or passively processing live animals. Manual processing was done with a soil sieve over white cloth within 24h; all pseudoscorpions were picked from these samples with a paintbrush and placed in 95% EtOH, kept cool in the field with ice packs, transported to AUMNH, and kept in a -20 °C freezer until a generic determination could be made. Passive processing used Tullgren funnels, in which soil arthropods were driven down a humidity gradient into a collection cup that was filled with 95% EtOH; samples were then sorted in 95% EtOH and all pseudoscorpions removed and identified to genus. No *Hesperochernes* were recovered from surface collecting that was otherwise highly efficient at collecting pseudoscorpions. Haphazard sampling of tree trunks and deadwood near cave entrances, exterior rock walls of cave entrances, and the entrance zones of caves all failed to recover *Hesperochernes* but did recover other pseudoscorpions. Eastern Phoebe (*Sayornis phoebe*) often nests at cave entrances. We dissected nests we encountered that did not show evidence of present occupation by nesting birds or have eggs inside of them. From these nest dissections we did not recover pseudoscorpions but did recover many potential *Hesperochernes* prey: parasitic mites (Mesostigmata), soil mites (Sarcoptiformes), and insect larvae.

2. DNA extraction

DNA extractions were generally whole-body extractions and done with Qiagen DNEasy kits. We followed the manufacturer's instructions except for two modifications: shaking samples during the initial lyse step on a shaker platform, and in the last step adding an extra wash of Buffer AE. Cuticles were preserved from filters during extractions to make them available for morphological study. Extracted DNA quality and quantity were verified by gel electrophoresis and Qubit. Samples were excluded from further analysis if extracted DNA only contained small fragments or could not be concentrated down into 13.3 ng/µL in a volume of 7.5 µL. Some samples from important localities were included despite being below 13.3 ng/µL or including smaller fragments

as seen in the gel. These represented significant range expansions or type locations. As needed, samples were brought to 13.3 ng/µL with a vacuum centrifuge to increase concentration or deionized distilled water to decrease concentration.

3. Library preparation

3.1 Protocol

RADseq libraries were prepared following the 3RAD protocol (Bayona-Vásquez et al., 2019; Glenn et al., 2017). RAD library preparation was done by CDRS at AUMNH for two libraries and at University of California at Davis for one library, following a 3RAD protocol based on Glenn et al. (2017). The complete protocol is provided in Supplementary Material 1.

3.2 Sample loading, combinatorial barcoding, restriction enzymes

Following concentration standardization, a map of a 96-well plate was generated and a combination of iTru5 and iTru7 barcodes were assigned to each well. Technical replicates were included in each plate. Using this map, 7.5 µL of each sample was loaded into each assigned well in the 96-well plate. Restriction digest enzymes EcoRI-HF and ClaI were used to cut genomic DNA and the enzyme MspI was used as the third error-correcting enzyme.

3.3 Restriction digest

2 µL of 2.5 µM concentration annealed adapters of EcoRI-HF iTru7 and ClaI iTru5 were added to each well, following the assignment for adapters in the plate map. A restriction digest cocktail was prepared, with the following volumes calculated per well: 1.8 µL 10X Cutsmart buffer, 1 µL EcoRI-HF enzyme, 1 µL ClaI enzyme, 1 µL MspI enzyme, and 1.7 µL deionized distilled water. 6.5 µL of restriction digest cocktail was added to each well, so that the total volume in each well was 14 µL. The well plate was put into a thermocycler on a single-step program: 120 min at 37 °C.

3.4 Adapter ligation

A ligation cocktail was prepared, with the following volumes calculated per well: 0.6 µL 10X ligase buffer, 0.25 µL T4 DNA ligase, 1.8 µL of 10 mM concentration rATP, 3.35 µL deionized distilled water. The plate was removed from the thermocycler, kept on ice while preparing the

ligation cocktail, and then 6 µL of ligation cocktail was added to each well, bringing the total volume in each well to 20 µL. The plate was returned to the thermocycler and a two-step program started: 3 cycles of 20 min at 22 °C and then 10 min at 37 °C; 20 min at 80 °C; total incubation time 110 min.

3.5 Sample pooling, normalization, ligation of iTru5 adapter, library amplification

Pooling was decided for each plate, with at least two pools for each plate, and volumes of each well were extracted and pooled accordingly. A subset was kept as backup if needed. Pooled libraries were cleaned with magnetic beads to discard reagents. Pooled cleaned libraries were normalized into a combined tube of 75 µL containing all libraries. An amplification cocktail was prepared with the following reagents calculated per pool: 10 µL 5X KAPA Hifi Fidelity Buffer, 1.5 µL dNTP mix, 5 µL iTru5_8N, 20 µL deionized distilled water. To PCR tubes was added 36 µL amplification cocktail, 1 µL KAPA HiFi Hotstart DNA Polymerase, and 12.5 µL cleaned pooled normalized libraries, for a total volume of 50 µL in each PCR tube. Samples were placed in a thermocycler and the following three-step program was run: one cycle of 95 °C for 2 min; one cycle of 98 °C for 20 s, then 61 °C for 30 s, then 72 °C for 30 s; one cycle of 72 °C for 5 min. Following amplification, the amplified libraries were cleaned with magnetic beads to discard unwanted reagents.

3.6 Ligation of iTru5 and iTru7 adapters, library amplification

An amplification cocktail was prepared for volumes appropriate to each of 3 PCR tubes: 10 µL 5X KAPA HiFi Fidelity Buffer, 1.5 µL 10mM dNTP mix, 5 µL iTruP5, 1 µL KAPA HiFi Hotstart DNA Polymerase, 17.5 µL dH2O, 5 µL iTru7, 10 µL libraries from previous step. Following amplification, the amplified libraries were cleaned with magnetic beads to discard unwanted reagents.

3.7 Size selection, final amplification, verification

30 µL of libraries were size selected using a BluePippen for tight size selection at 550 bp +/- 10-20%. An amplification cocktail was prepared, with the following volumes for 4 50 µL PCR tubes: 10 µL 5X KAPA HiFi Fidelity Buffer, 1.5 µL 10 mM dNTP mix, 5 µL iTru5 adapters, 5 µL iTru7 adapters, 17.5 µL distilled deionized water, 1 µL KAPA HiFi Hotstart DNA Polymerase, 10 µL

size-selected DNA libraries. PCR tubes were transferred to a thermocycler with the following three-step program: one cycle of 95 °C for 2 min; 10 cycles of 98 °C for 20 s, then 61 °C for 15 s, then 72 °C for 45 s; one cycle of 72 °C for 5 min. Amplified libraries were cleaned with magnetic beads to discard unwanted reagents and pooled into a single tube. Following cleaning, concentration was verified with Qubit and DNA fragment length was verified on a gel. Final library product was then sent for sequencing.

4. Sequencing and loci assembly

4.1 Sequencing and verification of raw data

RAD libraries were sequenced on the Illumina NextSeq platform with paired-end 150 base pair sequencing. Two plates of samples were sequenced at the University of Georgia and one was sequenced at University of California at Davis. Sequenced libraries were downloaded to the high-performance computing cluster at the Alabama SuperComputer Facility, Huntsville, Alabama (ASC). Raw data files in Illumina basecall format were first converted to fastq format using bcl2fastq (Illumina) and then libraries were verified with FastQC (Babraham Bioinformatics, 2019).

4.2 Loci assembly

Demultiplexing, quality control, and loci assembly were done with the ipyrad pipeline (Eaton & Overcast, 2020) on ASC. Using ipyrad steps 1-2, combinatorial barcodes were separately used for each of three sequencing libraries of 96 samples to demultiplex and associate reads with a fastq file for each sample. Samples were then trimmed of barcode adapters and trimmed for quality. Technical replicates from the same individuals were concatenated. All subsequent analyses considered all samples as a single library. A new run of ipyrad in steps 1-7 assembled loci from the combined data set. Parameters used for ipyrad steps 1-2 for the separate libraries and for ipyrad steps 1-7 for the combined library are in Supplementary Material 2. To verify that all samples could be used, FastQC was run on all generated sample loci fastq and visualized simultaneously with MultiQC on a laptop computer (Babraham Bioinformatics, 2019; Ewels, Magnusson, Lundin, & Käller, 2016).

5. Phylogenetics

5.1 Phylogenetic analysis of the three described species

All phylogenetic analyses were run in IQ-TREE version 2.1.12 (Minh et al., 2020); a model test was run and the best substitution model was chosen using the Corrected Akaike Information Criterion (AICc), following which a likelihood analysis was run with 1000 replicate ultrafast bootstraps. Resulting trees were visualized in TreeViewer version 2.0.1 (Bianchini, 2021). Initially, the entire data set was run with GTR+F+I+G4 as the best model for the data (Fig. 1.4). Next, samples with less than 50% of possible loci from the assembly were excluded from the data set, bringing the total samples in the pruned data set, after merging technical replicates, from 132 to 50 (Fig. 1.5). In the pruned data set GTR+F+I+G4 was the best model for the data.

Branch support with ultrafast bootstraps (UFB) is credible only if >95% (Minh et al., 2020). In the full data set, UFB support was poor and branch length was very shallow for all but one sample from Flintknapper Cave in Madison Co., AL. With this longer branch pruned so shallow branches could be examined, populations located east and west of the Mississippi River were generally reciprocally monophyletic excepting one specimen from a Missouri cave, *H. holsingeri* was recovered as nested within *H. mirabilis*, and no clear patterns emerged between populations sampled from east of the Mississippi River. In the pruned data set, shallower nodes tended to have credible UFB support, several nodes had almost credible UFB support, western and eastern samples were not reciprocally monophyletic, described species were not reciprocally monophyletic, and no clear biogeographic pattern was evident.

6. Population genetics

6.1 Population analyses with F_{ST}

Using VCFtools (Danecek et al., 2011) running on Hopper, Weir and Cockerham mean F_{ST} estimates were calculated to make pairwise comparisons between populations defined by karst biogeography (Tab. 1.1): Ozarks, combined Appalachian Valley and Ridge and Interior Low Plateau, and Driftless karst regions. Comparisons between populations west and east of the Mississippi River were 0.24 whether north or south of the Ohio River. Complete panmixia was estimated within populations sampled from east of the Mississippi River.

6.2 Population analyses with STRUCTURE

Samples from the RAD data were assigned to a metagroup of all samples and STRUCTURE was run on ASC through IPython in a Jupyter Notebook. STRUCTURE uses a Bayesian framework, which estimates ancestry proportions of each specimen in the dataset to a given value of k (Perez & Granger, 2007; Porras-Hurtado et al., 2013). Starting with a matrix of 583,984 SNPs, we allowed for 50% missing data in group assignment (minmap=0.5), 40% missing data across the matrix (mincov=0.4), used a burnin of 1 million, used 1 million replicates, tested for k=2 to 5, and then replicated this process eight times. The R package toytreeplot (Francois, 2016) was used to visualize the STRUCTURE plot (Fig. 1.6). STRUCTURE analysis yielded k=3, with these three ancestral populations broadly having an east-west division between samples coming from caves in karst regions on either side of the Mississippi River. Mixing did occur across this significant river system, with >90% of specimens being assigned to three ancestral populations. *Hesperochernes* with the most equal share of all three ancestral populations came from Whites Cave, Edmonson Co., Kentucky, and from Cottrells Cave, Madison Co., Alabama. The specimen with the most equal share of the ancestral population dominating *Hesperochernes* collected west of the Mississippi River and the dominant ancestral population from collections east of it came from Flintknapper Cave, Madison Co., Alabama. Significant portions of the ancestral population that dominated the Ozarks specimens from caves in Arkansas, Missouri, and Oklahoma were found in the furthest east cave we sampled, a cave that we discovered and called Cueva Cellar, in Shenandoah Co., Virginia: ~1000 km from Ozark cave collections. Of the two ancestral populations dominant in specimens from eastern caves, there were no connections between the Driftless karst region and any one ancestral population. Specimens from the one Driftless karst region topotypic locality, that of *H. holsingeri* in Wilson Cave, Jefferson Co., Indiana, had a significant portion of all three ancestral populations. Collections from the two *H. mirabilis* type localities, Gilley Cave, Lee Co., Virginia, and Whites Cave, Edmonson Co., Kentucky, both shared all three ancestral populations. Biological replicates from these counties had varying degrees of shared population ancestry.

6.3 Population analyses with molecular PCA

Samples from the RAD data were assigned to different iterations of population groupings and molecular Principal Component Analyses (PCAs) of SNPs in assembled loci were run through the

iPyrad analysis toolkit. Computations were performed on a laptop computer (MacBook Air 2017 model with 2.2 GHz dual-core i7 processors and 8 GB RAM, operating system macOS 10.15) using IPython in a Jupyter Notebook. Iterations of PCAs were done with specimens in three themes: First, PCA1 used populations inferred from karst biogeography based on F_{ST} results; second, in PCA2 populations were situated west or east of the Mississippi River based on the STRUCTURE results; third, in PCA3, without *a priori* assignment and instead using the kmeans method of assigning specimens to populations. All PCAs started with 583,984 SNPs, which were reduced to 457,562 SNPs after indel and bi-allele filtering. As with the STRUCTURE analysis, parameters that could be altered affected strictness of allowance for missing data across the entire SNP matrix (parameter mincov) and SNPs present in *a priori* assigned populations (parameter minmap).

In PCA1 with *a priori* assigned populations using karst regions (Fig. 1.7), with strict parameter settings allowing 10% missing data, the set of SNPs available was reduced to 384, and all populations were tightly clustered, with western samples tending to be separated from eastern samples. Patterns emerged in the data when up to 60% missing data was allowed. In the first case of population assignment, by karst region, three regions were used: the Ozarks karst region (ozark), the combined Appalachian Valley and Ridge karst region and Interior Low Plateau karst region (appintplat), combined due to their extremely low recovered pairwise F_{ST} values, and the Driftless karst region (drift). Requiring minmap=0.35, mincov=0.2, and 300 replicates of subsampling the SNP matrix, ozark separated widely from the other groups on PC0 (16.9% variance explained), with separation also evident on PC1 (4.2% explained) between appintplat and drift, with appintplat exhibiting a tight cluster of SNPs. These separations were more evident when these same PCA parameters were subjected to t-distribution stochastic neighbor embedding modeling (TSNEM) with 1000 iterations.

In PCA2 examining eastern and western populations (Fig. 1.8), with strict parameter settings (minmap=0.5, mincov=0.8) and allowing for <10% missing data, no distinction could be made between populations as all clustered tightly together, and this was not improved when applying TSNEM with 1000 iterations. Patterns emerged in the data when up to 60% missing data was allowed with parameters minmap=0.3 and mincov=0.2, giving 20988 SNPs, from which 1342

SNPs were subsampled in 300 iterations. This gave an obvious distinction between eastern and western populations on PC0 and some separation within eastern populations on PC1 as seen in the first PCA looking at karst regions. Running TSNEM of the relaxed distribution with 1000 iterations did not change the general pattern but a larger spread in eastern populations was recovered.

In PCA3 samples were assigned into populations using the kmeans method (Fig. 1.9). Samples were colored by karst region for illustrative purposes only. This yielded 52040 SNPs of which 3120 were subsampled in 300 replicates. With relaxed filtering, samples generally grouped with their respective karst region, but did not group with the three karst regions with strict parameter settings allowing 10% missing data. Patterns were not clear when TSNEM was applied to PCA3 with 10000 iterations.

Discussion

A phylogenetic approach suggested that the three subterranean *Hesperochernes* species in eastern North America had shallow divergence and that *H. holsingeri* was paraphyletic with respect to *H. mirabilis*.

A population genetics approach using reciprocal F_{ST}, STRUCTURE, and molecular PCA all showed that karstic biogeography had little effect on restricting gene flow in *Hesperochernes*. This lack of restriction was apparent across putatively insurmountable biogeographic barriers to a terrestrial cave-restricted arthropod, such as the Mississippi, Ohio, and Tennessee rivers. These results indicated that there is significant gene flow between the three subterranean species to an extent that is more likely to be seen in populations of one species with connected populations rather than separate species. When allowing for high levels of missing data in the molecular PCA approach, some population structure was recovered that showed fidelity of SNPs to karstic regions. The strongest population structure was an east-west division over the Mississippi River, which was recovered in both STRUCTURE and molecular PCA. Caves centrally located in the distribution, such as in central Alabama and Kentucky, tended to belong to the three ancestral

populations recovered in STRUCTURE. Only samples collected west of the Mississippi River tended to have stronger fidelity to a single ancestral population. This suggests that the western populations may have been colonized by one of the eastern populations, resulting in a founder effect of reduced genetic diversity west of the Mississippi River.

Our results showing high rates of gene flow over remarkable distances are more typical for volant migratory trogloxenes such as bats than the high rates of population structuring, localized endemism, and high rates of localized speciation typically seen in nonvolant subterranean vertebrates and invertebrates. More localized intrageneric panmixis in populations previously thought to be heterospecific known from different limestone caves separated by distances of <10 km has been uncovered in subterranean *Vietbocap* scorpions in Vietnam (Prendini, Ehrenthal, & Loria, 2021). Prendini et al.'s (2021) result in scorpions is similar to our results for *H. holsingeri* and caves nearby with *H. mirabilis* in southern Indiana, but does not address the long-distance gene flow between *Hesperochernes* populations in the Ozarks and eastern Appalachian karst regions. A more typical population structure in subterranean fauna has highly localized or endemic populations with high degrees of population structure as shown in STRUCTURE analysis or haplotype networks, or a high F_{ST} between populations and/or recognized species. This more typical pattern has been shown in cave-obligate *Nesticus* spiders in the Appalachian and the Valley and Ridge karst regions (Hedin, 1997; Snowman et al., 2010); *Darlingtonia* beetles in the Interior Low Plateau karst region in Kentucky (Boyd, Philips, Johnson, & Nixon, 2020); *Ceuthophilus* crickets in the Edwards Plateau karst region in Texas (Weckstein et al., 2016); *Tetracion* millipedes in the Interior Low Plateau karst region in Alabama and Tennessee (Loria et al., 2011). The distribution of the widespread salamander *Eurycea lucifuga* mirrors much of the range seen in *Hesperochernes*, but shows expected levels of high population structuring that is largely concordant with the geographical isolation of populations expected from the biogeographic barriers separating the major karst regions of the southeastern USA (Edgington, Ingram, & Taylor, 2016).

It is unknown to what extant *Hesperochernes* pseudoscorpions can tolerate outside temperature fluctuations that seasonally occur within the distribution range that we have shown to occur through literature searches and our extensive sampling efforts. It has been postulated that *Hesperochernes mirabilis* is not a cave-obligate animal at all and is merely a troglophile that uses

caves for part of its life cycle or a trogloxene that occasionally visits caves but does not require them to complete its life cycle (Muchmore, 1994). If true, then the species should be found outside of caves. We recovered no *Hesperochernes* from leaf litter collections, haphazard sampling under bark of living trees and fallen deadwood, coarse woody debris sampling of tree hollows, or dissection of Eastern Phoebe nests at cave entrances. Nonetheless it is possible that *Hesperochernes* pseudoscorpions may be found in the tree canopy and are transported into caves by bats that roost in trees and in caves. The thermal tolerance limits of these three species are unknown. Given the data available for *H. holsingeri*, *H. mirabilis*, *H. occidentalis*, and individuals identified to genus, the most parsimonious assessment is that these are cave-obligate animals that have overcome the physical limitations of their size and lack of connectivity of cave systems across subterranean biogeographic barriers by means of phoretic hosts that transport them efficiently enough to not surpass the thermal tolerance limit of these pseudoscorpions.

Flight is the most efficient mode of transportation that poses the least risk to surpassing thermal limitations, provided the host reliably moves from cave to cave without spending overlong periods outside of the subterranean environment. Likely potential volant hosts include trogloxene bats and trogloxene insects retaining functional vision and flight. Birds in eastern Nearctic caves only make use of cave entrances for their nests so are unlikely to be a host. Although suggested as a potential phoretic host, a pseudoscorpion has yet to be recorded from a living bird (Ashmole & Ashmole, 1997).

While in the eastern Nearctic karst there is the widespread *Hesperochernes mirabilis*, a similar pattern with a widespread, apparently troglophilic chernetid associated with bats is found in the Caucasus region of central Asia: *Megachernes pavlovskyi* (Turbanov, Palatov, & Golovatch, 2016). Similarly, it has been hypothesized to have a large geographic distribution through phoresy on bats, and likewise there is not yet direct evidence for this. A molecular approach been not yet been used with *M. pavlovskyi*. The first report of a pseudoscorpion on any bat was made as late as 2015 on a forest bat (Finlayson, Madani, Dennis, & Harvey, 2015). A pseudoscorpion has yet to be recorded from a bat species that makes regular use of caves. Bats that do make use of caves regularly migrate between cave systems separated by rivers. Eleven bat species in the eastern United States annually migrate between maternity and overwintering caves (Whitaker & Hamilton,

1998). These migration endpoints may be separated by hundreds of kilometers. Given that these bat species make regular use of caves as roosts when they are not congregating in a maternity or bachelor colony, it is likely that individuals will stop in caves en route during migration periods and move between caves when not migrating. In our surveys, *Hesperochernes* tended to be found in the highest numbers in caves with large bat populations. For example, we observed several thousand individuals at Oaks Cave, Tennessee, in which a Gray Bat maternity colony comprising thousands of individuals of this bat species is present for several months each year. The four bat species that tend to have the largest colony sizes include Big Brown Bat (*Eptesicus fuscus*), Brazilian Free-tailed Bat (*Tadarida brasiliensis*), Gray Bat (*Myotis grisescens*), and Indiana Bat (*Myotis sodalis*); of these, the Gray Bat has a similar distribution to eastern subterranean *Hesperochernes* populations and ranges exclusively in the karst regions in which the genus occurs (Fong, Porter, & Slay, 2012; M. J. Harvey, Altenbach, & Best, 1999; Niemiller, Zigler, & Fenolio, 2013; Slay, Niemiller, Sutton, & Taylor, 2016).

Nonvolant trogloxene hosts such as ground-nesting rodents may harbor these animals in their burrows and act as phoretic carriers of pseudoscorpions in their movements outside of their burrows to forage and find mates (during which pseudoscorpions could move from one animal to another and enter another burrow). Several ground-nesting rodents (such as *Neotoma* spp.) make use of caves (Niemiller et al., 2013; Slay et al., 2016). In Little Mouth Cave, Indiana, we observed several hundred *Hesperochernes* in a multigenerational midden of the woodrat *Neotoma magister*. It is unlikely that woodrats cross major rivers, but they may be acting as a dispersal agent within river drainages of individual karst regions and contributing to the high gene flow in *Hesperochernes* that we document here.

A third possibility is dispersal via cave flooding, which regularly occurs in several caves in which we collected *Hesperochernes*. This was evidenced by water lines and debris at the ceilings and ceiling-height ledges of cave passages. Caves with streams are typically connected to groundwater aquifers. Flooding in caves has been observed to decimates terrestrial invertebrate populations in shallow caves, with terrestrial invertebrate population numbers tending to track an expected time since recolonization rather than survival of a flooding event (Dumnicka, Galas, Karlikowska, & Sznober, 2015). Nonetheless, if they can survive immersion in water while the cave is flooded, it

is possible that *Hesperochernes* pseudoscorpions may be washed between caves in events of rapid changes of water levels. Survival of periodic immersion has been noted in epigean chernetids (Anthony, Buddle, & Sinclair, 2016). Conversely, high waters may simply deposit *Hesperochernes* pseudoscorpions at the ceiling, where they may later be more readily able to climb onto a roosting migratory bat.

A separate study lead by CDRS is investigating these possible mechanisms using an experimental approach (Stephen et al., in prep). Our finding of widespread gene flow between species has taxonomic implications. A second separate study lead by CDRS is addressing these taxonomic implications, bringing in morphological data, and including a checklist of complete locality data for each currently described species (Stephen et al., in prep.).

Given that the three eastern species are mixing, it is possible that similar patterns may be found with the two other described subterranean-limited and mammal-associated *Hesperochernes* in North America: *H. vespertilionis* in the Greater Antilles and *H. bradybaughi* in Arizona (Muchmore, 1971).

When describing the species, Beier (1976) placed *H. vespertilionis* into *Hesperochernes* based on similarity to *H. crassopalpus*, but this is problematic as *H. crassopalpus* had been transferred to *Acuminochernes* thirty years earlier by Hoff (1949). No phylogeny is available for all Chernetidae genera and the single molecular phylogeny available for the order included neither *Acuminochernes* nor *Hesperochernes,* so their relationship remains unclear. The generic placement of *H. vespertilionis* is questionable, and warrants further research given its potential relationship to cave-associated *Hesperochernes* of the southeastern USA.

We hypothesize that *H. bradybaughi*, the subterranean species from Arizona, is the sister taxon to the eastern species and was separated through a vicariance event: the formation of the Rocky Mountains. Pseudoscorpions are an ancient clade, with fossils from the Devonian (Shear, Schawaller, & Bonamo, 1989). Ancestral *Hesperochernes* may have existed prior to the formation of the Rocky Mountains and the desert and raised plateau of the Great Plains created by the rain shadow from these mountains into the continental interior. Few caves are known in the Great Plains

compared to the Mississippi River valley and eastwards into the Appalachians, but caves are plentiful on the southwestern edges of the Rocky Mountains. Future work will investigate the relationships of the eastern, western, and Caribbean species of *Hesperochernes*. Given the potential for phoresy by migrating Brazilian Free-tailed bats that move between the Greater Antilles and mainland North America, there is potential for this highly morphologically variable and interbreeding species complex to be even more widely distributed than we describe here.

Acknowledgements

We thank the Alabama Supercomputing Authority for access to the computing resources of the Alabama Supercomputer. CDRS was funded by the Cave Conservancy Foundation for both a significant PhD Fellowship and also a grant enabling present an earlier version of this research at the International Society for Subterranean Biology in 2018; by a fellowship from the Cave Research Foundation by a Meredith Birchfield grant from the Auburn University Museum of Natural History; by a fellowship from National Speleological Society; and by an initial grant from Dogwood City Grotto, Georgia, that purchased initial caving gear used throughout the extensive fieldwork of this project. Fieldwork would not have been possible without the extraordinary assistance of Pamela B. Hart in TAG, Julian J. Lewis in Indiana and Ohio, and Tom Malabad in Virginia. CDRS also gives thanks to Gerald Moni for assistance in Tennessee, Wil Orndorff in Virginia, Michael B. Slay in Arkansas, and Rickard Toomey in Kentucky. Access to the tens of thousands of caves in the eastern USA would not be possible without the previous work of hundreds of cavers and speleologists that have contributed maps and location data we were privileged to obtain through membership in the Alabama Cave Survey, Georgia Speleological Survey, Tennessee Cave Survey, and through generous cavers in the National Speleological Society that enabled CDRS' access to caves outside of these states. All collections were made with permits issued by state and federal bodies governing natural resources in Alabama, Arkansas, Georgia, Indiana, Kentucky, Missouri, Ohio, Oklahoma, Tennessee, and Virginia.

Author contributions

CDRS conceived the study, collected specimens, prepared RAD libraries, did bioinformatic analyses, and partly funded the study. JRS trained CDRS in RAD library preparation, guided analyses, and contributed intellectually. JWA provided laboratory reagents and equipment, collected specimens, guided analyses, and contributed intellectually. MLN assisted in cave access, collected specimens, and contributed intellectually. JEB provided laboratory reagents and equipment, contributed intellectually, and partly funded the study.

References

Anthony, S. E., Buddle, C. M., & Sinclair, B. J. (2016). Thermal biology and immersion tolerance of the Beringian pseudoscorpion Wyochernes asiaticus. *Polar Biology*, *39*(7), 1351–1355. doi: 10.1007/s00300-015-1849-y

Ashmole, P., & Ashmole, M. J. (1997). The land fauna of Ascension Island: New data from caves and lava flows, and a reconstruction of the prehistoric ecosystem. *Journal of Biogeography*, *24*(5), 549–589.

Babraham Bioinformatics. (2019). *FastQC v. 0.11.9*. Retrieved from http://www.bioinformatics.babraham.ac.uk/projects/fastqc/

Back, W. (1961). Calcium carbonate saturation in ground water, from routine analyses. *U.S. Geological Survey Water Supply Paper*, *1535-D*, 1–14.

Bailey, V. (1940). Caves and cave life. *Bulletin of the Speleological Society of the District of Columbia*, *1*.

Banks, N. (1895). Notes on the Pseudoscorpionida. *Journal of the New York Entomological Society*, *3*(1), 1–13.

Banks, N. (1908). The pseudoscorpions of Texas. *Bulletin of the Wisconsin Natural History Society*, *6*(1–2), 39–42.

Barr, T. C., Jr. (1960). A synopsis of cave beetles of the genus *Pseudanophthalmus* of the Mitchell Plain in southern Indiana (Coleoptera, Carabidae). *American Midland Naturalist*, *63*(2), 307–320.

Barr, T. C., Jr. (1961). *Caves of Tennessee. Bulletin 64.* Nashville, TN, USA: State of Tennessee, Department of Conservation and Commerce, Division of Geology.

Barr, T. C., Jr. (1985). Pattern and process in speciation of trechine beetles in eastern North America (Coleoptera: Carabidae: Trechinae). In G. E. Bali (Ed.), *Taxonomy, Phylogeny, and Biogeography of Beetles and Ants (Series Entomologia 33)* (pp. 350–407). The Netherlands: Dordrecht.

Bayona-Vásquez, N. J., Glenn, T. C., Kieran, T. J., Pierson, T. W., Hoffberg, S. L., Scott, P. A., ... Faircloth, B. C. (2019). Adapterama III: Quadruple-indexed, double/triple-enzyme RADseq libraries (2RAD/3RAD). *BioRxiv*. doi: 10.1101/205799

Beier, M. (1976). Pseudoscorpione von der Dominicanischen Republik (Insel Haiti). *Revue Suisse De Zoologie*, *83*(1), 45–58.

Bianchini, G. (2021). TreeViewer (Version 2.0.1). Retrieved from https://github.com/arklumpus/TreeViewer

Boyd, O. F., Philips, T. K., Johnson, J. R., & Nixon, J. J. (2020). Geographically structured genetic diversity in the cave beetle Darlingtonea kentuckensis Valentine, 1952 (Coleoptera, Carabidae, Trechini, Trechina). *Subterranean Biology*, *34*, 1–23. doi: 10.3897/subtbiol.34.46348

Buddle, C. M. (2010). Photographic key to the Pseudoscorpions of Canada and the adjacent USA. *Canadian Journal of Arthropod Identification*, *10*, 1–77. doi: https://dx.doi.org/10.3752/cjai.2010.10

Cardoso, R. C., Ferreira, R. L., & Souza-Silva, M. (2021). Priorities for cave fauna conservation in the Iuiú karst landscape, northeastern Brazil: A threatened spot of troglobitic species diversity. *Biodiversity and Conservation*, *30*(5), 1433–1455. doi: 10.1007/s10531-021-02151-5

Chamberlin, J. C. (1931). The arachnid order Chelonethida. *Stanford University Publications, Biological Sciences*, *7*(1), 1–284.

Christman, M. C., Culver, D. C., Madden, M. K., & White, D. (2005). Patterns of endemism of the eastern North American cave fauna. *Journal of Biogeography*, *32*(8), 1441–1452. doi: 10.1111/j.1365-2699.2005.01263.x

Coleman, W. T., & Zigler, K. S. (2015). The rediscovery of *Caecidotea nickajackensis* in Tennessee and Alabama. *Speleobiology Notes*, *7*, 10–13.

Culver, D. C. (1970). Analysis of simple cave communities. I. Caves as islands. *Evolution*, *24*(2), 463–474.

Culver, D. C., Kane, T. C., & Fong, D. W. (1995). *Adaptation and natural selection in caves. The evolution of* Gammarus minus. Cambridge, Massachusetts, United States: Harvard University Press.

Culver, D. C., Master, L. L., Christman, M. C., & Hobbs, H. H., III. (2000). Obligate cave fauna of the 48 contiguous United States. *Conservation Biology*, *14*(2), 386–401.

Culver, D. C., & Pipan, T. (2014). *Shallow subterranean habitats*. New York, New York, United States: Oxford University Press.

Danecek, P., Auton, A., Abecasis, G., Albers, C. A., Banks, E., DePristo, M. A., ... 1000 Genomes Project Analysis Group. (2011). The variant call format and VCFtools. *Bioinformatics*, *27*(15), 2156–2158. doi: 10.1093/bioinformatics/btr330

Davies, W. E. (1960). Origin of caves in folded limestone. *National Speleological Society Bulletin*, *22*(1), 5–18.

Dumnicka, E., Galas, J., Karlikowska, J., & Sznober, N. (2015). Temporary co-existence of aquatic and terrestrial invertebrates in shallow periodically flooded and frozen cave. *Biologia*, *70*(9), 1201−1209.

Eaton, D. A. R., & Overcast, I. (2020). ipyrad: Interactive assembly and analysis of RADseq datasets. *Bioinformatics*, *36*(8), 2592−2594. doi: 10.1093/bioinformatics/btz966

Edgington, H. A., Ingram, C. M., & Taylor, D. R. (2016). Cyto-nuclear discordance suggests complex evolutionary history in the cave-dwelling salamander, *E urycea lucifuga* . *Ecology and Evolution*, *6*(17), 6121−6138. doi: 10.1002/ece3.2212

Engel, A. S., Niemiller, M. L., Zigler, K. S., Stephen, C. D. R., Carter, E. T., Paterson, A. T., ... Taylor, S. J. (2017). Invertebrate and vertebrate cave fauna records for the Appalachian Valley and Ridge. In K. Moore & S. White (Eds.), *Proceedings of the 17th International Congress of Speleology (Ed. 2), July 23−29, Sydney, NSW Australia, Volume 1* (pp. 82−86). Sydney, Australia: Australian Speleological Federation Inc. Retrieved from http://www.uis-speleo.org/index.php?option=com_content&view=article&id=92&Itemid=417

Ewels, P., Magnusson, M., Lundin, S., & Käller, M. (2016). MultiQC: Summarize analysis results for multiple tools and samples in a single report. *Bioinformatics*, *32*(19), 3047−3048. doi: 10.1093/bioinformatics/btw354

Finlayson, G., Madani, G., Dennis, G., & Harvey, M. (2015). First reported observation of phoresy of pseudoscorpions on an endemic New Zealand mammal, the lesser short-tailed bat, *Mystacina tuberculata*. *New Zealand Journal of Zoology*, *42*(4), 298−301. doi: 10.1080/03014223.2015.1063517

Fong, D. W., Porter, M. L., & Slay, M. E. (2012). *Cave Life of the Virginias*. Huntsville, AL, US: Biology Section of the National Speleological Society.

Francois, O. (2016). *Running Structure-like population genetic analyses with R*.

Glenn, T. C., Bayona-Vasquez, N. J., Kieran, T. J., Pierson, T. W., Hoffberg, S. L., Scott, P. A., ... Faircloth, B. C. (2017). *Adapterama III: Quadruple-indexed, triple-enzyme RADseq libraries for about $1USD per Sample (3RAD)*. doi: 10.1101/205799

Harlan, A. J., & Zigler, K. S. (2009). The phylogenetic position of *Eurycea lucifuga*, the Cave Salamander, and the evolution of cave-adapted species in *Eurycea*. *Journal of the Tennessee Academy of Science*, *84*(4), 77–82.

Hart, P. B., Niemiller, M. L., Burress, E. D., Armbruster, J. W., Ludt, W. B., & Chakrabarty, P. (2020). Cave-adapted evolution in the North American amblyopsid fishes inferred using Ultraconserved Elements. *Evolution*, *74*(5), 936–949.

Harvey, M. J., Altenbach, J. S., & Best, T. L. (1999). *Bats of the United States*. Arkansas, United States: Arkansas Game and Fish Commission.

Harvey, M. S. (2013). Pseudoscorpions of the World, version 3.0. Western Australian Museum, Perth. Retrieved June 23, 2019, from http://museum.wa.gov.au/catalogues-beta/pseudoscorpions

Harvey, M. S., & Wynne, J. J. (2014). Troglomorphic pseudoscorpions (Arachnida: Pseudoscorpiones) of northern Arizona, with the description of two new short-range endemic species. *Journal of Arachnology*, *42*(3), 205–219. doi: 10.1636/K14-34.1

Hedin, M. C. (1997). Molecular phylogenetics at the population/species interface in cave spiders of the southern Appalachians (Araneae: Nesticidae: *Nesticus*). *Molecular Biology and Evolution*, *14*(3), 309–324. doi: 10.1093/oxfordjournals.molbev.a025766

Hoff, C. C. (1949). The pseudoscorpions of Illinois. *State of Illinois Department of Registration and Education Natural History Survey Division Bulletin*, *24*(4), 411–499.

Hoff, C. C., & Bolsterli, J. E. (1956). Pseudoscorpions of the Mississippi River drainage basin area. *Transactions of the American Microscopical Society*, *75*(2), 155–179.

Juberthie, C., Delay, B., & Bouillon, M. (1980). Extension du milieu souterrain en zone non calcaire: Description d′un nouveau milieu et de son peuplement par les Coléoptères troglobies. *Mémoires de biospéologie*, *6*, 19–52.

Kaye, C. A. (1957). The effect of solvent motion on limestone solution. *Journal of Geology*, *65*(1), 35–46.

Lewis, J. J. (2003). *Pseudotremia reynoldsae*, a new species of troglobitic milliped (Diplopoda: Chordeumatida: Cleidogonidae), with a synopsis of the cavernicolous millipeds of the Hoosier National Forest in Indiana. *Proceedings of the Indiana Academy of Science*, *112*, 36–42. Retrieved from http://journals.iupui.edu/index.php/ias/article/viewFile/7277/7288

Lewis, J. J. (2009). Three new species of *Caecidotea*, with a synopsis of the asellids of Virginia (Crustacea: Isopoda: Asellidae). In S. M. Roble & J. C. Mitchell (Eds.), *A lifetime of contributions to Myriapodology and the natural history of Virginia: A Festschrift in honor of Richard L. Hoffman's 80th Birthday* (pp. 245–259). Martinsville, Virginia, United States: Virginia Museum of Natural History.

Loria, S. F., Zigler, K. S., & Lewis, J. J. (2011). Molecular phylogeography of the troglobiotic millipede *Tetracion* Hoffman, 1956 (Diplopoda, Callipodida, Abacionidae). *International Journal of Myriapodology*, *5*. Retrieved from http://search.ebscohost.com/login.aspx?direct=true&profile=ehost&scope=site&authtype=crawler&jrnl=18752535&AN=67270621&h=iKrlqvZyNejQwqm8F9sotXM610iOW1s

PHM45Ac21FnKGMxnsWkZLhFUx9hgQ1wo10dsoUIVCnEzyQ%2Fb%2F8D6rzw%3D%3D&crl=c

Miller-Butterworth, C. M., Vonhof, M. J., Rosenstern, J., Turner, G. G., & Russell, A. L. (2014). Genetic structure of Little Brown Bats (*Myotis lucifugus*) corresponds with spread of White-Nose Syndrome among hibernacula. *Journal of Heredity*, *esu012*, 1−11. doi: 10.1093/jhered/esu012

Minh, B. Q., Schmidt, H. A., Chernomor, O., Schrempf, D., Woodhams, M. D., von Haeseler, A., & Lanfear, R. (2020). IQ-TREE 2: New models and efficient methods for phylogenetic inference in the genomic era. *Molecular Biology and Evolution*, *37*(5), 1530−1534. doi: 10.1093/molbev/msaa015

Muchmore, W. B. (1971). Phoresy by North and Central American pseudoscorpions. *Proceedings of the Rochester Academy of Science*, *12*(2), 79–97.

Muchmore, W. B. (1974). Clarification of the genera *Hesperochernes* and *Dinocheirus* (Pseudoscorpionida, Chernetidae). *Journal of Arachnology*, *2*, 25−36.

Muchmore, W. B. (1992). Cavernicolous pseudoscorpions from Texas and New Mexico (Arachnida: Pseudoscorpionida). *Texas Memorial Museum, Speleological Monographs*, *3*, 127−153.

Muchmore, W. B. (1994). Some pseudoscorpions (Arachnida: Pseudoscorpionida) from caves in Ohio and Indiana, U.S.A. *Transactions of the American Microscopical Society*, *113*(3), 316–324.

Nelson, S., Jr. (1975). A systematic study of Michigan Pseudoscorpionida. *American Midland Naturalist*, *93*(2), 257−301.

Niemiller, M. L., & Zigler, K. S. (2013). Patterns of cave biodiversity and endemism in the Appalachians and Interior Plateau of Tennessee, USA. *PLoS ONE*, *8*(5), e64177. doi: 10.1371/journal.pone.0064177

Niemiller, M. L., Zigler, K. S., & Fenolio, D. B. (2013). *Cave Life of TAG*. Huntsville, AL, US: Biology Section of the National Speleological Society.

Niemiller, M. L., Zigler, K. S., Hart, P. B., Kuhajda, B. R., Armbruster, J. W., Ayala, B. N., & Engel, A. S. (2016). First definitive record of a stygobiotic fish (Percopsiformes, Amblyopsidae, *Typhlichthys*) from the Appalachians karst region in the eastern United States. *Subterranean Biology*, *20*, 39–50. doi: 10.3897/subtbiol.20.9693

Ortuño, V. M., Gilgado, J. D., Jiménez-Valverde, A., Sendra, A., Pérez-Suárez, G., & Herrero-Borgoñón, J. J. (2013). The "Alluvial Mesovoid Shallow Substratum", a new subterranean habitat. *PLOS ONE*, *8*(10), e76311.

Palmer, A. N. (1975). The origin of maze caves. *National Speleological Society Bulletin*, *37*, 56–76.

Palmer, A. N. (2007). *Cave geology*. Dayton, OH, USA: Cave Books.

Peck, S. B. (1989). The cave fauna of Alabama: Part I. The terrestrial invertebrates (excluding insects). *Bulletin of the National Speleological Society*, *51*, 11–33.

Perez, F., & Granger, B. E. (2007). IPython: A System for Interactive Scientific Computing. *Computing in Science & Engineering*, *9*(3), 21–29. doi: 10.1109/MCSE.2007.53

Perez-Gelabert, D. E. (2008). Arthropods of Hispaniola (Dominican Republic and Haiti): A checklist and bibliography. *Zootaxa*, *1831*, 1–530.

Pipan, T., López, H., Oromí, P., Polak, S., & Culver, D. C. (2010). Temperature variation and the presence of troglobionts in terrestrial shallow subterranean habitats. *Journal of Natural History*, *45*(3–4), 253–273. doi: 10.1080/00222933.2010.523797

Pohl, E. R. (1955). Vertical shafts in limestone caves. *Occasional Papers of the National Speleological Society*, (2), 1–25.

Porras-Hurtado, L., Ruiz, Y., Santos, C., Phillips, C., Carracedo, Á., & Lareu, M. V. (2013). An overview of STRUCTURE: Applications, parameter settings, and supporting software. *Frontiers in Genetics*, *4*. doi: 10.3389/fgene.2013.00098

Prendini, L., Ehrenthal, V. L., & Loria, S. F. (2021). Systematics of the relictual Asian scorpion family Pseudochactidae Gromov, 1998, with a review of cavernicolous, troglobitic, and troglomorphic scorpions. *Bulletin of the American Museum of Natural History*, *453*(1). doi: 10.1206/0003-0090.453.1.1

Puechmaille, S. J., Wibbelt, G., Korn, V., Fuller, H., Forget, F., Muhldorfer, A. K., … Teeling, E. C. (2011). Pan-European distribution of White-Nose Syndrome fungus (*Geomyces destructans*) not associated with mass mortality. *PLoS ONE*, *6*(4), e19167.

Reiss, J., Perkins, D. M., Fussmann, K. E., Krause, S., Canhoto, C., Romeijn, P., & Robertson, A. L. (2019). Groundwater flooding: Ecosystem structure following an extreme recharge event. *Science of The Total Environment*, *652*, 1252–1260. doi: 10.1016/j.scitotenv.2018.10.216

Shear, W. A., Schawaller, W., & Bonamo, P. M. (1989). Record of Palaeozoic pseudoscorpions. *Nature*, *341*, 527–529.

Sket, B. (1997). Biotic diversity of the Dinaric karst, particularly in Slovenia: History of its richness, destruction, and protection. In I. D. Sasowsky, D. W. Fong, & E. L. White,

Special Publication 3. Conservation and Protection of the Biota of Karst. Extended Abstracts and Field-Trip Guide for the symposium held February 13 through 16, 1997. Nashville, Tennessee. (pp. 84–98). Charles Town, WV, USA: Karst Waters Institute.

Slay, M. E., Niemiller, M. L., Sutton, M., & Taylor, S. J. (2016). *Cave life of the Ozarks*. Huntsville, AL, US: Biology Section of the National Speleological Society.

Snowman, C. V., Zigler, K. S., & Hedin, M. (2010). Caves as islands: Mitochondrial phylogeography of the cave-obligate spider species *Nesticus barri* (Araneae: Nesticidae). *Journal of Arachnology*, *38*(1), 49–56. doi: 10.1636/A09-057.1

Turbanov, I. S., Palatov, D. M., & Golovatch, S. I. (2016). The state of the art of biospeleology in Russia and other countries of the former Soviet Union: A review of the cave (endogean) invertebrate fauna. 2. Arachnida—acknowledgments. *Entomological Review*, *96*(9), 1297–1333. doi: 10.1134/S0013873816090116

Vandel, A. (1965). *Biospeleology: The biology of cavernicolous animals* (B. E. Freeman, Trans.). Oxford, England, U.K.: Pergammon Press.

Weary, D. J., & Doctor, D. H. (2014). *Karst in the United States: A digital map collection and database. U.S. Geological Survey Open-File Report 2014-1156* (p. 23). Washington, District of Columbia: U.S. Geological Survey. Retrieved from U.S. Geological Survey website: http://dx.doi.org/10.3133/ofr20141156

Weckstein, J. D., Johnson, K. P., Murdoch, J. D., Krejca, J. K., Takiya, D. M., Veni, G., … Taylor, S. J. (2016). Comparative phylogeography of two codistributed subgenera of cave crickets (Orthoptera: Rhaphidophoridae: *Ceuthophilus* spp.). *Journal of Biogeography*, *43*(7), 1450–1463. doi: 10.1111/jbi.12734

Whitaker, J. O., & Hamilton, W. J. (1998). Chiroptera (Bats). In *Mammals of the eastern United States* (2nd ed., pp. 64–111). Ithaca, New York, United States: Cornell University Press.

Zhao, L., & Zhang, F. (2016). New cave species of *Sinella* Brook, 1882 from China (Collembola: Entomobryidae). *Zootaxa*, *4161*(4), 523. doi: 10.11646/zootaxa.4161.4.3

Zigler, K. S., Niemiller, M. L., Stephen, C. D. R., Ayala, B. N., Milne, M. A., Gladstone, N. S., ... Cressler, A. (2020). Biodiversity from caves and other subterranean habitats of Georgia, USA. *Journal of Cave and Karst Studies*, *82*(2), 125–167. doi: 10.4311/2019LSC0125

Fig. 1.1 Currently defined species of *Hesperochernes*: (a) *H. mirabilis*, topotypic specimen; (b) *H. holsingeri*, topotypic specimen; (c) *H. occidentalis*, specimen collected with 10 km of type locality. All specimens are females.

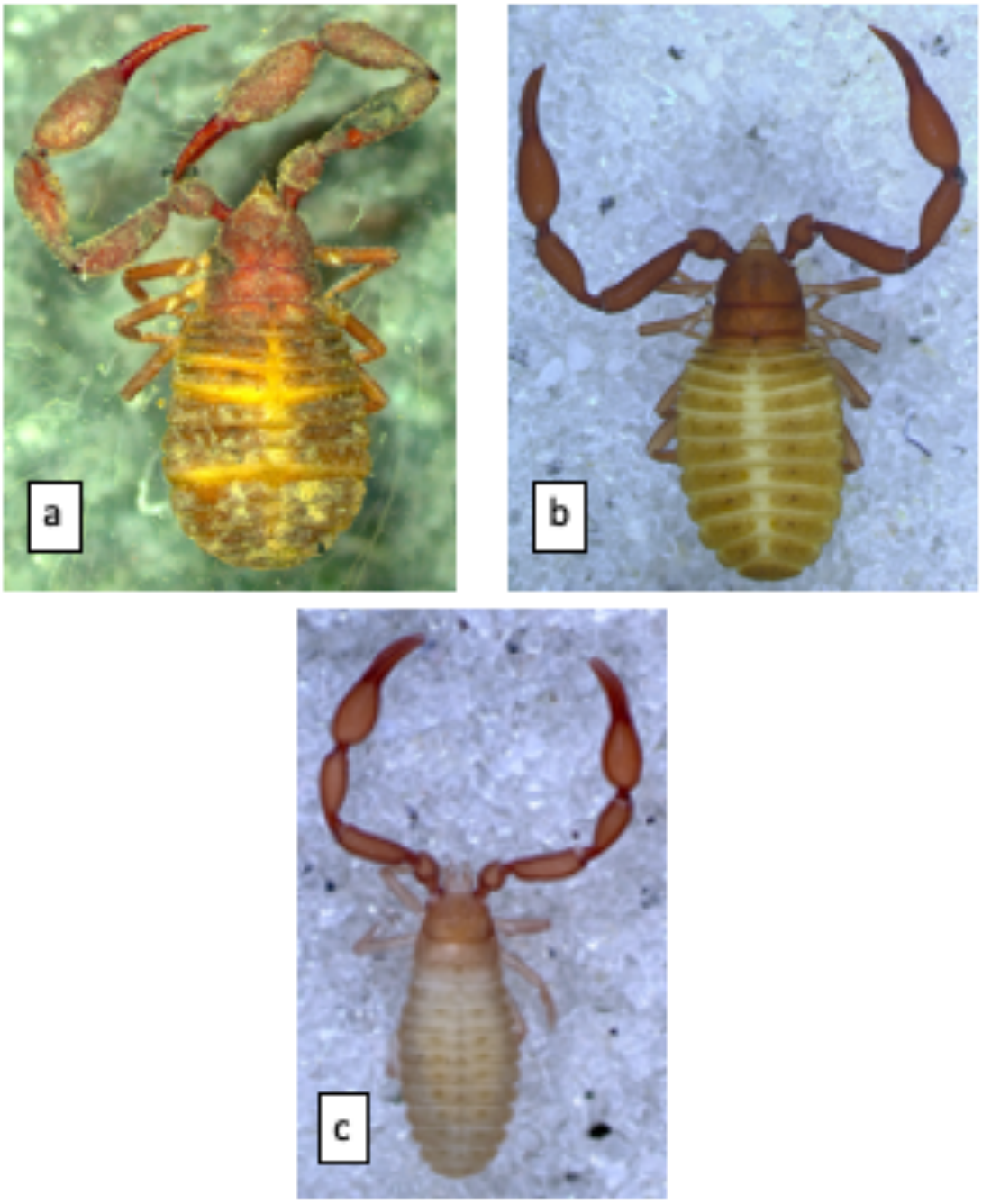

Fig. 1.2 Map of cave collection localities: green circles indicate caves from which samples of *Hesperochernes* were collected that generated usable RADseq loci with the iPyrad pipeline (Eaton & Overcast, 2020) following quality control steps. Grey regions indicate karstic regions (Weary & Doctor, 2014).

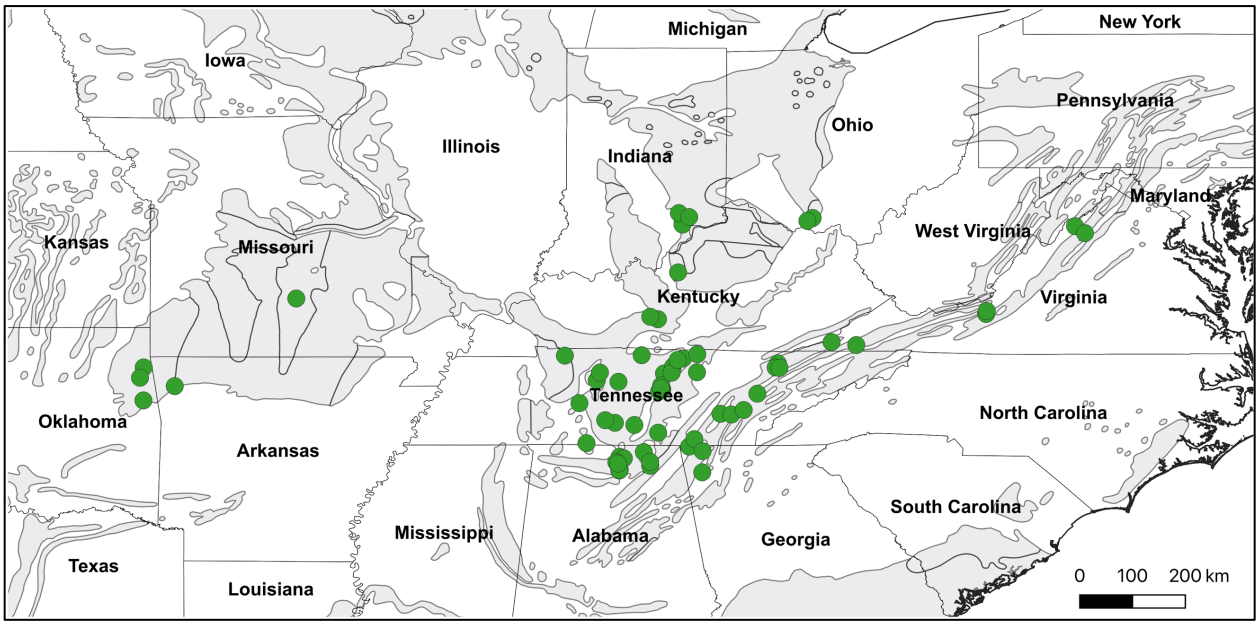

Fig. 1.3 Map of distribution of cave-obligate *Hesperochernes* east of the Great Plains.

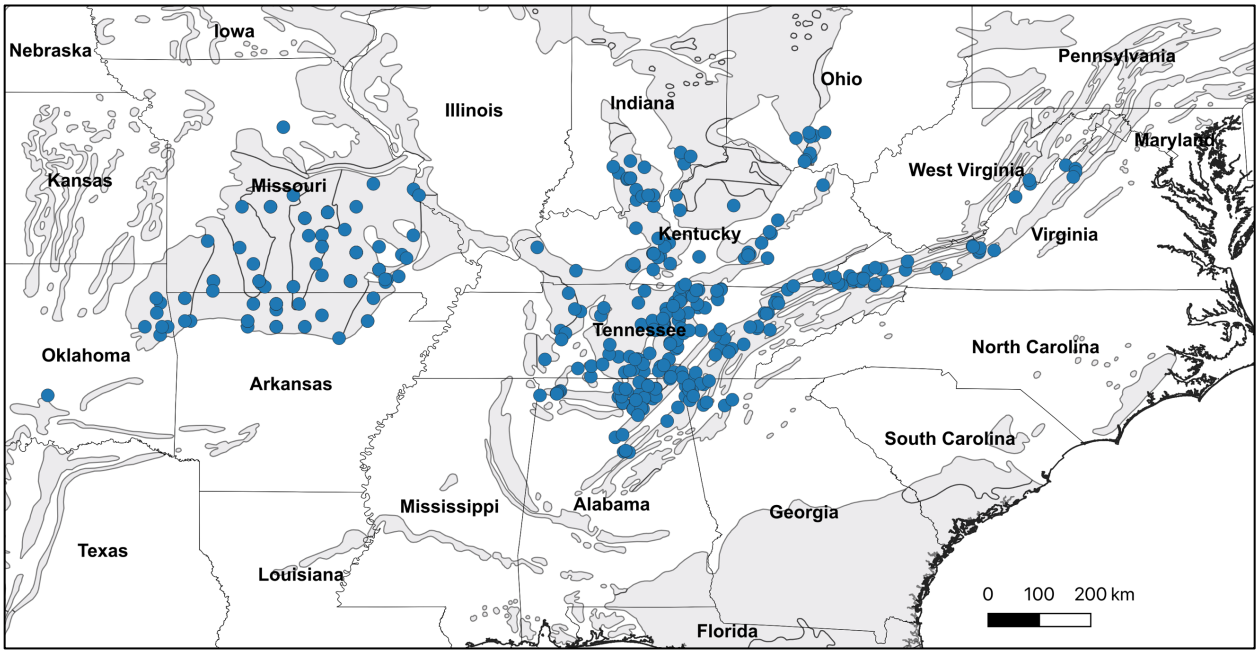

Fig. 1.4 Phylogeny of complete data set. (a) Tree rooted with furthest west Ozark karst region samples for display purposes only. Branches had poor UFB support and were very shallow; longer branches are pruned from tree for display purposes. 1, specimens collected from Oklahoma caves; 2, specimens collected from Arkansas caves; 3, specimen collected from a Missouri cave; 4, specimens collected from caves east of the Mississippi River; 5, specimens collected from Wilsons Cave, Indiana, type locality of *Hesperochernes holsingeri.* (b) Unrooted tree with longest branch from Flintknapper Cave, AL not pruned; tree rooted for display purposes with unpruned branch as sister to all other samples to illustrat shallowness of branch depth in Fig. 1.4a.

(a) (b)

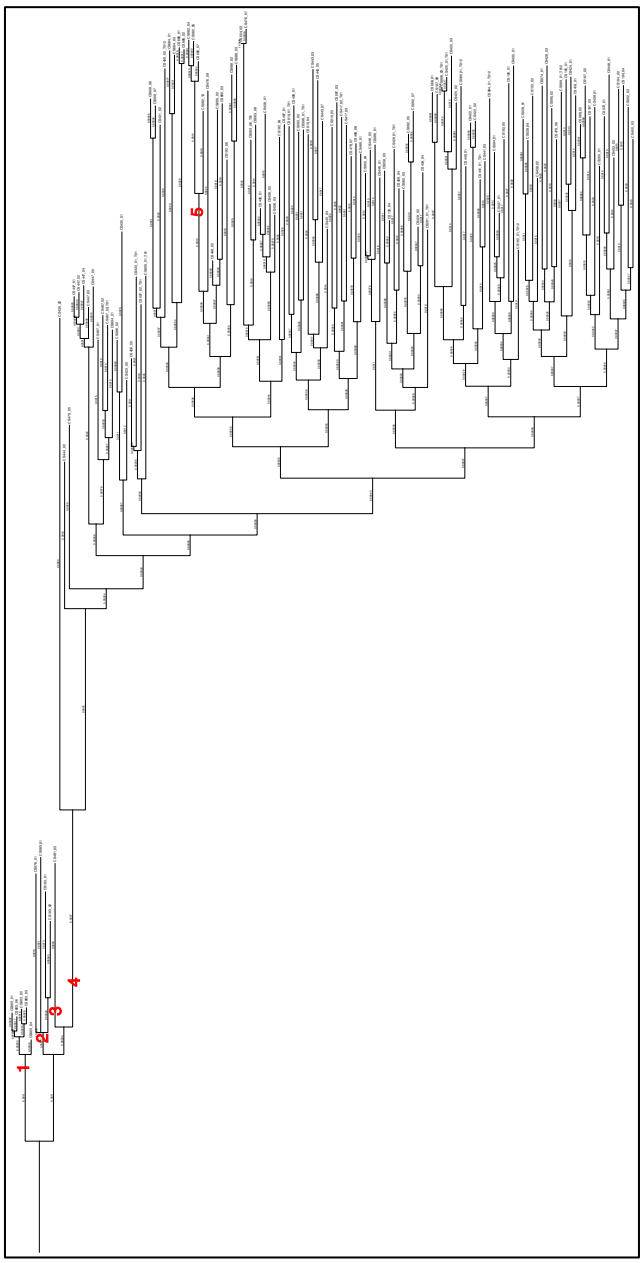

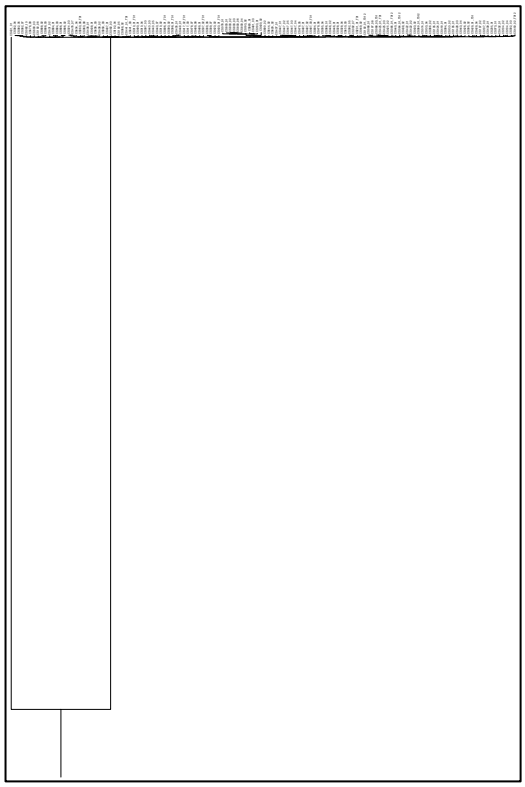

Fig. 1.5. Phylogeny of pruned data set. Used samples with at least 50% of possible loci; unlabeled internal nodes have >95% UFB support, black nodes have 80-95% UFB support, and nodes with <80% UFB support are collapsed into polytomies; Ozark sample is leaf with blank square, Driftless samples are leaves with black squares, Indian Cave type locality is leaf with grey square, unmarked leaves are from combined AVR and ILP karst regions. Tree rooted with inferred LCA (by TreeViewer) of Indian Cave and Ozark karst region samples; inferred sister clade samples are from Virginia.

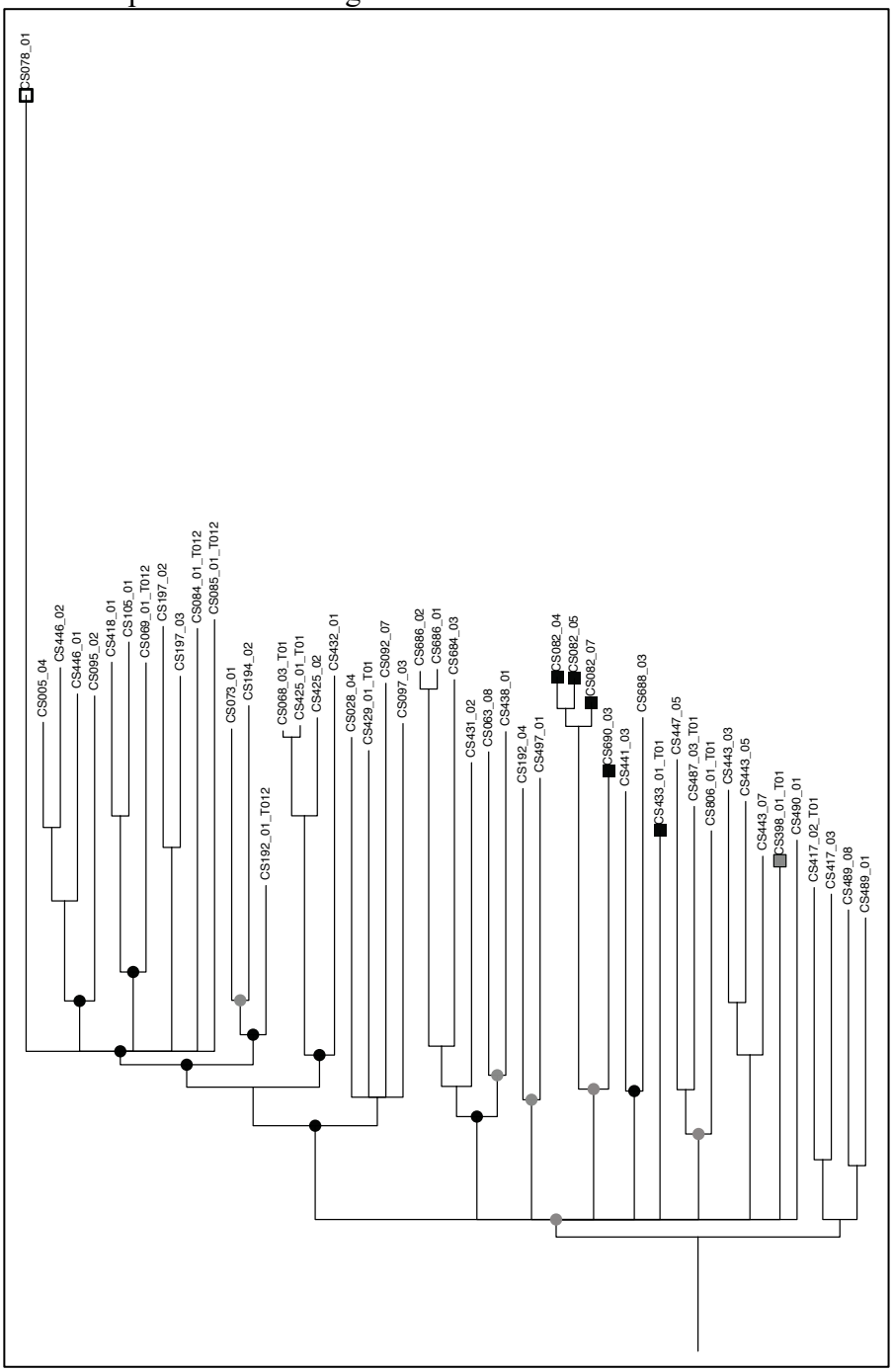

Fig. 1.6 Plot from STRUCTURE: blue bar on top of plot indicates specimens collected from caves in the Ozarks karst region; red bar on top of plot indicates specimens from caves in karstic regions east of the Mississippi River and south of the Ohio River (Appalachians, Interior Low Plateau, Valley and Ridge); green bar on top of plot indicates specimens from karstic regions that did not experience glaciation north of the Ohio River and east of the Mississippi River (Driftless); double bars indicate type localities.

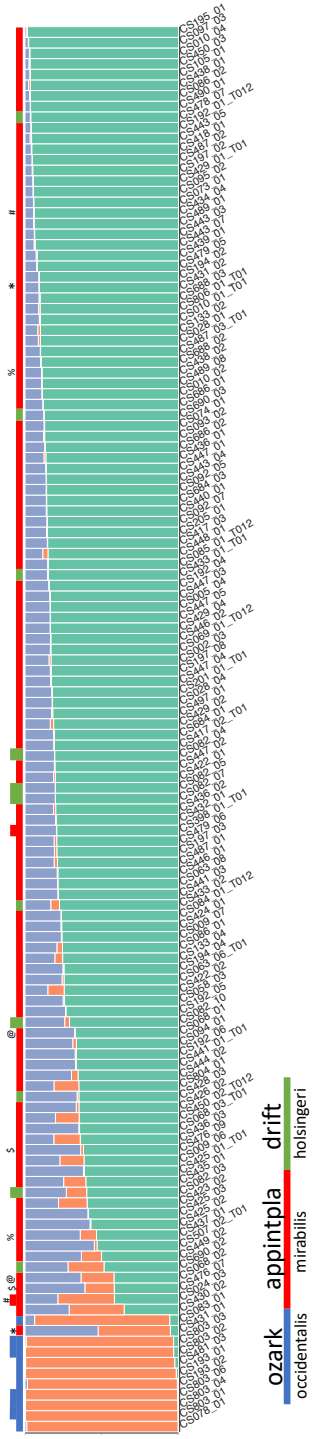

Fig. 1.7 Molecular PCA1, using *a priori* assigned populations based on karst regions: specimens grouped based on whether from caves in the combined Appalachians, Interior Plateau, and the Valley and Ridge karst regions (appintpla); Driftless Area karst region (drift); or Ozarks karst region (ozark). (a) PCA with strict filtering; (b) PCA with relaxed filtering; (c) PCA with relaxed filtering and TSNEM.

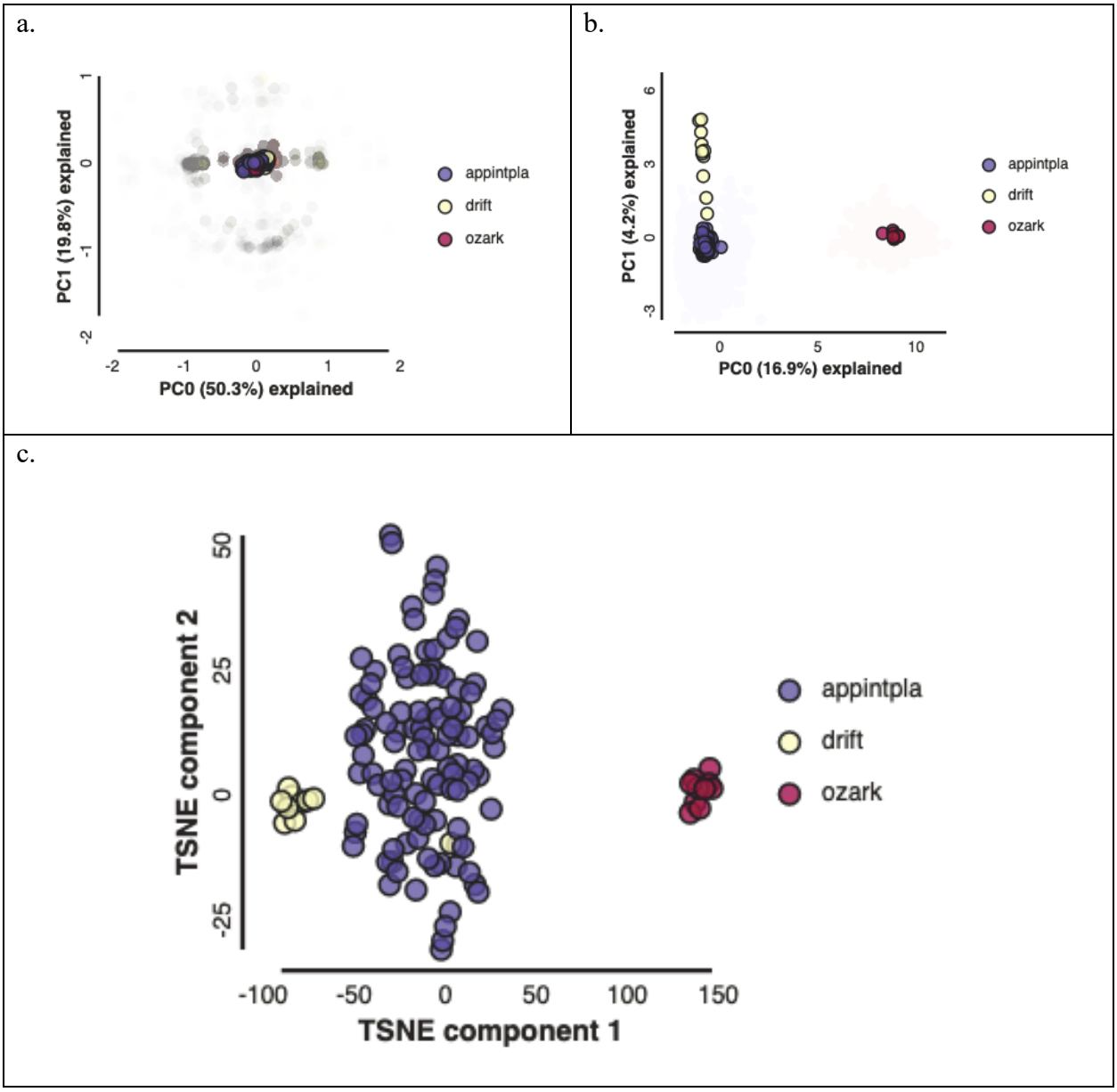

Fig. 1.8 Molecular PCA2, using *a priori* assigned populations based on the Mississippi River: specimens grouped based on whether from caves located east or west of the Mississippi River: (a) PCA with strict filtering; (b) PCA with relaxed filtering; (c) PCA with relaxed filtering and TSNEM.

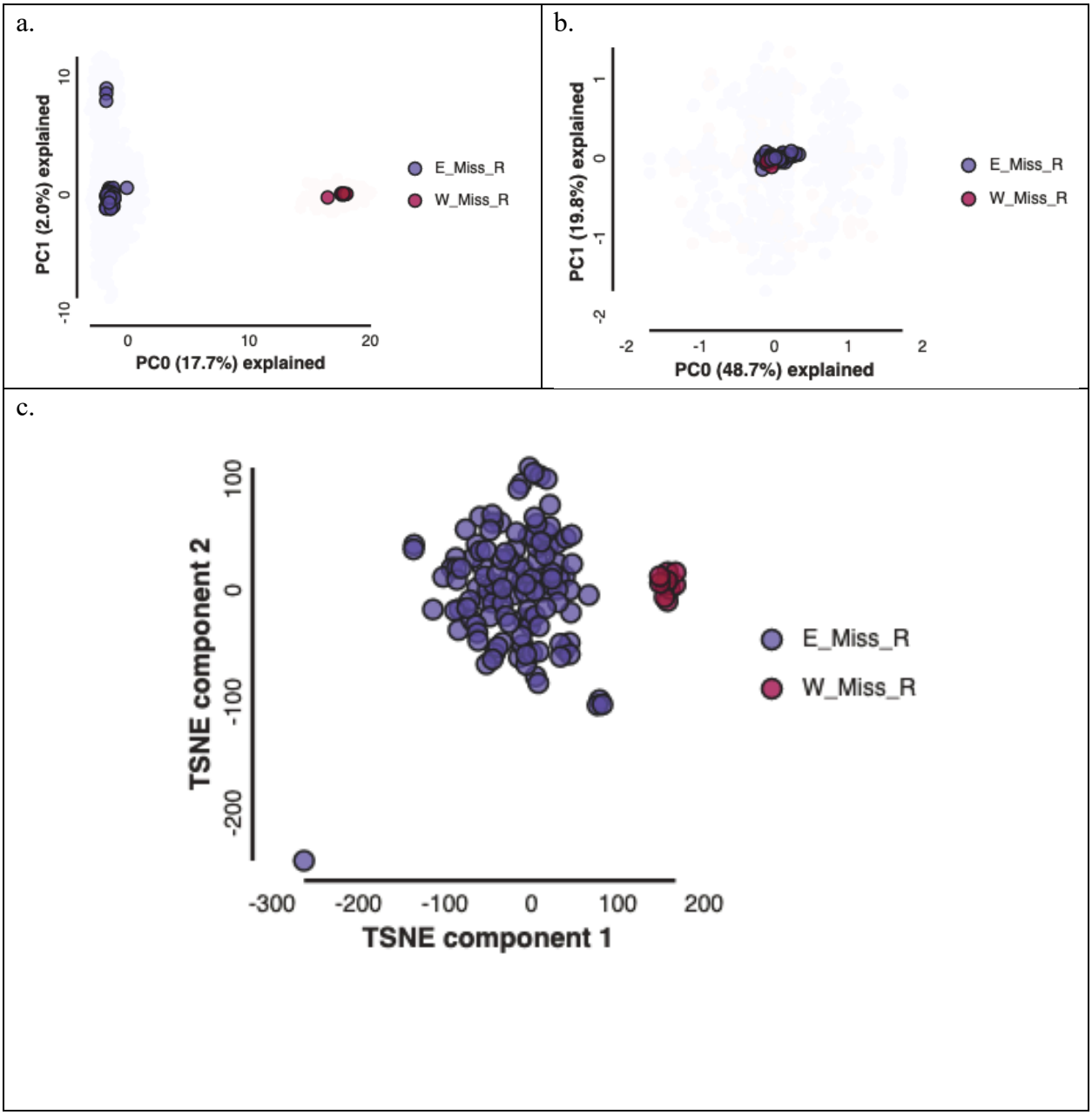

Fig. 1.9 Molecular PCA3, using *kmeans* method of assigning samples to populations. Specimens colored based on karst region groupings used in PCA1 but assigned to each population through *kmeans* method. (a) PCA with relaxed filtering; (b) PCA with relaxed filtering and TSNEM.

a.

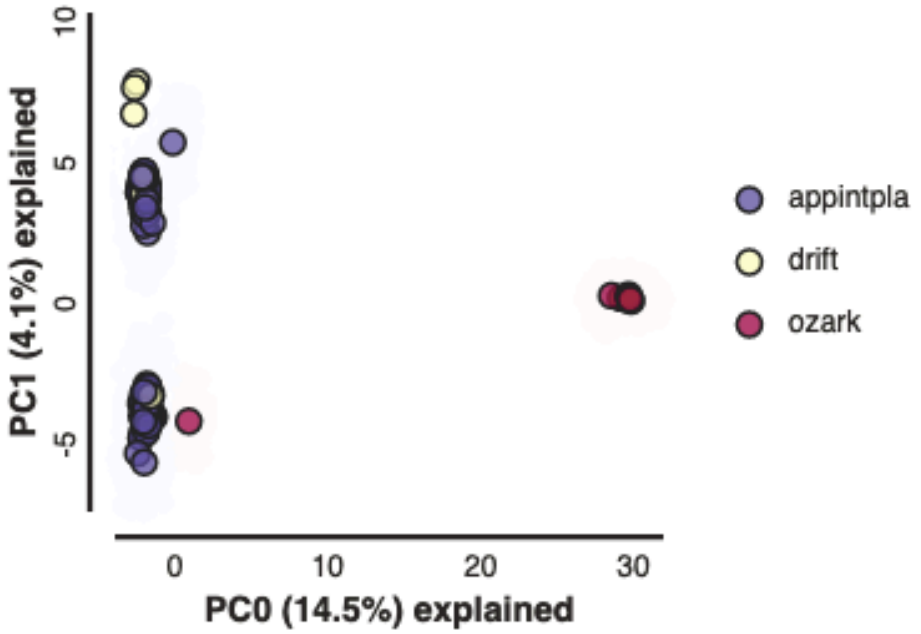

b.

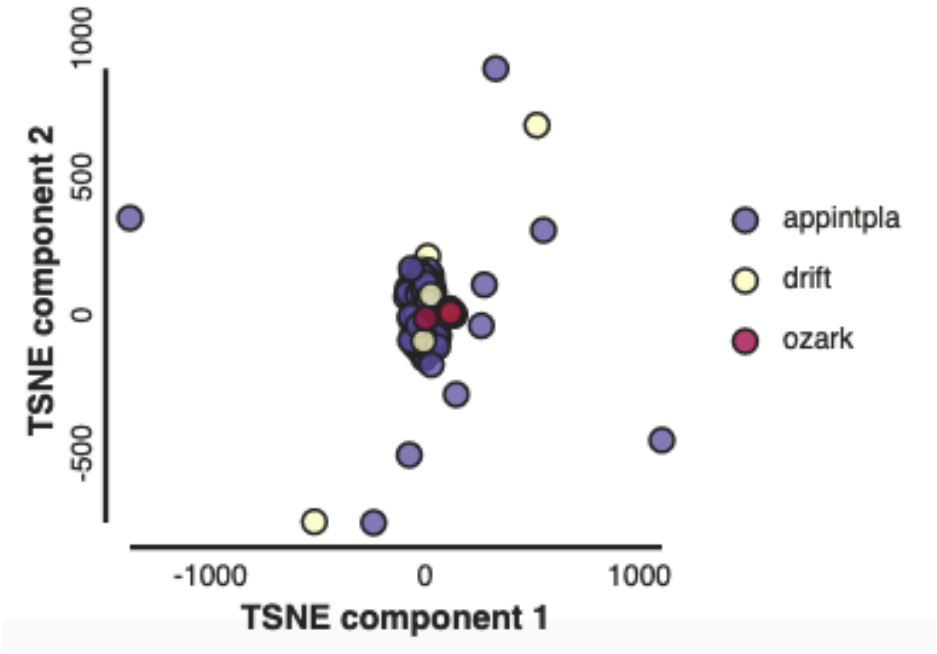

Tab. 1.1. F_{ST} results from VCFtools. AppIP, Appalachian Valley and Ridge and Interior Plateau karst regions (east of Mississippi River and south of Ohio River; Drift, Driftless karst region (east of Mississippi River and north of Ohio River); Ozark, Ozarks karst region (west of Mississippi River).

populations compared	**Weir and Cockerham mean F_{ST}**
AppIP vs. Drift	0
AppIP vs. Ozark	0.24
Drift vs. Ozark	0.24

Chapter 2

Standardized characters and landmarks for geometric morphometrics with Pseudoscorpiones: a case study assessing sexual dimorphism in *Hesperochernes mirabilis*

Authors

Charles D. R. Stephen[1,2,3], Jonathan W. Armbruster[1]

[1] Department of Biological Sciences, Auburn University, Auburn, Alabama, USA

[2] Department of Biology, Missouri State University, Springfield, Missouri, USA

[3] Corresponding author: cdr.stephen@gmail.com

Abstract

The powerful tools of molecular methods are unavailable to arthropods whose soft tissues have been dissolved in caustic clearing agents and are difficult to impossible with specimens that have been preserved in lower grade ethanol or other preservatives for decades to centuries. In pseudoscorpions these situations are typical in museum specimens. Species are generally diagnosed by qualitative characters and combinations of straight-line measurements, and often described based on few specimens. Upon additional specimens being found, measurements may no longer be considered diagnostic as variation is revealed. Intraspecific morphological investigations such as examinations of potential sexual dimorphism have relied on straight-line measurements for raw data. An alternate approach that has been used with success in insects and vertebrates is geometric morphometrics, which enables objective analysis of shape independent of size. Here through a case study investigating potential sexual dimorphism in *Hesperochernes mirabilis* (Banks, 1895) we provide geometric morphometrics landmarks for six body characters in standardized views and a walk-through guide that may be used for other investigations of pseudoscorpion morphology. Our approach found significant evidence for sexual dimorphism in *H. mirablilis*, the first time for which this has been found in this species.

Introduction

Molecular methods are making many advances in the understanding of relationships across life. At present and in the foreseeable future these methods remain unavailable for slide-preserved specimens. Permanent mounting on slides is a standard archival storage and examination medium for small arthropods, such as pseudoscorpions. Type specimens of North American pseudoscorpions tend to be cleared in lactic acid or potassium chloride then mounted on a permanent slide. Both straight-line measurements and generalized subjective notes on shape have been used in defining species based on the slide-mounted specimens. This is problematic with species that appear to be wide-ranging and are variable in size. The great advantage of geometric morphometrics is that it enables analysis of shape independent of size, eliminating this problem of size variation within a species due to environmental factors varying across its range, such as diet or temperature, or founder effects from scattered small populations (Bookstein 1991, Adams et al. 2013).

Geometric morphometrics provides a useful, inexpensive, and intuitive tool set for quantitatively addressing questions in ecology, ethology, taxonomy, and in phylogenetic comparative methods (Armbruster et al. 2016, Karanovic et al. 2016, Burress et al. 2017). The approach has been widely used in fish, birds, and humans, but has yet to be employed in pseudoscorpions. There are several open avenues of exploration where this approach would be of great use. For example, several pseudoscorpions are only known to be associated with subterranean habitat and have been deemed troglomorphic or strongly adapted to subterranean life by authors; however, sometimes the distinction is difficult to justify as their epigean congeners or species in the same family may share traits associated with subterranean life, such lack of eyes or presence of elongated limbs as seen in some subcortical species. Geometric morphometrics would provide a means to do this if combined with a phylogeny of epigean and subterranean congeners.

Quantitative studies of shape differences in pseudoscorpions are limited. Chamberlin (1931) gave the foundation of standard views of different body parts and standardized landmarks for measurements. Zeh (1987) examined sexual dimorphism in Neotropical chernetids. In this study chernetids were examined with straight-line measurements taken from silhouette images of a single character, the pedipalp chela in a lateral view. Linear regressions were utilized as a method

of assessing sexual dimorphism as seen in this character. Harvey (1985) used some statistics in sternophorids. Harvey (1987) used discriminant function analysis of pedipalp straight-line measurement characters in the garypid *Synsphyronus*. Muster et al. (2004) examined multivariate statistics of five straight-line measurements to assist in separating the chthoniid species *Chthonius fuscimanus* and *C. boldorii*. Christophoryová et al. (2016) used multivariate analyses to separate species of the chernetid *Lasiochernes*. With the exception of Zeh (1987), all previous quantitative studies of pseudoscorpion morphology have been motivated by a desire solve a taxonomically intractable problem. All literature to date on pseudoscorpion morphology using multivariate analyses has explored body characteristics examining size as a proxy for a shape providing a particular function, and not shape exclusive of size.

Quantitative tests of sexual selection as expressed in sexual dimorphism provide an example of testing evolutionary arms races. The two-fold purpose of this contribution is to first provide sets of standardized landmarks for different morphological characters, and second, to give a walk-through example of a case study using these landmarks to investigate potential sexual dimorphism in the subterranean-adapted chernetid *Hesperochernes mirabilis* (Banks, 1895). We provide sets of landmarks for six characters that may be used in the family Chernetidae or adapted for use across pseudoscorpion lineages. These characters and associated landmarks were chosen for their relative ease of access and their ease of analysis in freely available, user-friendly software.

Methods

Specimens of *Hesperochernes mirabilis* (Fig. 2.1) were collected and preserved in 80% EtOH at three collection events in 2017 and 2019 from a single large population located in Oaks Cave, Union County, Tennessee, USA (Fig. 2.2). This cave is given the code TUN5 by the Tennessee Cave Survey. In this study we used 20 females (Fig. 2.1a) and 20 males (Fig. 2.1b), all of which are accessioned into the Auburn University Museum of Natural History (AUMNH).

Six characters were analyzed: (1) carapace in dorsal view (Fig. 2.3, Fig. 2.9a, Tab. 2.1); (2) right leg IV femur and patella in prolateral view (Fig. 2.4, Fig. 2.9b, Tab. 2.2); (3) right pedipalp chela in dorsal view (Fig. 2.5, Fig. 2.10a, Tab. 2.3a); (4) right pedipalp chela in retrolateral view (Fig.

2.6, Fig. 2.10b, Tab. 2.3b); (5) right pedipalp fixed finger in retrolateral view (Fig. 2.7, Fig. 2.11a, Tab. 2.4a); and (5) right pedipalp movable finger in retrolateral view (Fig. 2.8, Fig. 2.11b, Tab. 2.4b). For each character, templates were created of standardized landmarks to capture shape from a standard view. Before starting to work with an individual specimen, it was examined to verify that there was no damage to all characters being analyzed, and then the right leg IV and the right pedipalp were dissected from it. All specimens were viewed for landmarking in a Stentor glass dish that was half-filled with fine-grained sand for orienting the specimen and filled with sufficient 80% ethyl alcohol to cover the specimen. Images were taken at the same magnification and in the same orientation. The standardized orientation is especially important for avoiding parallax problems. A set of three images was taken at different focal lengths for each specimen in each of the character sets. All images were taken with a Leica M165C stereomicroscope equipped with a Leica DFC425 camera and using the integrated software Leica Application Suite 1.1.1 ("LAS") that recorded magnification and scaling information for measurements. LAS metadata XML files containing precise magnification were used for scaling of images but a slide with a scale ruler in 0.01 mm increments could also be used without an integrated camera and software package.

Characters

Carapace in dorsal view: The specimen was placed in dorsal view so that it was balanced laterally with the top of the carapace in equal focus on its lateral sides and balanced longitudinally with the two transverse furrows in equal focus (Fig. 2.3). At the anterior edge, two lateral landmarks were placed at the base of the outer anterior edge setae, and one at the median line of the carapace and anterior edge. Six landmarks were associated with the two transverse furrows: at the anterior furrow, one at each lateral edge in alignment with the anterior furrow and one at the medial line; at the posterior furrow, one at each lateral edge and one at the medial line. Three landmarks were at the posterior edge of the carapace: two at the posterolateral points and one at the medial line. Descriptions of landmarks are in Tab. 2.1, a landmark guide is provided in Fig. 2.3, and an example of landmarks placed on a specimen is in Fig. 2.9a. Images were taken at 63X magnification for optimal viewing and placing of landmarks.

Leg IV femur and patella in prolateral view: The fourth walking leg (leg IV) femur and patella are fused in chernetids, with a visible suture line diving the greatly reduced, triangular femur from the comparatively elongate, trapezoidal patella. Some authors refer to the femur as femur I or basofemur and to the patella as femur II or telofemur (e.g., Chamberlin 1931, Hoff 1949, Muchmore 1990). From a prolateral view, that is, the anterior face of the leg when it is oriented perpendicular to the longitudinal axis of the body, the femur and patella lie more in a flattened straight line than in a retrolateral view (the posterior face of the leg), making the prolateral view easier to work with in two dimensions and standardize specimen placement for imaging to consistently place 2D landmarks. The dissected right leg IV was placed in prolateral view along its proximal-distal axis, so that the segment joints between the trochanter and femur and the patella and tibia were simultaneously in focus, and the retrolateral side was not visible (Fig. 2.4). Descriptions of landmarks are in Tab. 2.2, a landmark guide is provided in Fig. 2.4, and an example of landmarks placed on a specimen is in Fig. 2.9b. Images were taken at 80X magnification for optimal viewing and placing of landmarks.

Pedipalp chela in dorsal view: The dissected right pedipalp was placed in dorsal view such that it was balanced on its proximal-distal axis, with the fixed finger in focus along its entire length, the lateral edges of the fixed finger not visible, and the pedestal and base of the fixed finger in approximately equal focus (Fig. 2.5). Descriptions of landmarks are in Tab. 2.3a, a landmark guide is provided in Fig. 2.5, and an example of landmarks placed on a specimen is in Fig. 2.10a. Images were taken at 80X magnification for optimal viewing and placing of landmarks.

Pedipalp chela in retrolateral view: The dissected right pedipalp was placed in retrolateral view along its proximal-distal axis, with the joint between the fixed finger and movable finger in focus, and oriented so that this suture was perpendicular to the proximal-distal axis (Fig. 2.6). Retrolateral refers to the posterior face of an appendage when it is oriented perpendicular to the longitudinal axis of the body. Descriptions of landmarks are in Tab. 2.3b, a landmark guide is provided in Fig. 2.6, and an example of landmarks placed

on a specimen is in Fig. 2.10b. Images were taken at 80X magnification for optimal viewing and placing of landmarks.

Pedipalp fixed finger in retrolateral view: The dissected right pedipalp was placed in retrolateral view along its proximal-distal axis, such that the fixed finger trichobothria *esb* and *est* were in sharp focus (Fig. 2.7). Descriptions of landmarks are in Tab. 2.4a, a landmark guide is provided in Fig. 2.7, and an example of landmarks placed on a specimen is in Fig. 2.11a. Images were taken at 100X magnification for optimal viewing and placing of landmarks.

Pedipalp movable finger in retrolateral view: The dissected right pedipalp was placed in retrolateral view along its proximal-distal axis, such that the movable finger trichobothria *b* and *st* were in sharp focus (Fig. 2.8). Descriptions of landmarks are in Tab. 2.4b, a landmark guide is provided in Fig. 2.8, and an example of landmarks placed on a specimen is in Fig. 2.11b. Images were taken at 100X magnification for optimal viewing and placing of landmarks.

Image preparation and landmarking

The three images taken of each specimen in each of the six character sets were focal-stacked in ZereneStacker. This reduced the depth of field issue with these small, three-dimensional organisms such that all relevant features for marking landmarks were equally visible and in focus in a single composite image. Leica Application Suite (LAS) creates multiple files with each image taken with the integrated Leica DFC425 camera mounted on a Leica microscope; only the metadata XML file containing scale and magnification information was retained from each specimen character set. With the total pixel and mm per pixel scale information from the XML metadata files, mm / pixel was calculated in a spreadsheet for use in the Scale tab of StereoMorph. Alternatively, without an integrated camera it is possible to calculate mm / pixel with a scale slide having 0.01 mm increments on its ruler with the relevant pseudoscorpion character in the image frame at each magnification used.

In R 4.0.5 (R Core Team 2021), the function digitizeImages from the package StereoMorph (Olsen and Westneat 2015) was used to assign landmarks for each character on the stacked image of each of the 40 specimens in a graphical interface (Fig. 2.12). Landmark guides for each character are illustrated in Figs. 2.3-2.8 and are provided as reference landmarks for future studies; examples of landmarks placed in StereoMorph are in Figs. 2.9-2.11. Images were precisely scaled to within 0.001 mm through utilizing the tag XMetresPerPixel in the XML metadata files created by LAS. Following user input of scaling information (Fig. 2.13) and landmark assignment (Fig. 2.12) in the StereoMorph user interface, a text shape file (suffix ".shp") was generated for each specimen. Shape files were then concatenated and converted into a single text TPS file with the function writeLMtoTPS in StereoMorph.

Preliminary analysis steps

A classifier file consisting of a spreadsheet formatted as text CSV was created, with the first row the header, the first column an identifier code for each specimen for that character, and the second column the sex of that individual. The TPS file and the classifier file for each character were then used as input to the Java-based software package MorphoJ (Klingenberg 2011; available at https://morphometrics.uk/MorphoJ_page.html). The classifier file was imported through 'File > Import Classifier Variables' with default options; the TPS file was imported through 'File > Create Dataset'. To solely analyze shape, a Generalized Procrustes Analysis (GPA) was first run through 'Preliminaries > New Procrustes Fit', selecting the default option to align by principal axes. This generated a textual report file with GPA coordinates of the 40 observations and a graphic representation of the mean values for each landmark. By selecting 'Preliminaries > Create or Edit Wireframe' a wireframe was then created by linking landmarks along the outer edges, and also transversely for wireframes of the carapace transverse furrows, the leg IV suture between femur and patella, and the trichobothria of both pedipalp fingers. A covariance matrix required for ordination analysis was then generated through 'Preliminaries > Generate covariance matrix', selecting the dataset and pooled within-group covariance by sex (the group of interest in this case). Inputs for all subsequent analyses in MorphoJ consisted of the classifier file, GPA coordinates, and the covariance matrix.

Multivariate analysis of shape on GPA coordinates

Five analyses were run for each morphological character of pseudoscorpions examined. First, a Principal Components Analysis (PCA) was done through 'Variation > Principal Components Analysis', with graphical options selected to include 90% confidence ellipses grouped by the classifier sex. Second, a Procrustes ANOVA was run through 'Variation > Procrustes ANOVA', with sex used as the main effect and no additional main effects. Third, a regression analysis was run through 'Regression analysis' with Procrustes coordinates as the dependent variable and PC1 as the independent variable, and with a permutation test of 10000 iterations. Fourth, a Canonical Variate Analysis (CVA) was selected through 'Comparison > Canonical Variate Analysis', with the classifier variable sex chosen for grouping, and 10000 iterations selected for the permutation test for pairwise distances. Fifth, a Discriminant Function Analysis (DFA) was run through 'Comparison > Discriminant Function Analysis', with the classifier category sex comparing females and males, and with a permutation test of 10000 runs. All images generated in the 'Graphics' tab as image files and all text-based results in the 'Results' tab were exported as a text file.

Results

Carapace in dorsal view

Carapace in dorsal view had 12 landmarks from each specimen input into the GPA (Fig. 2.14a). In the PCA, PC1 explained 35.1% of the variance, PC2 14.5%, PC3 12.4%, and PCs 4-20 explained the remainder of the variance. In the PCA lollipop graphic (Fig. 2.14b), most shape changes in PC1 occurred at the landmarks 7,9,10,12, representing the lateral edges of the posterior furrow and the lateral edges of the posterior carapace; and then in 1,2,3,11, representing the anterior and posterior longitudinal length of the carapace. The plotted shape of the variance extremes in the wireframe graph inserts showed how the carapace shifted from more elongate and narrow to a more posteriorly widened shape. In the PCA scatterplot (Fig. 2.14c), females were more variable and males formed a tighter cluster.

In the Procrustes ANOVA, centroid size differed significantly between groups (individual df=1, F=38.14, P<0.001), as did shape (individual df=20, F=4.37, P<0.0001). In the regression analysis with Procrustes coordinates as the dependent variable and PC1 scores as the independent variable, some separation of females from males was evident, with males tending to cluster toward the origin and females away from the origin. The regression predicted 38% of sums of squares, and the permutation test returned a significant difference against the null hypothesis of independence (p<0.0001).

In the CVA, most variation in the CVA lollipop graph (Fig. 2.14d) occurred in landmarks 10,12, corresponding to the posterolateral edges of the carapace. This corresponded in the wireframe graph to a shape change between narrower and more posteriorly-widened shapes. In the histogram of CV1 values (Fig. 2.14e) females and males separated very strongly and without overlap.
In the DFA lollipop graph, most change occurred in landmarks 10,12 (Fig. 2.14f), corresponding to the posterolateral edges of the carapace. Shape changes in the wireframe graph corresponded to a slightly narrower vs. more posteriorly-widened shape. Females and males separated very strongly in the histogram of discriminant scores (Fig. 2.14g), and also strongly separated in the cross-validation scores, but with some overlap in the center only. The means of groups were significantly different (p<0.0001).

Leg IV femur and patella in prolateral view

Leg IV femur and patella in prolateral view had nine landmarks from each specimen input into the GPA (Fig. 2.15a). In the PCA, PC1 explained 30.4% of the variance, PC2 26.1%, PC3 21.1%, and PCs 4-14 explained the remainder of the variance. In the PCA scatterplot (Fig. 2.15b), males and females noticeably separated on PC1, with males tending to more negative and females more positive values. In the PCA lollipop graphic of PC1 (Fig. 2.15c) most shape changes occurred at landmarks one, three, and four, representing the basodorsal point of the femur and the dorsal and ventral points of the femur-patella suture. These landmark shifts corresponded to shape change between the variance extremes in the wireframe graph showing that the femur oscillated between a more stretched and elongate form to a more compact and robust shape.

In the Procrustes ANOVA, centroid size differed significantly between groups (individual $F=34.84$, $P<0.0001$, $df=1$), as did shape (individual $F=9.19$, $p<0.0001$, $df=8$). The regression analysis returned a linear plot of Regression1 vs. PC1, with sexes separating considerably, with males closer to the origin and female further from the origin.

In the CVA of CV1 (Fig. 2.15d) most variation between females and males centered on landmark 6, corresponding to the ventral point of the femur-patella suture, with a lesser amount of variation between the sexes in landmarks one and three, corresponding to the basoventral suture point with the trochanter and the distodorsal suture with the patella, respectively. Females and males separated strongly in the histogram of CV1 vs. Frequency (Fig. 2.15e).

The DFA lollipop graphic (Fig. 2.15f) showed the most variation in landmarks 6, corresponding to the ventral point of the femur-patella suture. A small amount of variation was also seen in landmark one, the ventral point of the trochanter-femur suture. Shape changes in the wireframe graph illustrated a change in the overall depth of the femur-patella, with a ventral bend occurring between females and males at the ventral point of the femur-patella suture. Females and males separated completely in the histogram of discriminant scores (Fig. 2.15g) with no overlap; in the cross-validation there was little overlap at the center. The means of groups were significantly different ($p<0.0001$).

Pedipalp chela in dorsal view

The pedipalp chela in dorsal view had nine landmarks from each specimen input into the GPA (Fig. 2.16a). In the PCA, PC1 explained 25.1% of the variance, PC2 18.6%, PC3 16.4%, and PCs 4-14 explained the remainder of the variance. In the PCA lollipop graphic (Fig. 2.5b), most shape changes in PC1 occurred at the landmarks one, two, and nine representing the tip and lateral basal edges of the fixed finger; and then in landmarks three and nine, representing the width and orientation of the widest point of the chela hand. The plotted shape of the variance extremes in the wireframe graph inserts showed how the pedipalp shifted from a more elongate and straightened shape of the finger to a more thickened chela hand and more curved finger. In the scatterplot (Fig. 2.16c), females and males had points mostly overlapping on both axes with some separation on PC1.

In the Procrustes ANOVA, centroid size differed significantly between groups (individual df=1, F=9.12, P=0.0045), as did shape (individual df=14, F=8.37, P<0.0001). In the regression analysis with Procrustes coordinates as the dependent variable and PC1 scores as the independent variable, a distinct separation of females from males was evident, with males tending to cluster toward the origin and females away from the origin. The regression predicted 33% of sums of squares, and the permutation test returned a significant difference against the null hypothesis of independence (p<0.0001).

In the CVA lollipop graph (Fig. 2.16d), most variation occurred in landmarks one, three, eight, and nine, corresponding to the tip of the fixed finger and lateral edge and the chela hand retrolateral widest point. In the wireframe graph this corresponded to a shape change between a more straightened fixed finger and narrow chela hand and a more prolaterally curved finger and thickened chela hand. Females and males separated strongly in the histogram of CV1 (Fig. 2.16e), with some central overlap.

In the DFA lollipop graph (Fig. 2.16f) most of the variation occurred in landmarks 1,3,9, corresponding to the tip of the fixed finger and lateral edge and the chela hand retrolateral widest point. In the wireframe graph this corresponded to a shape change between a slightly more straightened fixed finger and narrow chela hand and a slightly more prolaterally curved finger and thickened chela hand. Females and males separated strongly in the histogram of discriminant scores (Fig. 2.16g), with some central overlap, and separated but less strongly in the cross-validation scores. The means of groups were significantly different (p=0.0002).

Pedipalp chela in retrolateral view

The pedipalp chela in retrolateral view had 17 landmarks from each specimen input into the GPA (Fig. 2.17a). In the PCA, PC1 explained 24.2% of the variance, PC2 explained 15.5% of the variance, PC3 explained 12.7% of the variance, and PCs 4-30 explained the remainder of the variance. In the PCA lollipop graph (Fig. 2.17b) most shape changes in PC1 occurred in landmarks three, seven, eight, ten, 11, and 12, which altogether described a change in curvature of the pedipalp fingers; and in landmarks four and five, which affected the placement of the basal external

trichobothria. The plotted shape of the variance extremes in the wireframe graph inserts showed how the pedipalp chela in retrolateral view varied between a narrower hand and dorsally curved finger and thicker hand and straight finger. In the PCA scatterplot (Fig. 2.17c), sexes differed most strongly along PC2, with PC1 showing more extremes of females. Correspondingly, the wireframe graph for PC2 showed the most extremes of variance between a thicker hand and more straight but slightly dorsally curved finger and a thinner hand with a more dorsally curved finger. Differences in the shape of the curvature of the finger showed in both its outline and in the fixed finger external trichobothria.

In the Procrustes ANOVA, groups differed by centroid size (individual $F=8.08$, $p=0.007$, $df=1$) and shape (individual $F=6.26$, $p<0.0001$, $df=30$). The regression analysis returned a linear plot of Regression1 vs. PC1, with considerable overlap between groups. A second regression analysis plotting Regression Score1 vs. PC2 resulted in a wider and less straight line, more separation of the groups, with males tending to cluster away from the origin while females were throughout the scatterplot.

In the CVA very little variation is evident in the CVA lollipop graph (Fig. 2.17d); in the wireframe, an extreme of variance is shown between females and males in a slightly narrower and shorter hand and a slightly shorter finger, with some evidence of a difference in curvature of the finger showing mostly in the trichobothria. In the CVA histogram (Fig. 2.17e) females and males separated very strongly and without any overlap.

In the DFA lollipop graph (Fig. 2.17f) most variation occurred in landmarks 13, the basal juncture of the movable finger and ventral chela hand; and landmarks five and six, which corresponded to trichobothria *esb* and *est*. In the wireframe graph this corresponded to a shape change between a slightly more straightened fixed finger and narrow chela hand and a slightly more prolaterally curved finger and thickened chela hand. Females and males separated strongly in the histogram of discriminant scores (Fig. 2.17g) with some central overlap, and separated strongly in the cross-validation scores and with minimal central overlap. The means of groups were significantly different ($p<0.0001$).

Pedipalp fixed finger in retrolateral view

The pedipalp fixed finger in retrolateral view had nine landmarks from each specimen input into the GPA (Fig. 2.18a). In the PCA, PC1 explained 42.7% of the variance, PC2 26.7%, PC3 15.4%, and PCs 4-14 explained the remainder of the variance. In the PCA lollipop graph (Fig. 2.18b), most shape changes in PC1 occurred at landmark three, representing the proximal-distal placement of trichobothria *est*; in landmarks six and seven, representing the proximal-distal variation in the midpoint of the length of the finger along the marginal teeth; and landmarks eight and nine, representing the width of the finger at the basal origin of the marginal teeth. The plotted shape of the variance extremes in the wireframe graph showed how the pedipalp fixed finger shifted from curving ventrally or being more straightened, which approximated differences seen in dorsal view corresponding to a prolateral curve of the fingers. In the PCA scatterplot (Fig. 2.18c), males tended to a more central value while females tended more to extremes.

In the Procrustes ANOVA, centroid size did not differ significantly between groups (individual $F=0.78$, $P=0.382$, $df=1$), while shape did differ significantly (individual $F=2.59$, $p=0.0012$, $df=14$). The regression analysis returned a linear plot of Regression1 vs. PC1, with no clear separation on the graph between females and males, and males tending to cluster to more central values.

The CVA lollipop graphic (Fig. 2.18d) recovered the most variation in landmarks one, three, and four, corresponding to the centroid positions of *eb*, *est*, and *et*, affecting the distance between these trichobothria; and the ventral-dorsal position of the venedens, which reflected the degree of prolateral curvature as seen in dorsal view of the fingers. Females and males separated strongly in the histogram of CV1 vs. Frequency (Fig. 2.18e).

The DFA lollipop graphic (Fig. 2.18f) showed the most variation in landmarks one and three, corresponding to the trichobothria *eb* and *est*. Shape changes seen in the wireframe graph did not affect the overall shape of the finger, instead only affecting slight differences in the relative positioning of these trichobothria. Females and males separated in the histogram of discriminant scores (Fig. 2.18g) with little overlap in the middle and separated clearly if less strongly with some degree of overlap in the cross-validation histogram. The means of groups were significantly different ($p<0.0001$).

Pedipalp movable finger in retrolateral view

The pedipalp movable finger in retrolateral view had nine landmarks from each specimen input into the GPA (Fig. 2.19a). In the PCA, PC1 explained 55.3% of the variance, PC2 20.6%, PC3 8.7%, and PCs 4-14 explained the remainder of the variance. In the PCA scatterplot (Fig. 2.19b), males tended to a more central value on PC2 while females tended to more variable. The PCA lollipop graph of PC1 (Fig. 2.19c) indicated that most shape changes in this principal component occurred at the landmarks two and three, representing the proximal-distal placement of the center of trichobothria *esb* and *est*; and in landmarks six, seven, eight, and nine, representing the proximal-distal variation in the placement of the basal and midpoints of the finger on the dorsal and ventral sides. The shape of variance extremes in the corresponded to the movable finger shifting from curving ventrally to being more straightened; this is correlated with the differences seen in dorsal view that corresponded to a prolateral curve of the finger.

In the Procrustes ANOVA, centroid size did not differ significantly between groups (individual $F=0.01$, $P=0.90$, $df=1$), while shape did differ significantly (individual $F=4.65$, $p<0.0001$, $df=14$). The regression analysis returned a linear plot of Regression1 vs. PC1, with sexes overlapping considerably, with two outlier males closer to the origin and an outlier female far from the origin.

The CVA lollipop graphic of CV1 (Fig. 2.19d) showed subequal variation in all landmarks except the placement of the venedens and trichobothria *eb*. Females and males separated strongly in the histogram of CV1 vs. Frequency (Fig. 2.19e).

The DFA lollipop graphic (Fig. 2.19f) showed the most variation in landmarks two, three, and four, corresponding to trichobothria *esb*, *est*, *et*; and some variation in landmarks six and seven, corresponding to the midpoint of the length of the finger on the dorsal and ventral sides. The landmark shifts corresponded to shape changes in the wireframe graph that did not affect the overall shape of the finger, rather only slightly affecting differences in the relative positioning of these trichobothria. Females and males separated in the histogram of discriminant scores (Fig. 2.19g) with little overlap in the middle but separated less strongly with considerable overlap in the cross-validation histogram. The means of groups were significantly different ($p=0.0002$).

Discussion

In each of the six characters investigated evidence was recovered for significant sexual dimorphism in the results of PCAs, Procrustes ANOVAs, CVAs, and DFAs (Figs. 2.4-8). The characters mostly strongly separating males and females in the DFAs were carapace, pedipalp chela in retrolateral view, and leg IV femur and patella in prolateral view. The six characters investigated are located at different regions of the body, which is highly useful in situations where some characters are unavailable. This may happen in the process of collection, dissection, or mounting on a permanent slide. Characters with more landmarks did not necessarily perform better than those with fewer landmarks, although the pedipalp chela in retrolateral view with 17 landmarks was by far the best at discriminating sexes. It is also remarkable that relatively small characters on the body such as the pedipalp movable finger with only nine landmarks were useful for discriminating sexual dimorphism.

The principal advantage of 2D geometric morphometrics is that it may be done with tools already at hand by the average pseudoscorpion researcher: a microscope, a camera, and a dish for placing specimen. Provided characters examined maintain a consistent standardized view, this method may also be used with drawings of types and redescriptions of species found in literature or of slide-mounted specimens. Although we used a camera integrated and manufactured by Leica, less expensive cameras capable of high-resolution images are now available by other manufacturers. These may be used in an optic tube of a trinocular microscope or by utilizing one of the eyepieces in a binocular stereomicroscope setup.

For landmarking and inputting scale of images we used the digitizeImages function in StereoMorph for its ease of use in landmarking and inputting scale for each image. However, alternative methods exist should it cease to be developed or distributed, such as the older program tps2dig2 (Rohlf 2010) or the R package geomorph function digitize2D (Adams and Otárola-Castillo 2013). Automated methods using neural networks are being developed, particularly for 3D landmarking, but acquiring 3D landmarks and the processing power needed for them preclude researchers without access to these computing resources. Although only fixed landmarks of homologous points were used in this study, both curves and sliding semilandmarks are alternative

means of exploring shape analysis in pseudoscorpions. We did not incorporate curves in this study for the sake of simplicity as MorphoJ does not have this functionality.

In our case we took scale date from Leica Application Suite metadata XML files, but alternatively this could have been achieved with a combination of a micrometer eyepiece and a ruler slide with millimeter marks, or through magnification metadata generated by alternative integrated microscope imaging software. Regardless of the methods used, landmark and scale data are required for each image in a geometric morphometrics analysis of any character assessed to address a question on pseudoscorpion morphology.

All post-landmarking analyses were done in the freely available software MorphoJ. MorphoJ is an operating system-agnostic, Java-based graphical interface of code that may also be used directly in the R package Morpho. Alternatively, GPA and PCA (and 3D geometric morphometrics, amongst other functions) may be done in the R package geomorph (Adams and Otárola-Castillo 2013). However, CVA and DFA are not presently available in geomorph. Visualizations of geomorph results may be implemented with the R package ggplot2 (Wickham et al. 2019).

Landmarking in 3D is becoming increasingly common with technological advances and increases in access to technology such as microCT. For analysis of 3D data generated from microCT data of pseudoscorpions the software SlicerMorph (Rolfe et al. 2020) could be used for landmarking and analysis. Genitalic structures in pseudoscorpions are both internal and three-dimensional. A particularly exciting avenue of further exploration of geometric morphometric applications to pseudoscorpions would be with microCT to examine these complex internal structures that are generally ignored by taxonomists when describing new species.

Literature Cited

Adams DC, Otárola-Castillo E (2013) geomorph: an R package for the collection and analysis of geometric morphometric shape data. Paradis E (Ed.). Methods in Ecology and Evolution 4: 393–399. https://doi.org/10.1111/2041-210X.12035

Adams DC, Rohlf FJ, Slice DE (2013) A field comes of age: geometric morphometrics in the 21st century. Hystrix, the Italian Journal of Mammalogy 24: 7–14.

Armbruster JW, Stout CC, Hayes MM (2016) An empirical test for convergence and social mimicry using African Barbs (Cypriniformes: Cyprinidae). Evolutionary Ecology 30: 435–450.

Bookstein FL (1991) Morphometric tools for landmark data: geometry and biology. Cambridge University Press, New York, New York, United States, 456 pp.

Burress PBH, Burress ED, Armbruster JW (2017) Body shape variation within the Southern Cavefish, *Typhlichthys subterraneus* (Percopsiformes: Amblyopsidae). Zoomorphology 136: 365–377. https://doi.org/10.1007/s00435-017-0360-0

Chamberlin JC (1931) The arachnid order Chelonethida. Stanford University Publications, Biological Sciences 7: 1–284.

Christophoryová J, Krajčovičová K, Henderickx H, Španiel S (2016) A multivariate study of differentiating characters between three European species of the genus *Lasiochernes* Beier, 1932 (Pseudoscorpiones, Chernetidae). ZooKeys 629: 51–81. https://doi.org/10.3897/zookeys.629.8445

Harvey M (1987) A revision of the genus *Synsphyronus* Chamberlin (Garypidae : Pseudoscorpionida : Arachnida). Australian Journal of Zoology Supplementary Series 35: 1. https://doi.org/10.1071/AJZS126

Harvey MS (1985) The systematics of the family Sternophoridae (Pseudoscorpionida). Journal of Arachnology 13: 141–209.

Hoff CC (1949) The pseudoscorpions of Illinois. State of Illinois Department of Registration and Education Natural History Survey Division Bulletin 24: 411–499.

Karanovic T, Djurakic M, Eberhard SM (2016) Cryptic species or inadequate taxonomy? Implementation of 2D geometric morphometrics based on integumental organs as landmarks for delimitation and description of copepod taxa. Systematic Biology 65: 304–327. https://doi.org/10.1093/sysbio/syv088

Klingenberg CP (2011) MorphoJ: an integrated software package for geometric morphometrics: COMPUTER PROGRAM NOTE. Molecular Ecology Resources 11: 353–357. https://doi.org/10.1111/j.1755-0998.2010.02924.x

Muchmore WB (1990) Pseudoscorpionida. In: Dindal DL (Ed.), Soil Biology Guide. John Wiley and Sons, New York, New York, United States, 503–527.

Muster C, Schmarda T, Blick T (2004) Vicariance in a cryptic species pair of European pseudoscorpions (Arachnida, Pseudoscorpiones, Chthoniidae). Zoologischer Anzeiger 242: 299–311. https://doi.org/10.1078/0044-5231-00106

Olsen A, Westneat MW (2015) StereoMorph: an R package for the collection of 3D landmarks and curves using a stereo camera set-up. Methods in Ecology and Evolution 6: 351–356. https://doi.org/10.1111/2041-210X.12326

R Core Team (2021) R: a language and environment for statistical computing. R Foundation for Statistical Computing, Vienna, Austria. Available from: https://www.R-project.org.

Rohlf FJ (2010) tpsDig2 version 2.16. Department of Ecology and Evolution, State University of New York, Stony Brook.

Rolfe S, Pieper S, Porto A, Diamond K, Winchester J, Shan S, Kirveslahti H, Boyer D, Summers A, Maga AM (2020) SlicerMorph: an open and extensible platform to retrieve, visualize and analyze 3D morphology. bioRxiv: 2020.11.09.374926. https://doi.org/10.1101/2020.11.09.374926

Wickham H, Chang W, Henry L, Pedersen TL, Takahashi K, Wilke C, Woo K, Yutani H, RStudio (2019) ggplot2: Create elegant data visualisations using the grammar of graphics. Available from: https://cran.r-project.org/package=ggplot2.

Zeh DW (1987) Aggression, density, and sexual dimorphism in chernetid pseudoscorpions (Arachnida: Pseudoscorpionida). Evolution 41: 1072–1087.

Fig. 2.1. *Hesperochernes mirabilis*. Dorsal habitus of (a) female (specimen CS98.1, accessioned at AUMNH); (b) male (specimen CS48.1, accessioned at AUMNH).

a.

b.

Fig. 2.2. Location of Oaks Cave, Tennessee, USA. Grey areas denote karstic regions.

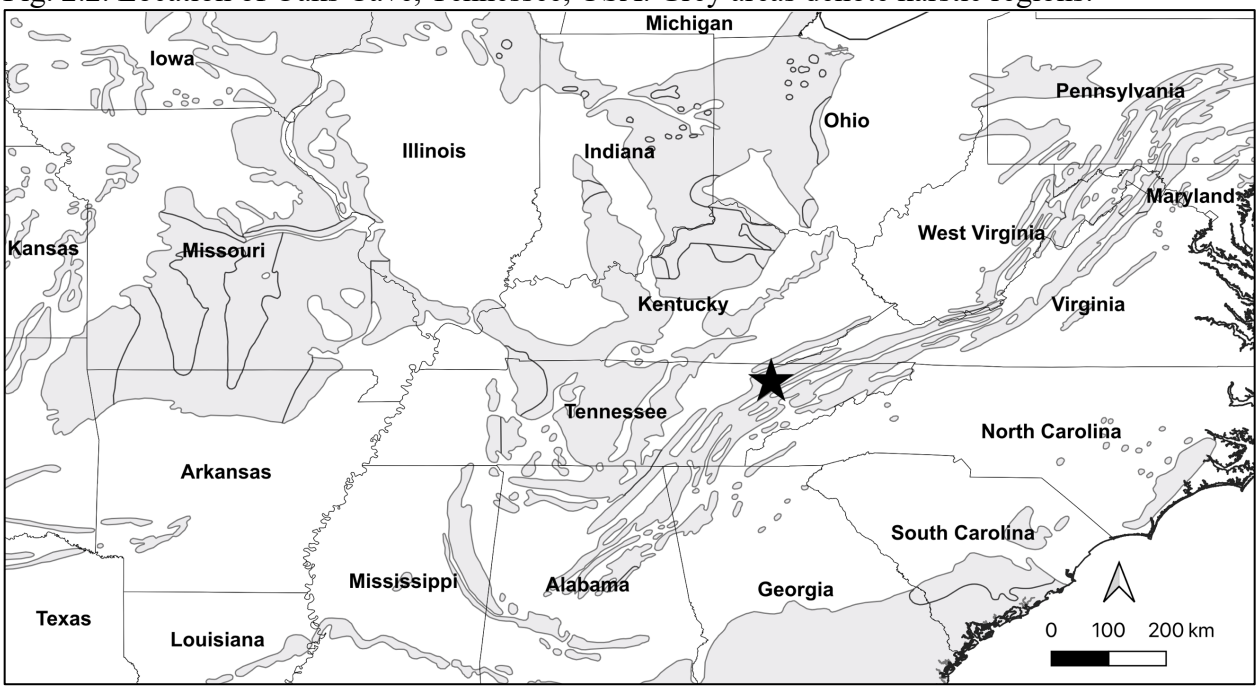

Fig. 2.3. Landmark guide for carapace in dorsal view. Specimen must be level in substrate immersed in ethanol, such that both furrows are in are in focus. Specimen may also be mounted on a slide. Description of each landmark given in Table 1.

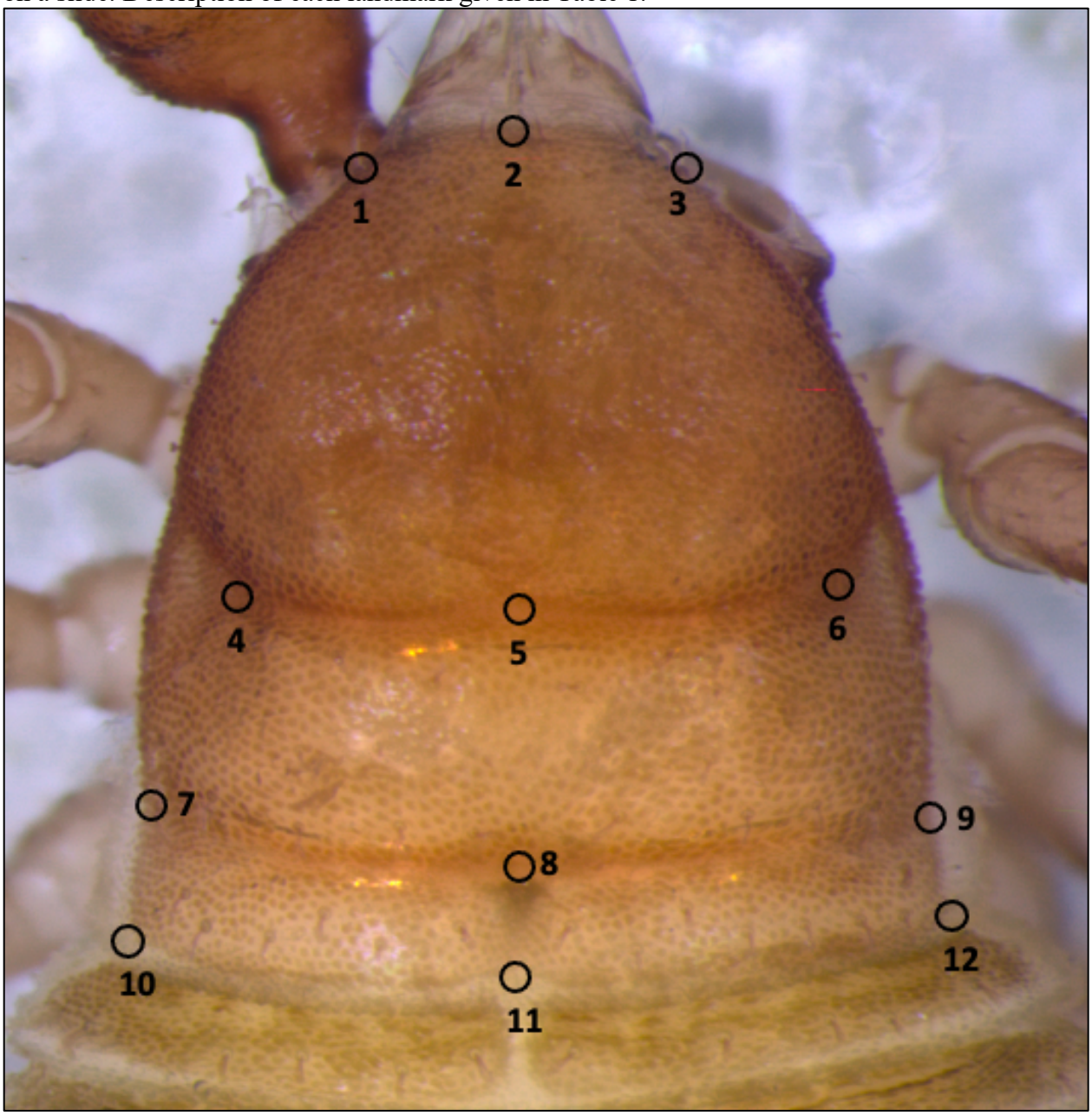

Fig. 2.4. Landmark guide for leg IV femur and tibia in prolateral view. Right leg IV illustrated. Specimen must be level in substrate immersed in ethanol, such that the basal and distal parts of the anterior and posterior parts of the tibia (landmarks 3, 4, 5, 6, respectively) are equally in focus. This view may also be achieved in a temporary slide with wire propping up the slide coverslip, and may also be found in specimens mounted on a permanent slide. Description of each landmark given in Table 1.

Fig. 2.5. Landmark guide for pedipalp chela in dorsal view. Right pedipalp illustrated. Specimen must be level in substrate immersed in ethanol, such that the basal part of the fixed finger and the distal part of the chela pedestal are equally in focus. This view is difficult to achieve on a temporary slide with wire propping up the slide coverslip, and the specimen will likely be crushed and landmarks distorted if the specimen has been mounted in a permanent slide. Description of each landmark given in Table 1.

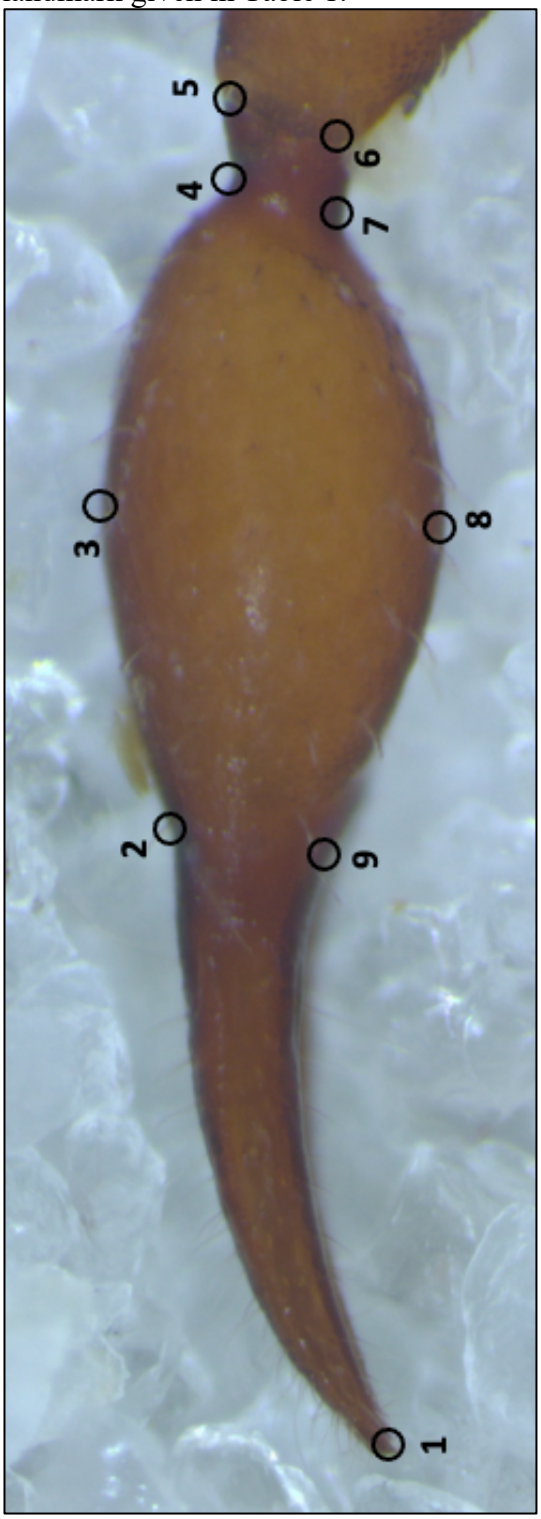

Fig. 2.6. Landmark guide for pedipalp chela in retrolateral view. Right pedipalp illustrated. Specimen must be level in substrate immersed in ethanol, such that the basal part of the fixed finger, basal attachment condyle of the movable finger, narrowest points of the chela pedestal (landmarks 11, 13, 2, and 15, respectively) are equally in focus. This view may also be achieved in a temporary slide with wire propping up the slide coverslip, and may also be found in specimens mounted on a permanent slide. Description of each landmark given in Table 1.

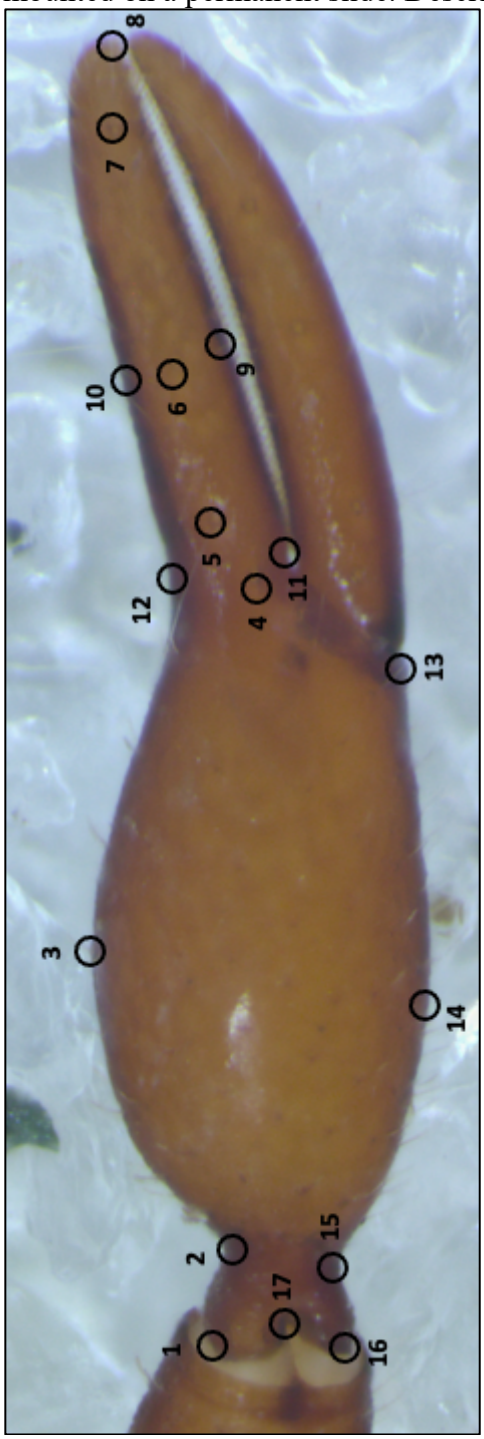

Fig. 2.7. Landmark guide for pedipalp fixed finger in retrolateral view. Right pedipalp illustrated. Specimen must be level in substrate immersed in ethanol, such that the basal part of the fixed finger and trichobothrium *est* (landmarks 8, 9, and 3, respectively) are equally in focus. This view may also be achieved in a temporary slide with wire propping up the slide coverslip, and may also be found in specimens mounted on a permanent slide. Description of each landmark given in Table 1.

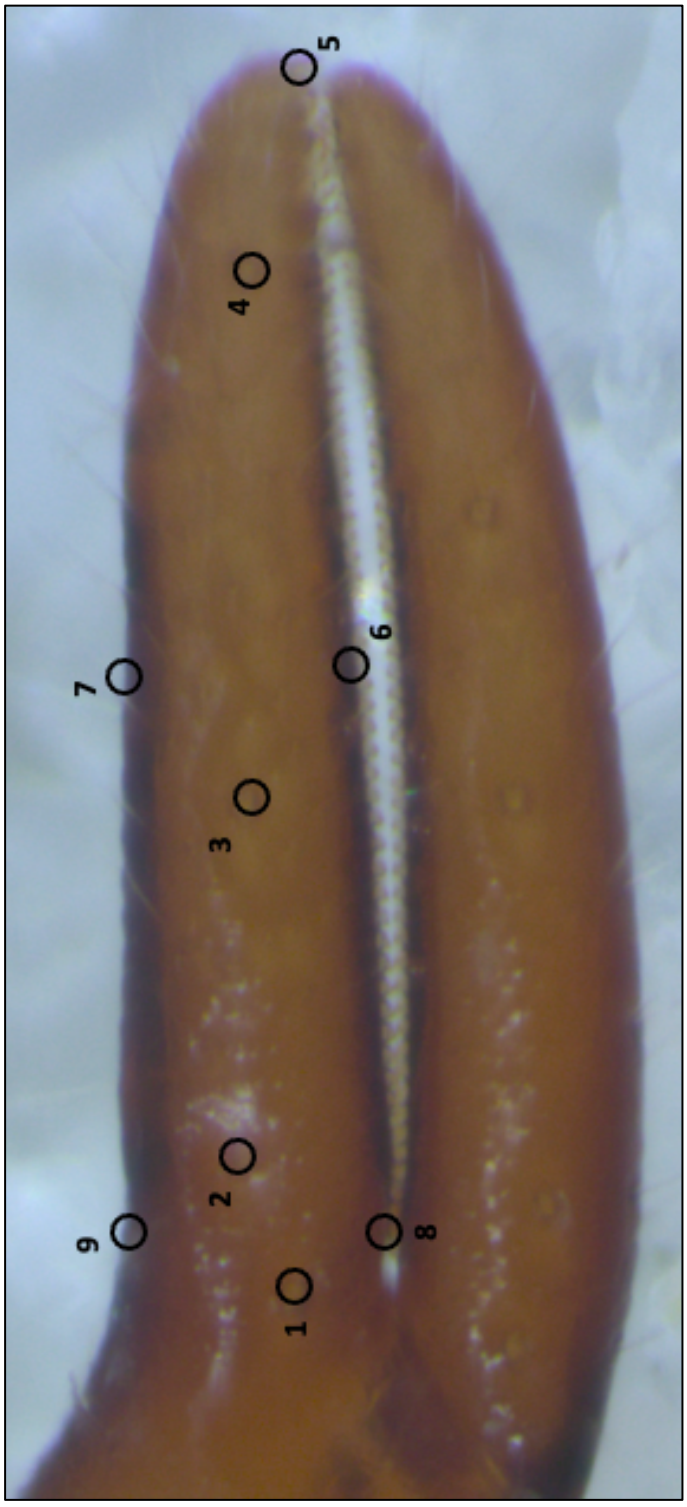

Fig. 2.8. Landmark guide for pedipalp movable finger in retrolateral view. Right pedipalp illustrated. Specimen must be level in substrate immersed in ethanol, such that the trichobothriia *sb* and *t* (landmarks 2 and 4, respectively) are equally in focus. This view may also be achieved in a temporary slide with wire propping up the slide coverslip, and may also be found in specimens mounted on a permanent slide. Description of each landmark given in Table 1.

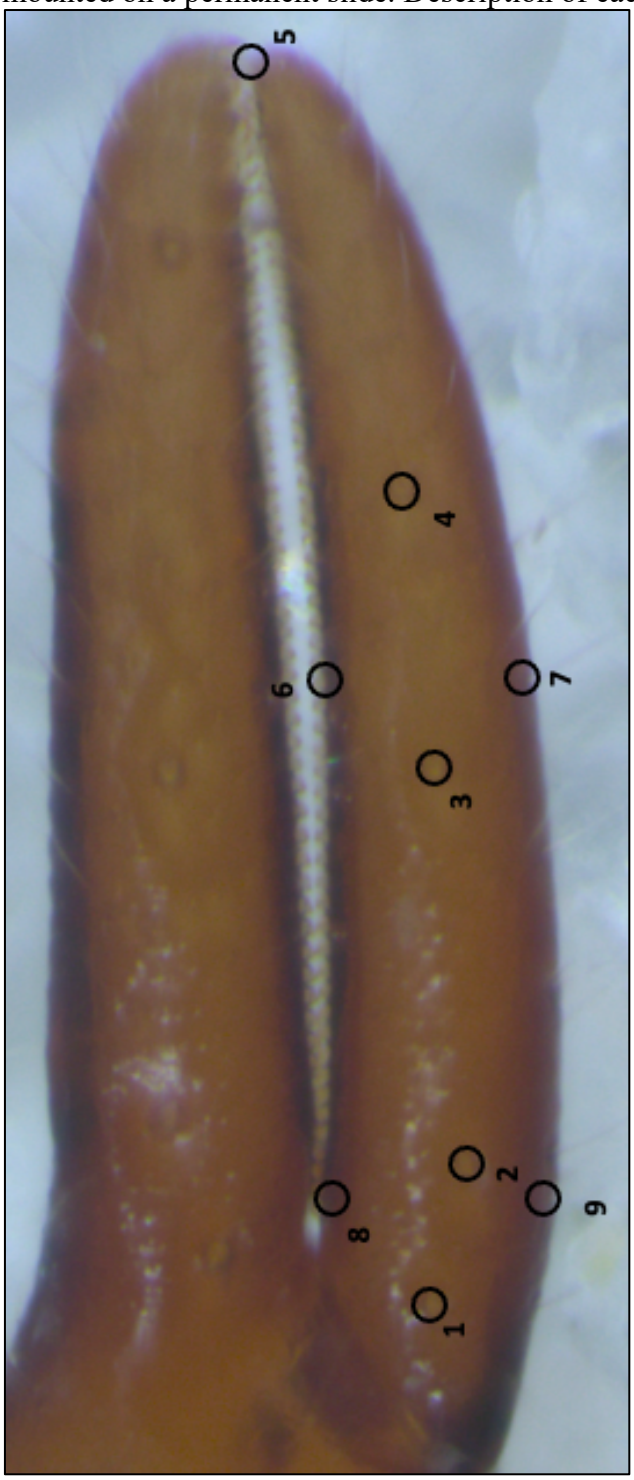

Fig. 2.9. Examples of placed landmarks on carapace and legs: (a) carapace in dorsal view; (b) leg IV femur and patella in prolateral view. Specimens of *H. mirabilis* with landmarks placed as they appear in StereoMorph. Points placed outside of each character for measuring scale. Descriptions of these landmarks are in Tab. 2.1 and Tab. 2.2 for carapace and leg IV femur and patella, respectively.

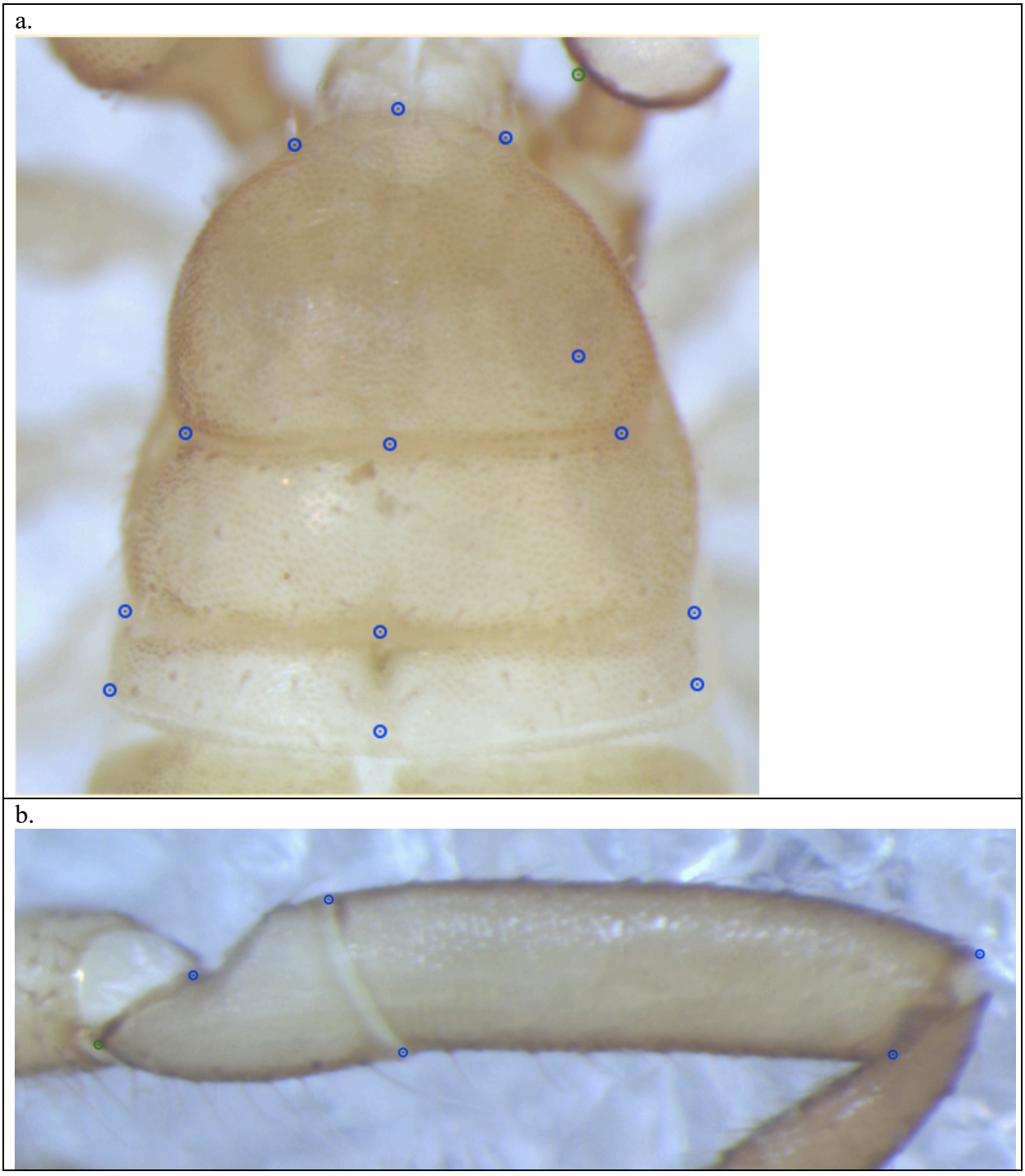

Fig. 2.10. Examples of placed landmarks on pedipalp chela: (a) right pedipalp chela in dorsal view; (b) right pedipal chela in retrolateral view. Specimens of *H. mirabilis* with landmarks placed as they appear in StereoMorph. Points placed outside of each character for measuring scale.

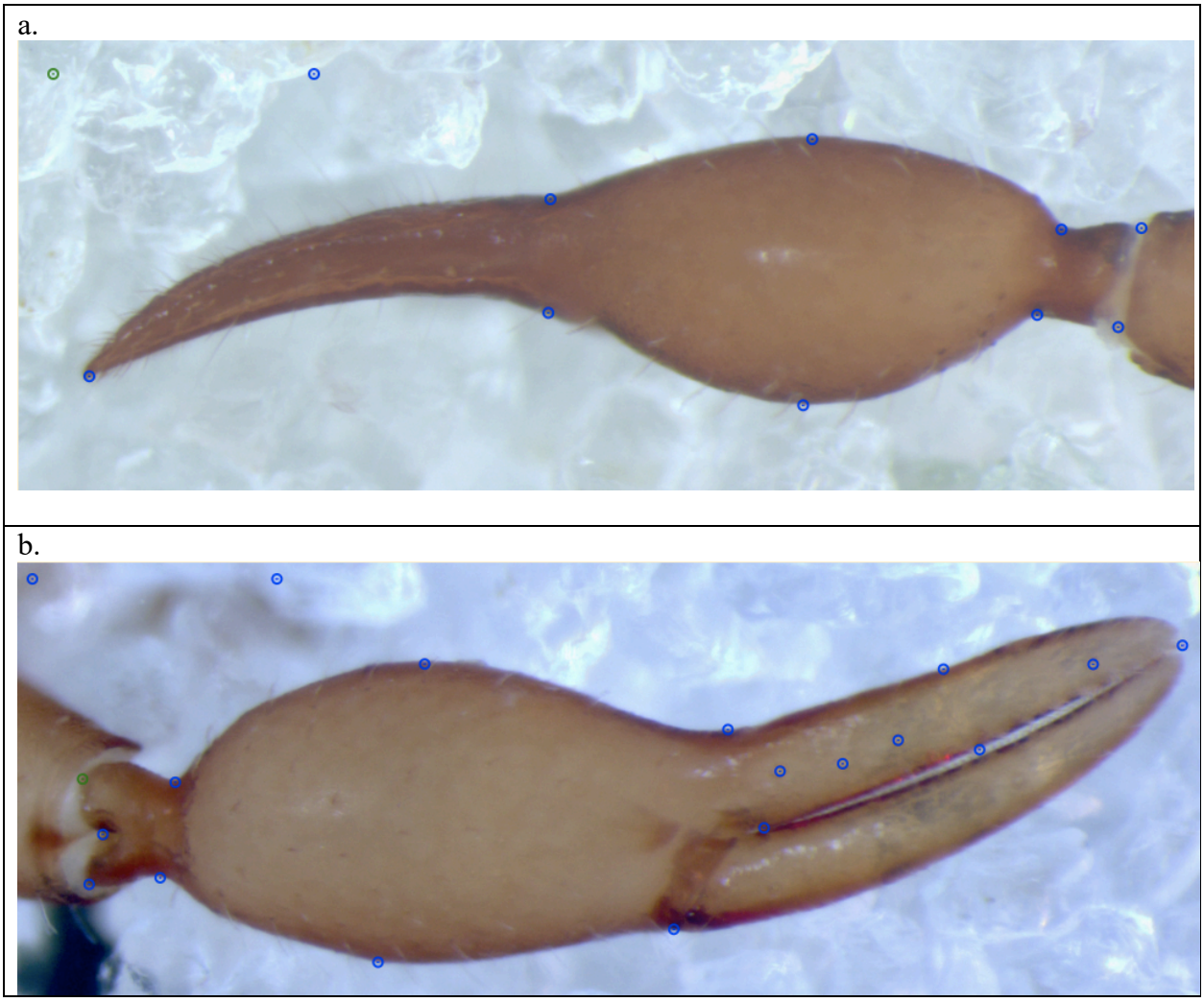

Fig. 2.11. Examples of placed landmarks on pedipalp chela fingers: (a) right pedipalp fixed finger in retrolateral view; (b) right pedipalp movable finger in retrolateral view. Specimens of *H. mirabilis* with landmarks placed as they appear in StereoMorph. Points placed outside of each character for measuring scale.

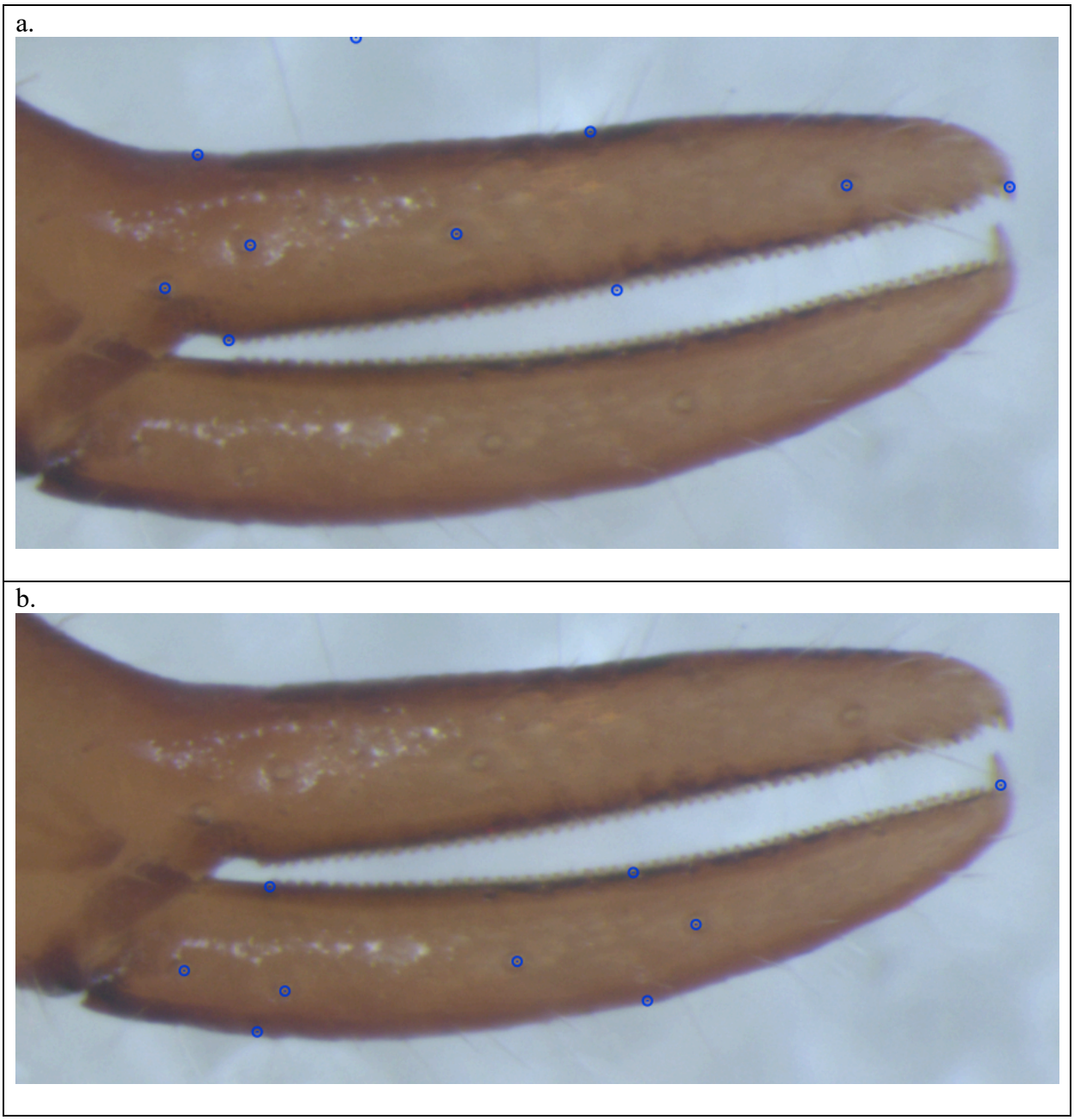

Fig. 2.12. StereoMorph user interface for inputting landmarks. Landmarks tab is shown. Points outside the character in the top left of the frame are for measuring scale.

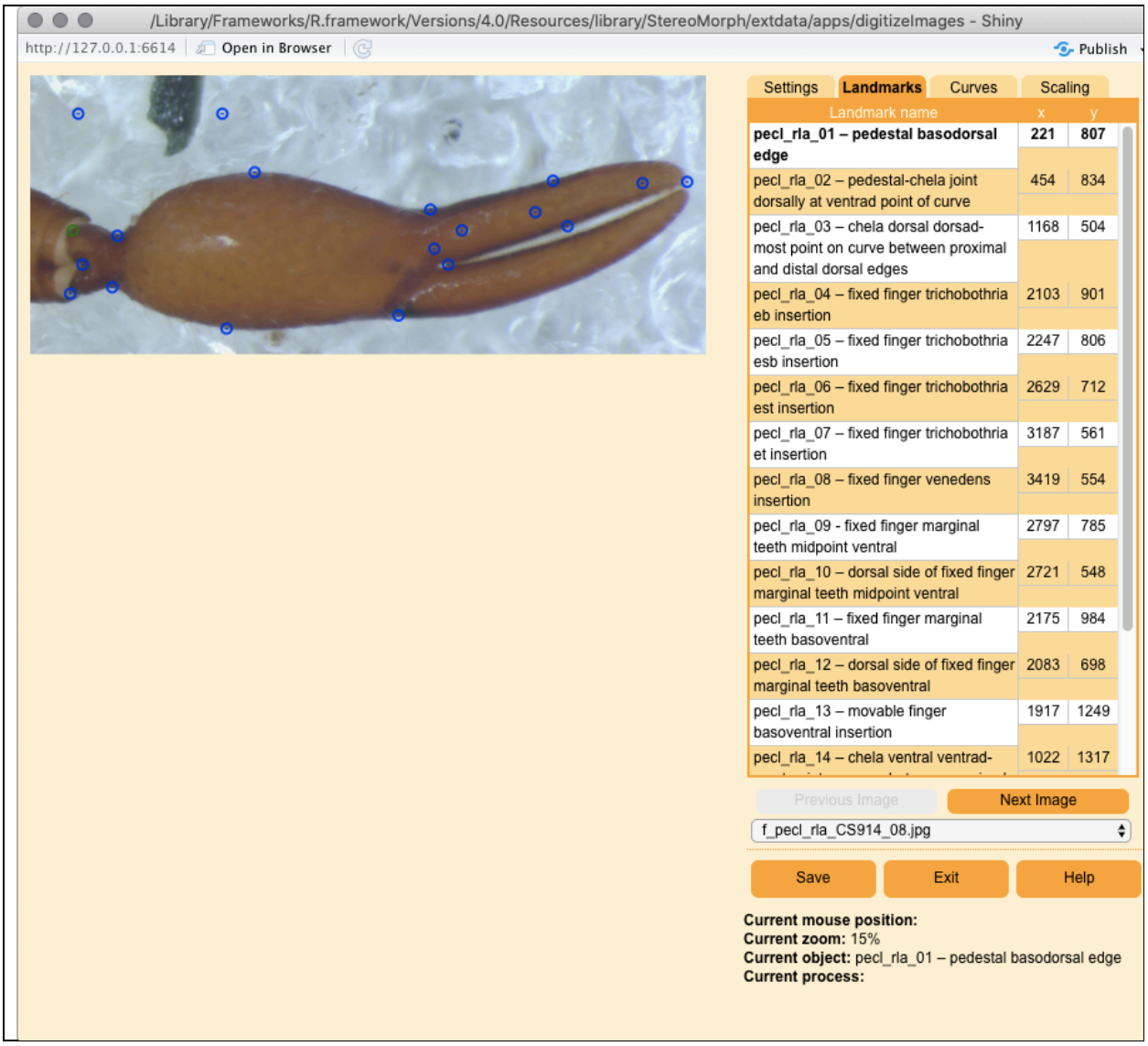

Fig. 2.13. StereoMorph user interface for inputting scale. Points were placed outside the character in the top left of the frame outside character landmarked used. The ruler interval was calculated in a spreadsheet for each image taken through scaling information in xml files output by Leica Application Suite software imaging software integrated with the Leica DFC camera.

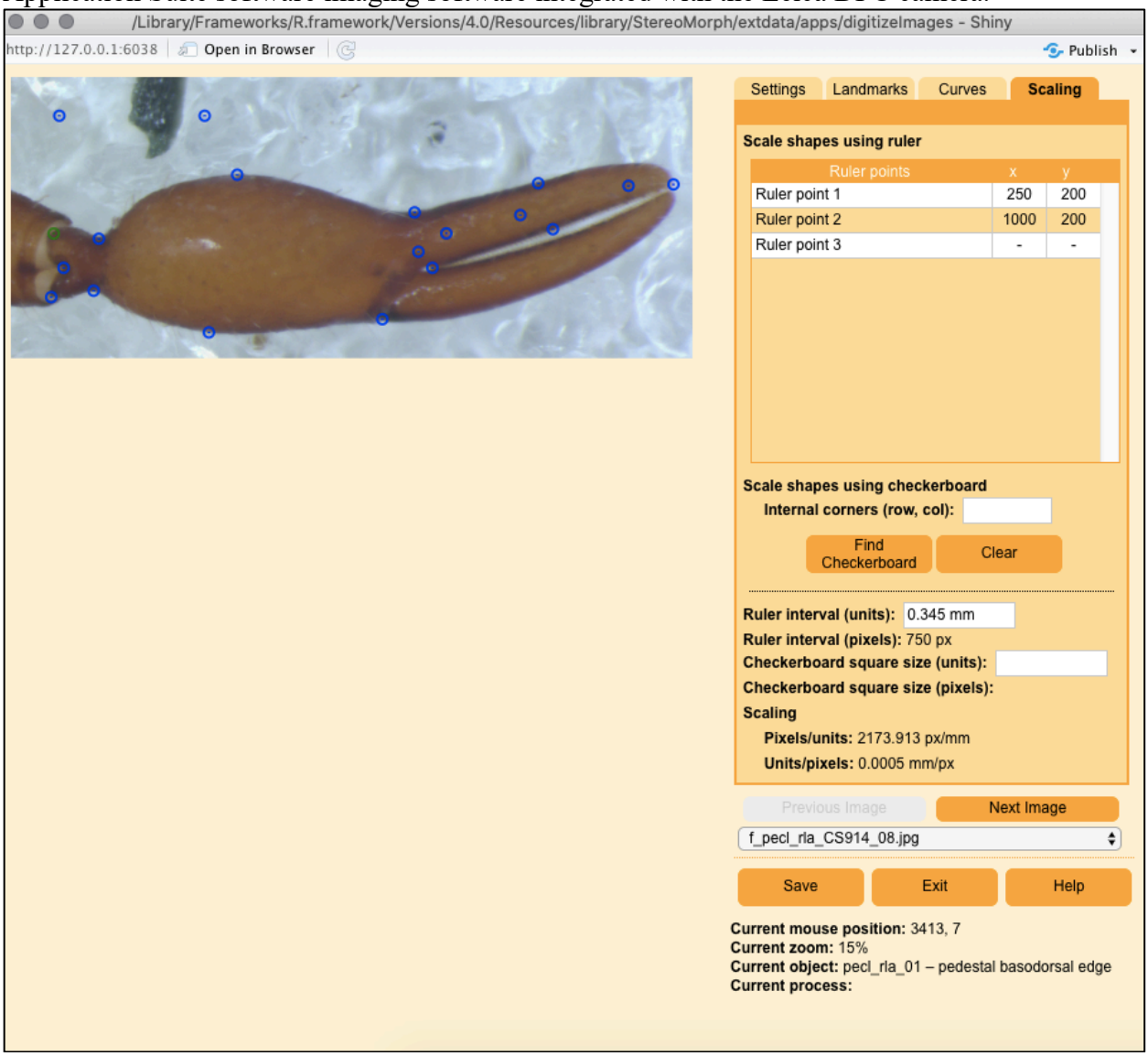

Fig. 2.14. Shape analyses of carapace: (a) GPA lollipop graph; (b) PCA lollipop graph of PC1; (c) PCA scatterplot graph of PC1 and PC2, red circle and dots indicating females and blue circle and dots indicating males; (d) CVA lollipop graph with wireframe; (e) CVA histogram of frequency of canonical variates, red indicating females and blue indicating males; (f) DFA lollipop graph with wireframe; (g) DFA histogram of discriminant scores, red indicating females and blue indicating males.

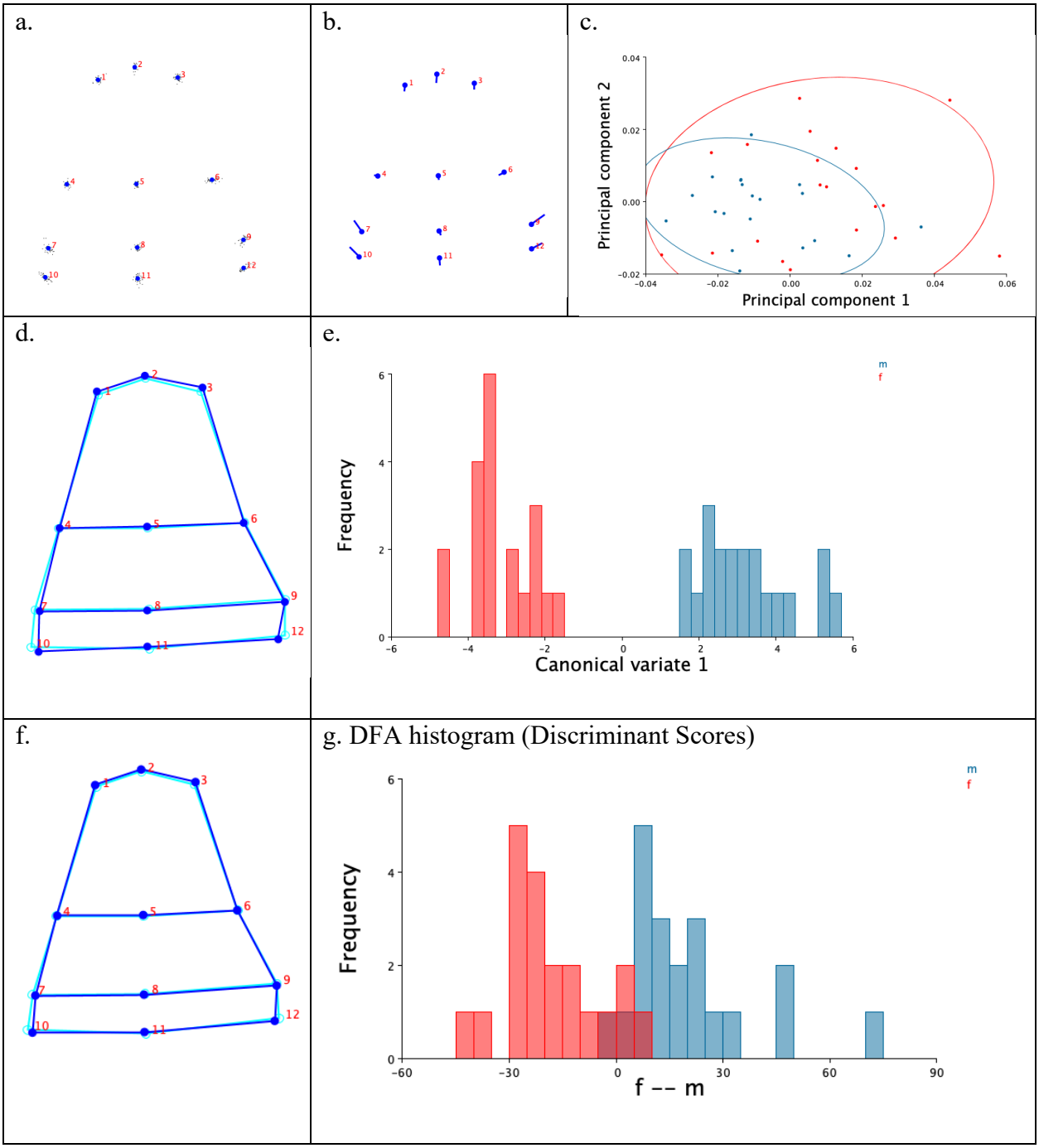

Fig. 2.15. Shape analyses of leg IV femur and patella: (a) GPA lollipop graph; (b) PCA lollipop graph of PC1; (c) CVA lollipop graph; (d) DFA lollipop graph with wireframe; (e) PCA scatterplot graph of PC1 and PC2, red circle and dots indicating females and blue circle and dots indicating males; (f) CVA histogram of frequency of canonical variates, red indicating females and blue indicating males; (g) DFA histogram of discriminant scores, red indicating females and blue indicating males.

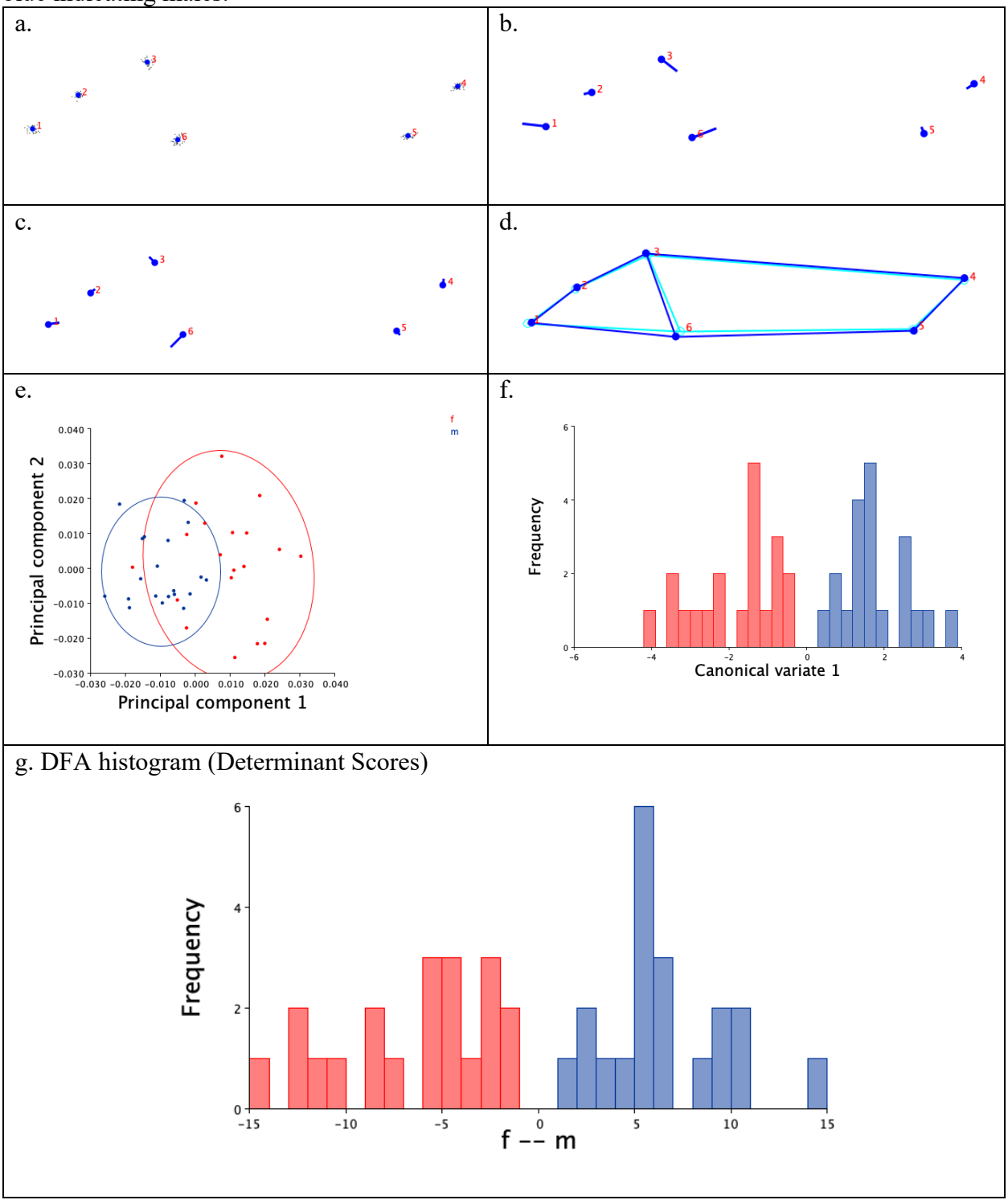

Fig. 2.16. Shape analyses of pedipalp chela in dorsal view: (a) GPA lollipop graph; (b) PCA lollipop graph of PC1; (c) CVA lollipop graph; (d) DFA lollipop graph with wireframe; (e) PCA scatterplot graph of PC1 and PC2, red circle and dots indicating females and blue circle and dots indicating males; (f) CVA histogram of frequency of canonical variates, red indicating females and blue indicating males; (g) DFA histogram of discriminant scores, red indicating females and blue indicating males.

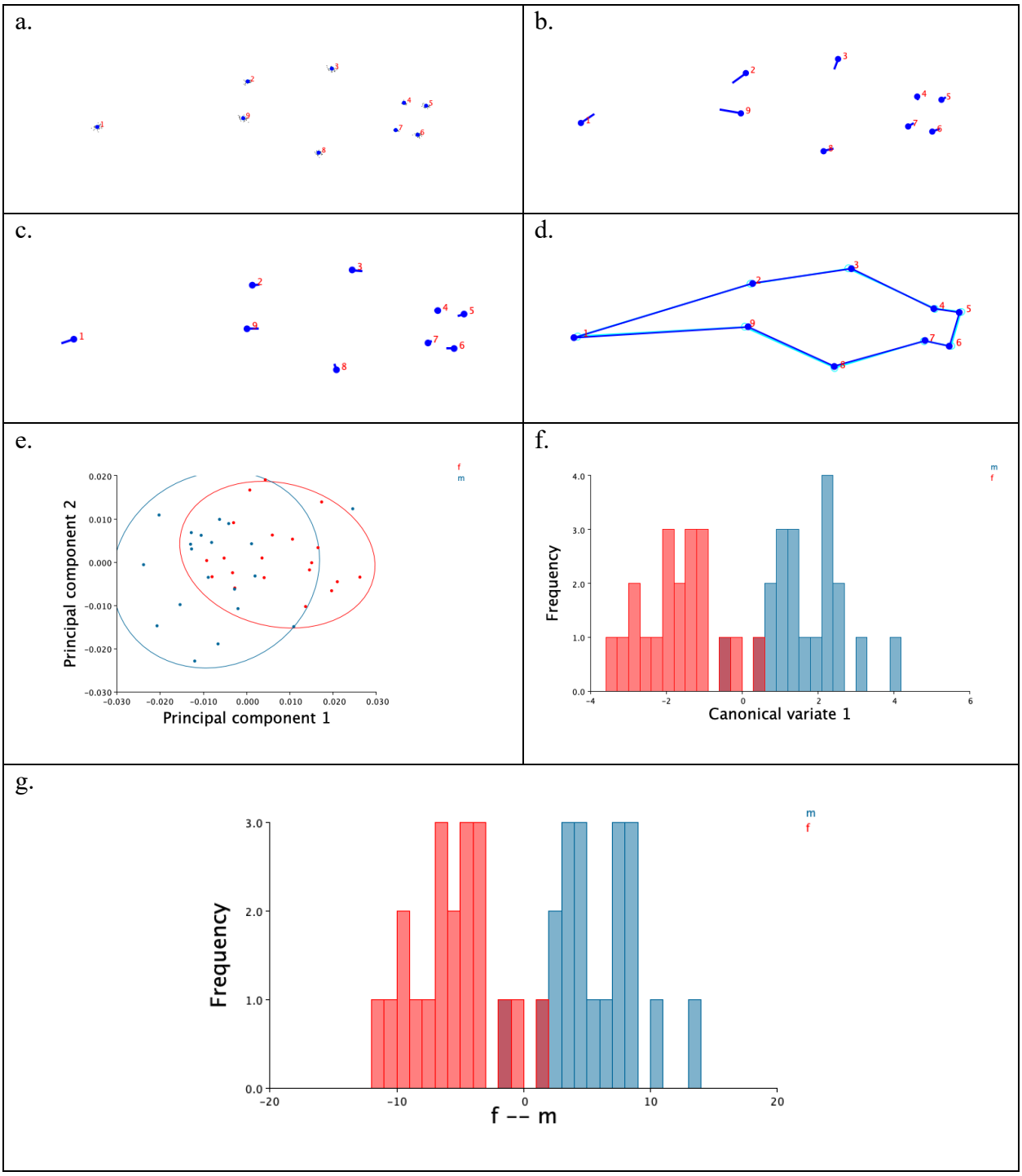

Fig. 2.17. Shape analyses of pedipalp chela in retrolateral view: (a) GPA lollipop graph; (b) PCA lollipop graph of PC1; (c) CVA lollipop graph; (d) DFA lollipop graph with wireframe; (e) PCA scatterplot graph of PC1 and PC2, red circle and dots indicating females and blue circle and dots indicating males; (f) CVA histogram of frequency of canonical variates, red indicating females and blue indicating males; (g) DFA histogram of discriminant scores, red indicating females and blue indicating males.

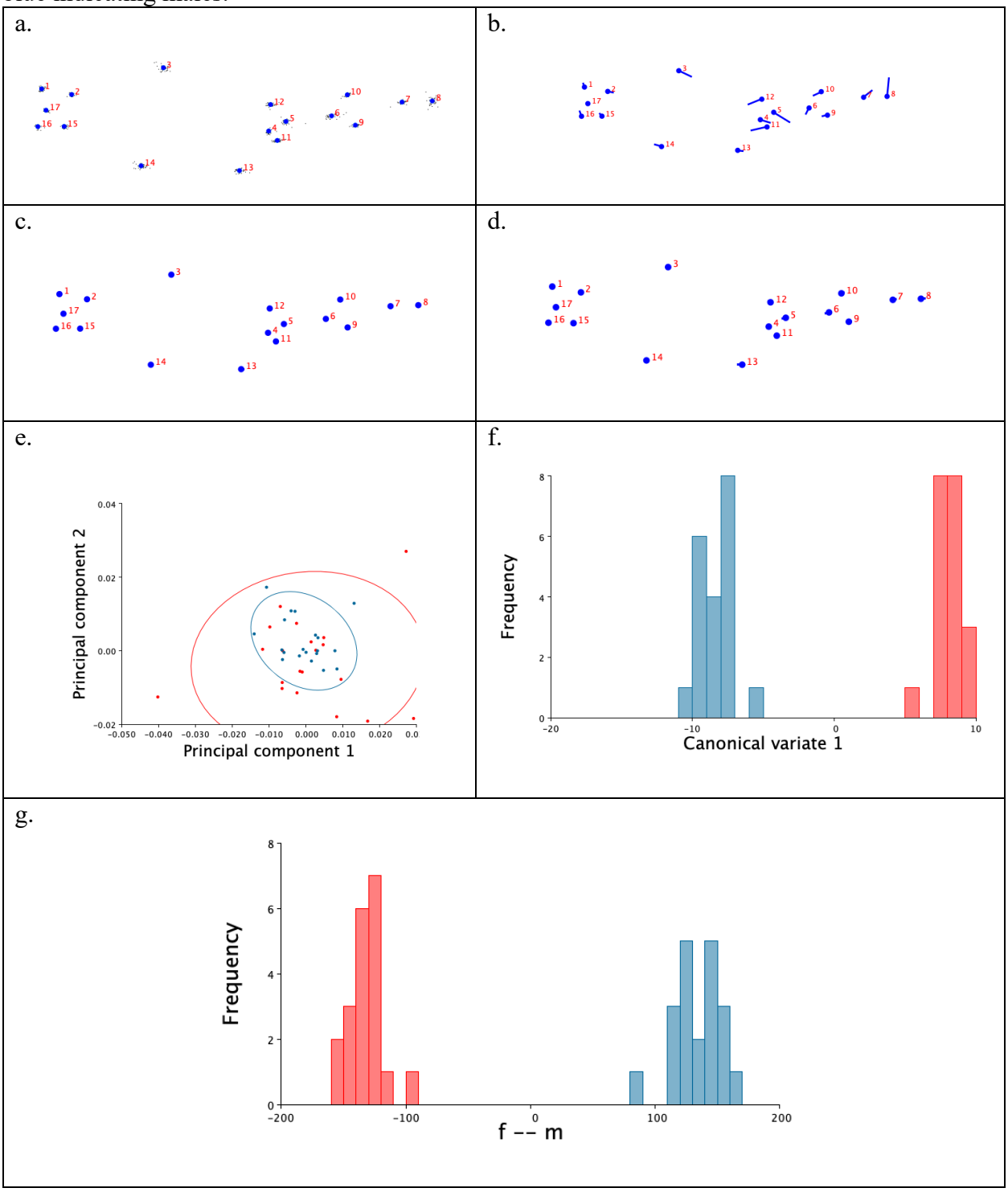

Fig. 2.18. Shape analyses of pedipalp fixed finger in retrolateral view: (a) GPA lollipop graph; (b) PCA lollipop graph of PC1; (c) CVA lollipop graph; (d) DFA lollipop graph with wireframe; (e) PCA scatterplot graph of PC1 and PC2, red circle and dots indicating females and blue circle and dots indicating males; (f) CVA histogram of frequency of canonical variates, red indicating females and blue indicating males; (g) DFA histogram of discriminant scores, red indicating females and blue indicating males.

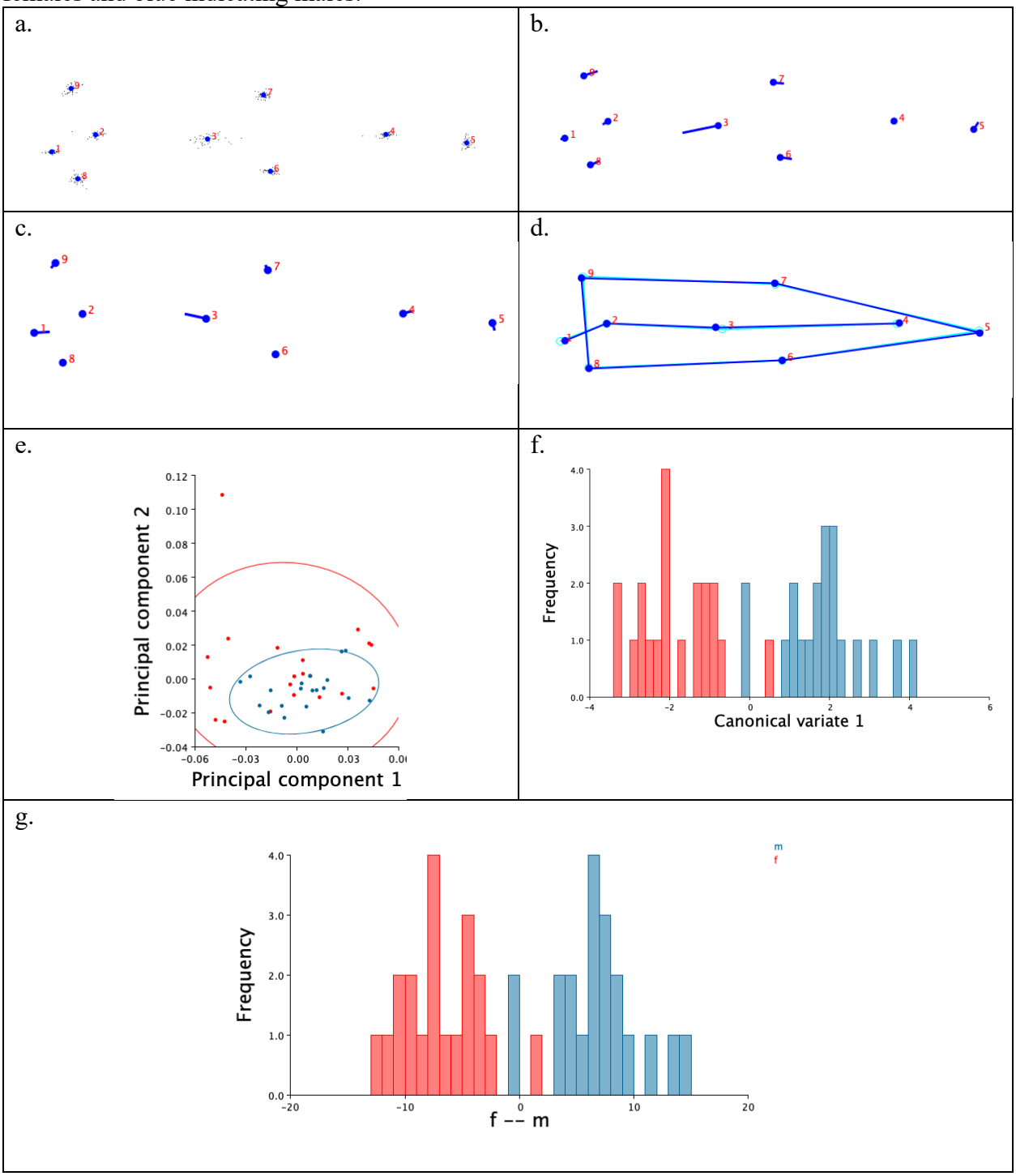

Fig. 2.19. Shape analyses of pedipalp movable finger in retrolateral view: (a) GPA lollipop graph; (b) PCA lollipop graph of PC1; (c) CVA lollipop graph; (d) DFA lollipop graph with wireframe; (e) PCA scatterplot graph of PC1 and PC2, red circle and dots indicating females and blue circle and dots indicating males; (f) CVA histogram of frequency of canonical variates, red indicating females and blue indicating males; (g) DFA histogram of discriminant scores, red indicating females and blue indicating males.

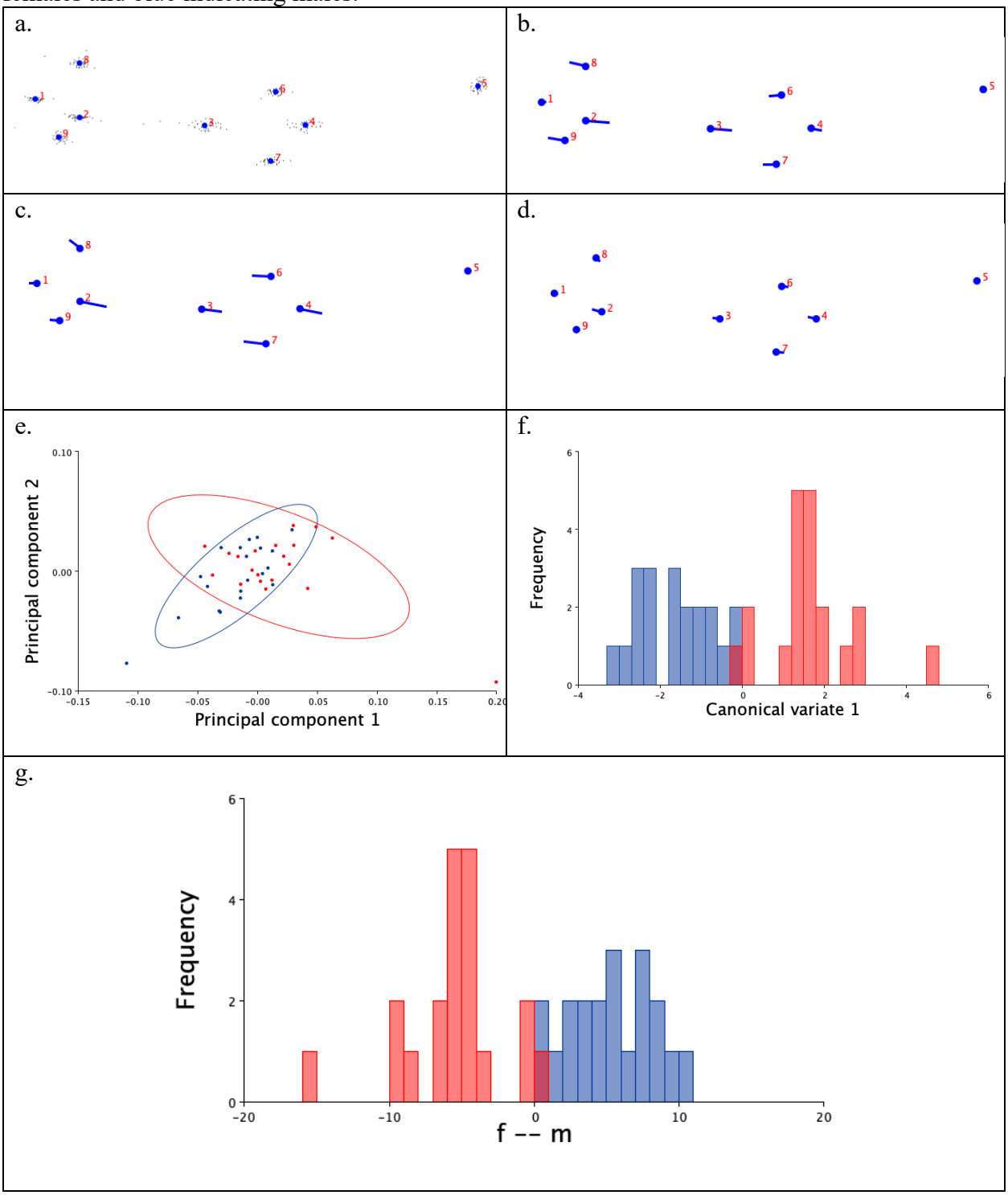

Tab. 2.1. Description of landmarks for carapace in dorsal view. Landmarks plotted on a specimen in Fig. 2.9a.

Landmark	Description
1	anterior margin seta, lateral-most seta socket, left side
2	anterior marginal edge, at point median to pair of anterior-medial setae
3	anterior margin seta, lateral-most seta socket, right side
4	anterior carapace transverse furrow, lateral-most edge, left side, if furrow splits or widens anteriorly then at intersection of anterior-most part of furrow edge and lateral margin
5	anterior carapace transverse furrow, median, at anterior-posterior midpoint of furrow if furrow is widened, at point in line with AM2 and PF2
6	anterior carapace transverse furrow, lateral-most edge, right side, if furrow splits or widens anteriorly then at intersection of anterior-most part of furrow edge and lateral margin
7	posterior carapace transverse furrow, left side, at lateral margin of sclerotized tissue, if furrow splits or widens anteriorly then at anterior-most part of furrow edge and lateral margin
8	posterior carapace transverse furrow, median, at anterior-posterior midpoint of furrow if furrow is widened, at point in line with center of darkened region located just posterior to posterior furrow
9	posterior carapace transverse furrow, right side, at lateral margin of sclerotized tissue, if furrow splits or widens anteriorly then at anterior-most part of furrow edge and lateral margin
10	posterior margin, lateral edge, left side, at greatest sclerotized width
11	posterior margin, median, in line with abdomen tergite 1 median and posterior margin median furrow (point 8)
12	posterior margin, lateral edge, right side, at greatest sclerotized width

Tab. 2.2. Description of landmarks for leg IV femur and tibia in prolateral view. Landmarks plotted on a specimen in Fig. 2.9b.

Landmark	Description
1	femur and trochanter joint, basoventral at femur
2	femur and trochanter joint, basodorsal at femur
3	femur and patella joint, posterioventral at femur
4	patella and tibia joint, posteriorventral at patella
5	patella and tibia joint, posteriodorsal at patella
6	femur and patella joint, basodorsal at femur

Tab. 2.3. Description of landmarks for pedipalp chela: (a) in dorsal view; (b) in retrolateral view. Landmarks plotted on a specimen in Fig. 2.10a and Fig. 2.10b for dorsal and retrolateral views, respectively.

(a)

Landmark	Description
1	distal tip of fixed finger
2	basoretrolateral edge of fixed finger
3	retrolateral widest point of chela
4	retrolateral basal edge of chela and pedestal
5	retrolateral basal pedestal edge and femur
6	prolateral basal pedestal edge and femur
7	prolateral basal edge of chela and pedestal
8	prolateral widest point of chela
9	prolateral edge of fixed finger

(b)

Landmark	Description
1	pedestal basodorsal edge
2	pedestal-chela joint dorsally at ventrad point of curve
3	chela dorsal dorsad-most point on curve between proximal and distal dorsal edges
4	fixed finger trichobothria *eb* insertion
5	fixed finger trichobothria *esb* insertion
6	fixed finger trichobothria *est* insertion
7	fixed finger trichobothria *et* insertion
8	fixed finger venedens insertion
9	fixed finger marginal teeth midpoint ventral
10	dorsal side of fixed finger marginal teeth midpoint ventral
11	fixed finger marginal teeth basoventral
12	dorsal side of fixed finger marginal teeth basoventral
13	movable finger basoventral insertion
14	chela ventral ventrad-most point on curve between proximal and distal dorsal edges
15	pedestal-chela joint ventrally at dorsad point of curve
16	pedestal basoventral edge
17	pedestal basomedian notch at proximad point

Tab. 2.4. Description of landmarks for pedipalp fingers in retrolateral view: (a) fixed finger; (b) movable finger. Landmarks plotted on a specimen in Fig. 2.11a and Fig. 2.11b for fixed finger and movable finger, respectively.

(a)

Landmark	Description
1	fixed finger trichobothria *eb* insertion
2	fixed finger trichobothria *esb* insertion
3	fixed finger trichobothria *est* insertion
4	fixed finger trichobothria *et* insertion
5	fixed finger marginal teeth distad tooth at ventral insertion
6	fixed finger marginal teeth midpoint ventral
7	dorsal side of fixed finger marginal teeth midpoint ventral
8	fixed finger marginal teeth basoventral
9	dorsal side of fixed finger marginal teeth basoventral

(b)

Landmark	Description
1	movable finger trichobothria *b* insertion
2	movable finger trichobothria *sb* insertion
3	movable finger trichobothria *st* insertion
4	movable finger trichobothria *t* insertion
5	movable finger venedens insertion on ventral side
6	movable finger marginal teeth midpoint dorsal
7	ventral side of movable finger marginal teeth midpoint ventral
8	movable finger marginal teeth basodorsal
9	ventral side of movable finger marginal teeth basodorsal

Chapter 3

Consolidation of three eastern Nearctic subterranean pseudoscorpions into *Hesperochernes mirabilis* (Pseudoscorpiones: Chernetidae), a cave-obligate species with a remarkably large distribution

Authors

Charles D. R. Stephen[1,2,3], Jonathan W. Armbruster[1], Jason E. Bond[4]

[1] Auburn University, Auburn, Alabama, USA

[2] Missouri State University, Springfield, Missouri, USA

[3] Corresponding author: cdr.stephen@gmail.com

[4] University of California at Davis, Davis, California, USA

Abstract

The karst regions of the eastern United States are a recognized biodiversity hotspot for cave fauna. Within this region, subterranean pseudoscorpions are some of the best examples of this remarkable biodiversity: as a group they are speciose, most are endemic, and many have highly restricted ranges. However, as is the case with most cave fauna, knowledge of this region's subterranean pseudoscorpions is restricted to species descriptions and regional species lists. No critical evaluations of these understudied fauna have been done to date with molecular or advanced morphological tools. Applications of these tools may uncover cryptic species or reveal overestimations of species richness. In this study we evaluate eastern members of subterranean *Hesperochernes*, a genus widespread through much of the United States from the Mississippi River basin region and eastwards. Uniquely to cave pseudoscorpions, the species tend to be found in high populations relatively easily accessible to biologists. East of the Mississippi River, all specimens of *Hesperochernes* have been assigned to *H. mirabilis*, with the exception of two specimens collected from one cave north of the Ohio River, from which *H. holsingeri* was described as a single-cave endemic. West of the Mississippi River, in the Ozarks karst region, *H. occidentalis* appears to be distributed throughout this karstic region, with specimens known as far west as northeastern Oklahoma and some potentially questionable records from northeastern

Texas. Westward into the Great Plains, caves are sparse and no *Hesperochernes* are yet known, until the southwestern extent of the Rocky Mountains range in Arizona, where *H. bradybaughi* was recently described from one cave in Parashant National Monument. We increase the total range in the eastern USA of subterranean *Hesperochernes* congeners to 316 caves distributed through twelve states. These records come from our extensive field collection, use of material we identified from museum collections and previously identified material, past published records, and previously unpublished data recovered from reports to government bodies and private agencies. Notably, an extensive effort of surface-based collection from leaf litter and subcortical habitat recovered no *Hesperochernes* but was otherwise highly successful in collecting other genera and families of pseudoscorpions. Caves with *Hesperochernes* populations straddle multiple biogeographic barriers that should be significant to a flightless, thermally restricted animal. Instead of cryptic speciation, our total evidence approach presents multifaceted arguments we use to synonymize the three cave-obligate species known from the Ozarks karst region and eastwards into the oldest available name: *Hesperochernes mirabilis* (Banks 1895).

Introduction

Pseudoscorpions are small (1-4 mm) predators, that within caves are known to prey upon mammal parasites and other small arthropods in bat guano and woodrat nests (Knudsen 1956, Barr 1968). They have in turn been documented to be consumed by larger predators such as salamanders (Salvidio et al. 2014). Cave-obligate pseudoscorpions tend to have highly restricted geographic ranges. This pattern has been widely reported in cave regions in the eastern USA, South America, Europe, eastern Asia, and Australia (Chamberlin 1952, Harvey 1989, 1990, Holsinger et al. 2013, Cardoso et al. 2021, Viana and Ferreira 2021). Two significant exceptions to this pattern are in the genus *Hesperochernes* in the karst regions of eastern North America: *H. mirabilis* and *H. occidentalis* (Hoff and Bolsterli 1956, Muchmore 1974). One additional cave-obligate congener is known from the eastern karst regions with a more typical geographically restricted range: *H. holsingeri* (Muchmore 1994). With the exception of one subcortical species from Japan, the remaining 20 species placed in this genus are endemic to North America and the Greater Antilles (Sato 1983, Harvey 1990, Harvey and Wynne 2014). In North America, congeners that are epigean or shallowly subterranean (i.e., from animal burrows) have been collected from west of the Great

Plains, in northern Mexico, in northern regions in western Canada and in Montana, in the northeast from Vermont, and from southeastern Florida (Banks 1893, 1895, 1908, Ellingsen 1910, Moles 1914, Chamberlin 1924, 1935, Beier 1930, Hoff 1945, 1948, 1956, Hoff and Clawson 1952). Several species are known to be associated with mammals (Beier 1930, Hoff and Clawson 1952, Muchmore 1971b, 1992). The two cave-restricted species known from outside of the eastern USA karst regions are *H. bradybaughi* from Arizona and *H. vespertilionis* from the Greater Antilles islands of Cuba and Hispaniola (Beier 1976, Perez-Gelabert 2008, Harvey and Wynne 2014). Interestingly, *Hesperochernes* is the only genus of family Chernetidae with known species collected from caves in the USA (Harvey 1990, 2013).

Here, we assess the taxonomic status of cave-obligate North American *Hesperochernes*, within a geographic boundary of the karstic regions located east of the Great Plains, south and east of the Great Lakes, and excluding Florida. There are three species within this region, located on either side of the Mississippi River and extending eastward approximately bounded by the Ohio and Tennessee Rivers to the Appalachian Mountains and then northeast into northeastern Virginia. *Hesperochernes holsingeri* and *H. mirabilis* are exclusively found east of the Mississippi River, while *H. occidentalis* is endemic to the Ozarks karst region west of the Mississippi River. Several ancient geographic barriers to dispersal within this range should post significant barriers to gene flow for terrestrial subterranean-restricted arachnids incapable of aerial dispersal by their own means. In addition to the three large rivers mentioned and their extensive drainage basins of tributaries, this also includes regions without cave-forming limestone that have delineated distinct faunal assemblages in each of the five major karstic regions in which *Hesperochernes* species have been found (Culver et al. 2003, Niemiller and Zigler 2013, Niemiller et al. 2016, Engel et al. 2017, Zigler et al. 2020).

Due to similar extreme selective pressures across caves, cave-adapted species often converge on a similar external form (Darwin 1872). It may be that the practice of defining species based on select external characters alone has led to overly inclusive diagnostic characters in the cases of the apparently widely-dispersed *H. mirabilis* and *H. occidentalis* (Hoff 1956). Alternatively, as seen in other genera of surface-dwelling Chernetidae, *Hesperochernes* species may engage in phoresy, enabling transportation between caves on wide-ranging cave-associated animals, such as bats,

moths, or rodents, so long as time spent outside caves does not exceed these cave-obligate animals' tolerance to humidity and thermal fluctuations (Hagen 1879, Muchmore 1971a, Holsinger et al. 2013, Niemiller et al. 2013, Finlayson et al. 2015, Slay et al. 2016).

Specimens were first identified as *Hesperochernes* using traditional methods, which currently is limited to the single reliable diagnostic character in females of the spermathecae consisting of a pair of narrow, convoluted tubes that terminate in bulbs (Harvey and Wynne 2014). The degree of variation and overlap within other traditional characters, predominantly morphometrics, of the two wide-ranging species and one single-cave endemic renders reliable assignment of individuals to a given species questionable with traditional morphometrics or qualitative shape characteristics (Hoff 1956). Significant geographic features, such as the Mississippi River, Ohio River, or fidelity to karstic regions could all play a useful role as diagnostic characters in the absence of good morphological features, but this assumes a lack of gene flow between populations across these presumed barriers.

A revision of the subterranean members of this genus in eastern North America is long overdue. Using specimens identified to genus, we tested the existing species hypotheses of the three eastern subterranean *Hesperochernes* lineages using molecular and morphological methods.

We took on a massive collection effort to obtain fresh material and incorporated museum specimens to address this long-standing taxonomic problem. We expected our results to either indicate that overlooked diversity exists and that we would then describe several species, or alternatively, that these chernetids comprise as many or fewer than the current set of three described species, due to an ability to move between caves irrespective of presumed biogeographic barriers to dispersal.

Methods

1. Collection.

1.1. Field collection

1.1.1 Collection method for known and potential cave localities

The primary method of sampling was through visual encounter surveys done by teams as detailed in Zigler et al. (2020). Briefly, all habitat within the cave was searched within limits of available personnel and time, starting with the entrance zone, proceeding into the transition zone, and then the maximum extent of accessible passages in the dark zone. At each cave where *Hesperochernes* was found a set of 1-10 specimens were collected upon discovery using a paintbrush. The number collected varied with permit limitations at the site visited. Between caves, gear decontamination protocols were followed to avoid our sampling contributing to the spread of White-Nose Syndrome, a fungal disease that is decimating bat populations in the United States as the fungal pathogen *Geoymces destructans* continues to spreads westward from its origin introduction from Europe into a New York cave (Samoray 2011, Maher et al. 2012, WNS Decontamination Team 2012, Zukal et al. 2014). All specimens collected in the field were potentially useful for our molecular approach, so all were collected live or immediately preserved in 95% EtOH. Following collection, specimens were kept cool and transported to the lab at the Auburn University Museum of Natural History (AUMNH). Here they were sorted and identified, then transferred to cryotubes into fresh 95% EtOH and stored at -20 °C until DNA extraction. Some specimens were not subjected to DNA extraction for the purposes of morphological work and their potential future utility as a type specimen. All voucher specimens were accessioned into AUMNH. Permission was obtained to enter caves from government agencies managing caves and from landowners of caves on private lands. Permits to collect specimens were obtained from the federal National Parks Service for Mammoth Cave National Park and as required by state agencies managing caves in Alabama, Arkansas, Georgia, Indiana, Kentucky, Missouri, Ohio, Oklahoma, Tennessee, and Virginia. Additionally, close coordination, cave location, in-cave guidance, and collection help were gratefully received from members and employees of the Alabama Cave Survey, Georgia Speleological Survey, owners and managers of Hidden River Cave (Kentucky), Illinois Natural History Survey, Indiana Cave Survey, Kentucky Speleological Society, the owner of Marengo Cave (Indiana), National Speleological Society, Tennessee Cave Survey, The Nature

Conservancy, Southeastern Cave Conservancy, Virginia Speleological Survey, and volunteers from local grottoes in several states visited through the course of field collection.

1.1.2 Collection method for potential surface localities

To test the hypothesis that *Hesperochernes* species are not cave-obligate animals and thus may be found outside of subterranean habitat, we extensively sampled from surface localities in karstic and non-karstic regions near where subterranean *Hesperochernes* species were known to occur, we discovered new subterranean populations, or we suspected subterranean populations may exist. We used three methods: haphazard sampling, bulk sampling of sifted leaf litter, and sticky traps.

Haphazard sampling occurred near cave entrances and on hikes to caves. Methods included subcortical sampling of deadwood, searches of boulders, rocks, and loose debris along rocky stream beds and surface rocks in karstic regions, and haphazard sampling of bird nests when unoccupied nests were discovered at cave entrances. Three abandoned Eastern Phoebe nests were extracted from cave entrances in Alabama and Tennessee, placed in a bag, returned to the AUMNH laboratory, and completely picked apart by hand to search for pseudoscorpions.

Bulk samples of leaf litter were collected while traveling on foot to cave entrances, adjacent to cave entrances, on either side of the drip line of cave entrances, from a systematic survey of sinkhole invertebrate fauna in southern Indiana, and from opportunistic stops in protected areas while traveling by vehicle through karstic regions to known caves. This method was employed throughout the breadth of the geographic range of known and discovered sites, southward to regions with no known or subsequently discovered *Hesperochernes* populations in the southern Florida Lime Sink karst region encompassing northern Florida, parts of southeastern Alabama, and southwestern Georgia, and northward into southern Quebec, Canada. Leaf litter sampling for pseudoscorpions was done following the recommendations of Hoff (1949). Briefly, we typically processed ca. 10 L of leaf litter material (leaves and soil hummus) through a Winkler sifter to concentrate litter to finer particles, temporarily stored sifted material in a plastic bag kept at ambient temperature and outside of direct sunlight during transport, and then manually or passively processed live animals. Manual processing was done with a soil sieve or by hand over white cloth within 24h; all pseudoscorpions were picked from these samples with a paintbrush and placed in

95% EtOH, kept cool in the field with ice packs, transported to AUMNH, and kept in a -20 °C freezer until a generic determination could be made. Passive processing used Tullgren funnels, a highly efficient and pragmatic modification of Berlese funnels, in which a bulk sample is placed in a funnel on a wire mesh, and soil arthropods are driven downwards through the funnel by a gradient of heat, light, and humidity created by an incandescent light bulb hanging over the sample; soil fauna drop through the funnel into a collection cup, which in this case was filled with 95% EtOH (Berlese 1904, Tullgren 1918, Hoff 1949, Macfadyen 1953). Extracted samples were then sorted, pseudoscorpions removed from bulk extractions, and pseudoscorpions then identified using Muchmore's (1990) synoptic key to family, and then to genus in the event of Chernetidae being identified from a sample. Eastern Phoebe (*Sayornis phoebe*) often nests at cave entrances. We dissected nests we encountered that did not show evidence of present occupation by nesting birds or have eggs inside of them.

Chernetid pseudoscorpions are known to be phoretic on larger flies. Species of robust flies in the family Heleomyzidae that occur in caves of eastern North America concomitant with *Hesperochernes* include *Amoebaleria defessa*, *A. sackeni*, and four species of *Heleomyza*. These flies as larvae consume organic inputs to caves such as mammal carcasses, mammal feces, and fungi; while adults have well-developed eyes, were observed to readily fly in-cave, and presumably may move between caves (Barr 1961, Gill 1962, Garnett and Foote 1966, 1967, Gill and Peterson 1987, Zigler et al. 2020). These flies are potential phoretic vectors of *Hesperochernes* and may transport them across the landscape. A single record of *Hesperochernes mirabilis* on a heleomyzid was noted by Muchmore on an adult fly close to a cave entrance, the fly being tentatively identified as either *Amoebaleria defessa* or *A. sackeni*. Two extensive sticky trap sampling programs in Alabama were used. The first was designed by the senior author for sampling winged dispersing reproductives of subterranean termites (Rhinotermitidae) over the course of two years of continuous sampling in 2010-2011 (Stephen 2012). This included approximately 1000 sticky traps that were placed at a height of 1m over one year of continuous sampling in triplicate at each sampling site in 17 counties across Alabama. Coverage included Interior Low Plateau, Valley and Ridge, and Appalachian karstic regions, and the Florida Lime Sink karstic region, in which no subterranean sampling was done in this study (Fig. 3.3a). The second sticky trap sampling program was designed for monitoring of *Lymantria dispar*, an invasive forest pest. Sticky

traps were placed at breast height on trees on the right of way of smaller roads in mostly rural areas that were forested. Traps were put up in May and taken down at the end of August and then checked for *L. dispar*; the target moth, rhinotermitid termites, harvestmen, and any pseudoscorpions were removed from traps by CDRS with a citrus-based solvent. Traps were located in counties of the northern half of Alabama, with approximately 80 traps placed per county monitored; 26 counties in 2010 only, two counties in 2010 and 2011, and two counties in 2011 only (Fig. 3.3b). Coordinates were taken with a handheld GPS at each trap and traps sampled in more than one year were located on the same tree whenever possible. In all, 2287 *L. dispar* traps were checked for pseudoscorpions.

1.1.3 Type localities

Collections were made at type locality caves and in caves throughout all major eastern karst regions for which we could gain access through the course of the study. The type locality for *H. mirabilis* is ambiguous as Banks (1895) implied two caves: Indian Cave, Kentucky, and "cave at Pennington Gap", Virginia. The type specimen for Indian Cave was located by Hoff in the Museum of Comparative Zoology, Cambridge, MA, USA. Hoff (1946), apparently unaware that the type from Pennington Gap cave was in France at Musuém d'histoire naturelle, Paris, assumed this type was lost and designated the Indian Cave specimen as the lectotype. Several caves are located in Pennington Gap, a geographic feature bisecting a ridge marking the border of southwestern Virginia and northeastern Tennessee. The largest, most well-known cave that casual travelers from Europe in the 1800s would have entered is Gilley Cave. A French expedition collecting subterranean fauna passed through this region at this time and the most probable large cave on this route would have been Gilley Cave (Packard 1888, 1894). They gave their collections to Alfeus S. Packard and perhaps from here specimens made their way to Nathan Banks. This is the most likely source of Banks' specimens from Kentucky and Virginia, as he did not publish otherwise on cave-collected specimens and is unlikely to have collected arachnids in caves himself (Packard 1888, Banks 1895). Thus without explicit information in Banks' (1895) text, we infer the Virginia type locality as Gilley Cave. The type locality for the remaining species is less controversial. *Hesperochernes holsingeri* is only unambiguously associated with its type locality, Wilsons Cave, Indiana (Muchmore 1994). *Hesperochernes occidentalis* has been reported from numerous caves in the Ozarks karst region west of the Mississippi River, with the type locality Fincher Cave,

Arkansas (Hoff and Bolsterli 1956). The allotype was collected from Caroll Cave, Arkansas, and paratypes were collected from Stevensons Cave, Arkansas, and from a series of unknown caves in Washington County, Arkansas (Hoff and Bolsterli 1956).

1.2 Published records

A thorough literature review was conducted in search of occurrence records from caves and potential surface localities for *Hesperochernes* within the prescribed sampling region. Primary literature was searched to compile known records on a state by state basis for Alabama (Peck 1989), Arkansas (Hoff and Bolsterli 1956, McDaniel et al. 1979, Graening et al. 2006), Georgia (Zigler et al. 2020), Indiana (Lewis 1983, Lewis et al. 1997), Kentucky (Banks 1895, Lewis and Lewis 2005a), Missouri (Gardner 1986), Ohio (Hobbs and Flynn 1981, Muchmore 1994, Hobbs and Hazelton 2010), Tennessee (Muchmore 1971b, Lewis et al. 2010, Dixon and Zigler 2011), and Virginia (Banks 1895, Holsinger 1963, Holsinger and Culver 1988, Holsinger et al. 2013). Emendations to published locality records from Georgia may be found in Zigler et al. (2020) and to avoid confusion this is the only source used here for this state. Records also exist for *H. occidentalis* from Edwards Co., Texas (Muchmore 1992, Cokendolpher 2009); representatives of the genus may extend further westward than previously known into the Edwards Plateau karst region. Gardner (1986) lists a potential new species of *Hesperochernes* identified by Muchmore in FS Cave 135, Texas Co., Missouri, but this is not correct: in Muchmore's catalog of identified specimens for this cave he determined specimens not as *Hesperochernes* but potential representatives of *Acuminochernes* and *Dinocheirus*. Graening et al.'s (2006) record of *Hesperochernes* in Fitton Spring Cave and Van Dyke Spring Cave, both in Newton Co., AR, are considered in error, as Muchmore did all their pseudoscorpion identifications and no specimens from these caves are in his catalog of identified specimens.

1.3 Museum specimens and unpublished records

Many useful records and specimens were yielded from an examination of museum catalog entries, identifying material determined only to family or order in museum collections, and from unpublished occurrences in grey literature. These records or specimens worked with and in many cases loaned to the senior author came from the American Museum of Natural History, New York, NY, USA; Field Museum of Natural History, Chicago, IL, USA; Florida State Collection of

Arthropods (FSCA), Gainesville, FL, USA; Muséum d'histoire naturelle, Paris, France; and Museum of Comparative Zoology, Cambridge, MA, USA. The potential record for *H. occidentalis* from the Edwards Plateau karst region in Texas (Cokendolpher 2009) was not examined nor was this region sampled by the authors for fresh material that could be used in morphological and molecular approaches. Significant material, especially collected by Julian J. Lewis, previously not accessioned into any museum were given to the senior author and accessioned into the Auburn University Museum of Natural History (AUMNH), Auburn, AL, USA. Many specimens that have remained unpublished records were given to and identified by William L. Muchmore. Muchmore described the majority of extant North American pseudoscorpion cave species and remains an important figure in pseudoscorpion literature (Stephen and Harvey 2018). Muchmore's personal catalog of specimens is housed in its original handwritten hardcopy form as a card catalog at FSCA, along with the majority of his life's work of identified specimens (Stephen and Harvey 2018). Museum records expanded the known occurrences and were useful in verifying previously published records. Unpublished grey literature occurrence records from reports delivered to government agencies and private organizations were used in compiling records from Indiana (Lewis 1998), Kentucky (Harker Jr. and Barr Jr. 1980), Missouri (Gardner 1986), Ohio (Hobbs and Hazelton 2011), and Tennessee (Lewis 2005, Lewis and Lewis 2005b, 2007).

2. Molecular approach.

2.1 DNA extraction

DNA extractions were generally whole-body extractions and done with Qiagen DNEasy kits, using a protocol modified from the manufacturer's instructions that was found to increase yield. Cuticles were preserved from filters during extractions to make them available for morphological study. Extracted DNA quality and quantity were verified by gel electrophoresis and Qubit, and samples without at least 13.3 ng/µL in a volume of 7.5 µL were excluded.

2.2. Library preparation for COI

A pilot study using specimens collected from Alabama, Tennessee, and Oklahoma (Fig. 3.4) used the mitochondrial gene for cytochrome oxidase *c* submit I (COI). At Auburn University primers from Murienne et al. (2008) were used to amplify COI, quality and size were verified on a gel, and

PCR products submitted to an in-house sequencing center at Auburn University for Sanger sequencing.

2.3. Library preparation for RADseq

RADseq libraries were prepared following the 3RAD protocol (Glenn et al. 2017, Bayona-Vásquez et al. 2019). RAD library preparation was done by CDRS, at Auburn University for two libraries and at University of California at Davis for one library. All libraries followed an identical 3RAD protocol based on Glenn et al. (2017). The complete protocol is provided in Supplementary Material 1 and additional details are available in Chapter 1. Prepared libraries were sequenced on the Illumina MiSeq platform with paired-end sequencing, at University of Georgia and at University of California at Davis. Loci were assembled with the ipyrad pipeline (Eaton and Overcast 2020), as detailed in Chapter 1.

2.4 Phylogenetic analysis of the three described species

With the COI data set of individuals from Tennessee and Oklahoma a maximum likelihood analysis was done using RAxML on the CIPRES cluster (Miller et al. 2011, Stamatakis 2014) (Fig. 3.5).

Using IQ-TREE 2 (Minh et al. 2020), a maximum likelihood analysis with ultrafast bootstraps (UFB) was performed on the RADseq loci (Figs. 1.4, 1.5). Reciprocal monophyly was not recovered for *H. holsingeri*, *H. mirabilis,* or *H. occidentalis*. Support was low except in some shallow branches, branch lengths were shallow, and groups separated by great geographic distances were recovered as clades with weak to good UFB support.

2.5 Population genetics analyses of specimens used in RADseq data set

Methods for these analyses are detailed in Chapter 1. Using the total RADseq loci set generated with ipyrad, we used VCFtools to analyse F_{ST} among presumed populations (Danecek et al. 2011, Eaton and Overcast 2020).

3. Morphological approach.

In this approach we used three methods: straight-line measurements, geometric morphometrics, and qualitative assessments. Straight-line measurements were done using standardized views and measuring between standardized landmarks (Chamberlin 1931) on subjectively-defined characters diagnostic for the genus and the three species under consideration (Hoff and Bolsterli 1956, Muchmore 1994). The geometric morphometrics approach used characters and landmarks appropriate for chernetid pseudoscorpions (Chapter 2). The qualitative approach involved drawing diagnostic characters from different specimens for visual comparison (Harvey and Wynne 2014).

3.1. Straight-line measurements

Straight-line measurements were made of total body length, the carapace, pedipalp segments, and leg IV segments. Preserved specimens from our collection efforts were chosen from across the geographic range we uncovered for the purpose of providing additional morphometric data and for a Principal Components Analysis (PCA). Chamberlin (1931) was used for standardized views, straight-lines axes, and landmarks for measuring. All measurements were done using photographs taken with a Leica DFC425 camera integrated with a Leica M165C stereomicroscope, from which images were imported into Leica Application Suite (LAS) and measurements taken from the saved images to a precision of a hundredth of a millimeter. Measurements were log-normal transformed to reduce variation inherent in the different dimensions of the characters used. Transformed values were inputted into a matrix, upon which a PCA was run in R with a custom script using the R package ggplot2 (Wickham et al. 2019). Four characters were used in the PCA, with a sample size of 54 specimens collected from caves in nine states. For reference, we also included measurements from the holotype and paratype series of *Hesperochernes tamiae*, a surface species with a published distribution of one ground squirrel nest in Tomkins County, New York (Beier 1932) and an unknown habitat in Ingam County, Michigan (Snider and Nelson 1991). *Hesperochernes tamiae* is the only surface congener known from east of the Great Plains and south of the Great Lakes.

3.2. Geometric morphometrics

Images taken for straight-line measurements were also used in geometric morphometric analyses. Specifically, the carapace in dorsal view was used to investigate shape differences that may covary

with recovered cryptic species or populations. This was done using a geometric morphometrics approach with landmarks defined in Chapter 2 that were successful with uncovering sexual dimorphism in this sclerotized part of the body that does not vary with starvation or gestation. Briefly, representative specimens were selected, placed in an ethanol dish in beads and adjusted so that they were oriented in standardized view (see Chapter 2 for details). Using a Leica DFC425 camera at its maximum resolution attached to a Leica M165C stereomicroscope and integrated with it via LAS, a set of images taken were taken at different focal lengths to capture the depth of features required. Using ZereneStacker, focal stacks of 10-50 images were then used to generate composite images of the character. Focal stacking was used to overcome the depth of field problem encountered when working at high magnifications. Composite images were calibrated with scaling information in LAS metadata files. Using standardized landmarks (Stephen and Armbruster, unpublished), in the R package StereoMorph each 2D image was landmarked and then a tps files summarizing the coordinates of landmarks and scaling was generated. The tps file was then imported into MorphoJ, where a Generalized Procrustes Analysis (GPA) removed the effects of size variation, a covariance matrix was generated, a wireframe graph was created from the landmark set, and then a PCA and a Canonical Variants Analysis (CVA) was run.

3.3. Qualitative approach

A set of specimens were selected for slide-mounting: topotypic material of *H. holsingeri*; topotypic material of *H. mirabilis*; near-topotypic material of *H. occidentalis*; and the holotype and female paratypes of *H. tamiae*. All specimens were collected through the course of this study, except for the type series of *H. tamiae* that was on loan from Museum für Naturkunde, Berlin. Prior to slide-mounting, specimens were cleared in lactic acid for 24h at room temperature (~20 °C). Specimens were then temporarily mounted on glass slides in a glycerol medium. Specimens were examined with a Leica microscope with a drawing tube attachment. Spermathecae and associated structures were examined and drawn in the female, and internal genital structures were drawn in the males. Drawings were photographed with an iPhone 11 running on iOS 15.2.1 using the native Camera application, which allowed for using the device's gyroscope to take level, undistorted, and high-quality digital photographs. Images of female drawings were imported into Inkscape, where the pencil lines were electronically traced to make vector graphic versions of the drawings; images of males were retained as pencil drawings (Figs. 3.6-3.13).

Results

1. Collection.

For *Hesperochernes mirabilis,* we located the caves listed as type localities by Banks (1895): Indian Cave Barren County, Kentucky and Gilley Cave, Lee County, Virginia. Both caves are gated and privately-owned. We obtained landowner permission to access and collect specimens and obtained topotypic specimens from both caves. For *H. holsingeri*, the type locality is Wilsons Cave, Jefferson County, Indiana. This cave is privately-owned and closed to visitation but we did obtain landowner permission to access the cave and collect samples, and successfully collected topotypic specimens. For *H. occidentalis*, the type locality for the holotype and paratypes are both in Washington County, Arkansas: Fincher Cave for the holotype and Carroll Cave for the paratype. Both caves are privately-owned and closed to visitation. We were unable to obtain landowner permission to access these caves. However, we did obtain samples from McNeely Cave, which is located within 20 km of both Fincher Cave and Carroll Cave. Through the course of this study, we have directly collected or observed specimens, borrowed specimens from institutions, and found records of specimens in both published reports and reputable grey literature sources. Our combined effort yielded 318 records of populations of subterranean *Hesperochernes* in caves located east of the Great Plains, all in the United States and distributed across 12 states (Fig. 3.1): Alabama (48 caves in eight counties); Arkansas (20 caves in five counties); Georgia (16 caves in five counties); Illinois (one cave in one county); Indiana (18 caves in eight counties); Kentucky (17 caves in 11 counties); Missouri (47 caves in 20 counties); Ohio (nine caves in four counties); Oklahoma (seven caves in four counties); Tennessee (96 caves in 41 counties); Texas (three caves in two counties); and Virginia (36 caves in 13 counties). The widest extent of this distribution is about 1000 km.

No *Hesperochernes* were recovered from surface collecting that was otherwise successful at collecting pseudoscorpions. Our surface collection effort included bulk samples of leaf litter, a large sticky trap sampling program in Alabama only, and haphazard opportunistic sampling in the vicinity of all caves visited. Bulk samples of leaf litter were taken from 124 localities (Fig. 3.2). Taking the two Alabama-based sticky trap programs together, traps were placed at 2322 localities, for a total of 3807 sticky traps that were examined for pseudoscorpions (Fig. 3.3). All sampled cave sites (Fig. 3.1) also included some effort of opportunistic surface rock and subcortical sampling. Leaf litter extractions from cave entrance zones and sinkholes, haphazard sampling of

tree trunks and deadwood near cave entrances, exterior rock walls of cave entrances, and the entrance zones of caves all failed to recover *Hesperochernes*. These methods were successful in recovering pseudoscorpions of families Atemnidae, Chernetidae (not *Hesperochernes* but did recover *Americhernes* and *Illinichernes*), Chthoniidae, Neobisiidae, and Syarinidae. No pseudoscorpions were found in extractions of abandoned Eastern Phoebe bird nests. Bird nest dissections did recover many potential *Hesperochernes* prey: parasitic mites (Mesostigmata), soil mites (Sarcoptiformes), external insect parasites (Siphonaptera), and insect larvae. Sticky trap sampling yielded no *Hesperochernes* but did recover *Americhernes oblongus*. Finally, in addition to our efforts, through the course of this study colleagues would sporadically donate phoretic pseudoscorpions discovered on moths and beetles while sampling via Malaise traps, sweep netting, and light trapping. Some of these were identified to family Chernetidae but none were *Hesperochernes*.

2. Molecular approach.

In the pilot study, the mitochondrial gene COI was amplified from samples taken from 12 caves located across Tennessee in the Interior Low Plateau and Valley and Ridge karst regions, and from two caves from eastern Oklahoma in the Ozarks karst region (Fig. 3.4). Approaches included Bayesian inference with MrBayes and Maximum Likelihood with RAxML. Analyses reconstructed ambiguous relationships among the 14 samples from the three karst regions.

None of the resulting trees recovered a monophyletic clade from Wilsons Cave, Indiana (i.e., *H. holsingeri*), a monophyletic clade of specimens from west of the Mississippi River (i.e., *H. occidentalis*), or a monophyletic clade of specimens east of the Mississippi River and generally south of the Ohio River (i.e., *H. mirabilis*).

With the RADseq data set, F_{ST} values recovered were significantly lower than the expected value of 1, which would be expected in genetically isolated species without gene flow. These results strongly support gene flow between described species. A more extensive analysis of the unusual population structure of eastern Nearctic subterranean *Hesperochernes* is presented in Chapter 1, where evidence is presented for gene flow between all geographic regions included in this data set and little barriers to genetic exchange between the described species are evident.

3. Morphological approach.

The single diagnostic character for separating *Hesperochernes* from other genera in the tribe Chernetini of family Chernetidae is that females possess a pair of spermathecae characterized by a long, convoluted, narrow tube ending in a bulb. In the qualitative approach, the spermathecae of slide-mounted female specimens occidentalis were compared through drawings made through a camera lucida from type localities for *H. holsingeri* (Fig. 3.6) and *H. mirabilis* (Fig. 3.7), near the type locality for *H. occidentalis* (Fig. 3.8), and from a female paratype of the surface species *H. tamiae* (Fig. 3.9). Beier (1930) did not include a figure showing the shape of the spermatheca, nor have other authors since; here we provide the first illustration of this character. All female specimens drawn and examined to confirm the identity to genus had this feature. In comparing surface and cave forms, tubes of spermatheca were shorter in *H. tamiae* but the bulb was of equivalent size and shape. Male structures showed variation amongst *H. holsingeri* (Fig. 3.10), *H. mirabilis* (Fig. 3.11), *H. occidentalis* (Fig. 3.12), and *H. tamiae* (Fig. 3.13). The principal difference in males was a horizontal vs. vertical orientation of lateral sac structures and a lack of a posteriomedial sac when subterranean species (Figs. 3.10-3.12) were compared to the surface species (Fig. 3.13).

In the straight-line measurement analysis, specimens were grouped by putative species: *H. holsingeri* (single cave in Indiana; n=2), *H. mirabilis* (all caves east of Mississippi River; n=46), and *H. occidentalis* (all caves west of Mississippi River; n=5), and *H. tamiae* (ground squirrel nest in New York; n=1). The PCA revealed no clear pattern separating specimens from eastern caves, western caves, or the single-cave endemic (Fig. 3.14). The surface species *H. tamiae* was near some *H. mirabilis* and *H. occidentalis* in PC1 and PC2. Body length has been used in species descriptions and we included this character in straight-line measurements, but it is a poor indicator of size, as pleural membranes of the abdomen may swell or shrink in different conditions, such as gestation or starvation. Carapace length is a better indicator of organism size.

In the geometric morphometrics analyses, specimens were grouped by northern vs. southern localities, with the Ohio River as the boundary, and by eastern vs. western localities, with the Mississippi River as the boundary. The PCA revealed no clear grouping of eastern vs. western (Fig. 3.15a) or northern vs. southern caves (Fig. 3.15b). The CVAs, which maximize differences

among a covariance matrix, did show a covariance in shape of the carapace with some overlap in specimens collected from eastern vs. western caves (Fig. 3.16a), but also revealed no clear pattern in specimens from northern vs. southern caves (Fig. 3.16b).

Discussion

The type locality of a species is the location associated with its type specimen, so having two type specimens without a clearly defined holotype is problematic when the two type localities for *H. mirabilis* are not geographically close to one another. The straight-line distance between the localities defined by Banks (1895) is 270 km, a distance cut by large rivers and regions without karstic rock that serve in part to define three separate karst regions (Interior Low Plateau, Valley and Ridge, and Appalachians) (Fig. 3.17). Both the print and online world catalogs of pseudoscorpion species reiterate this disjunct distribution (Harvey 1990, 2011, 2013). Additional collection efforts in the southwestern Appalachian karst and surrounding region since the 1895 description by Banks expanded the species' reported distribution to six Ohio caves, one Indiana cave, nine Georgia caves, and 17 Virginia caves (Muchmore 1994, Reeves et al. 2000, Holsinger et al. 2013, Zigler et al. 2020). However, the genus is far from ubiquitous. Systematic collections finding pseudoscorpions of other genera in 77 caves located in Alabama, Illinois, and South Carolina did not report *Hesperochernes* (Reeves 2001, Lewis et al. 2003, Campbell et al. 2011). We sampled *Hesperochernes* from 318 caves, but it is far from ubiquitous—of 203 cave sampling trips led by CDRS, only 54 resulted in a collection of *Hesperochernes*. Caves with repeat visits typically did not recover *Hesperochernes* in all sampling trips when observed populations were nonexistent or small (less than 10 individuals) in a successful visit, although our intensive sampling did usually recover at least one specimen of a pseudoscorpion of some taxon on every trip. West Virginia has no records for *Hesperochernes* but is rich with caves and likely new records are waiting to be discovered (Muchmore 1994). We obtained permits for West Virginia but were unable to sample in this state. Similarly, southern Pennsylvania and western Maryland have karstic cave systems that likely harbor *H. mirabilis* but we did not sample in these states (Culver et al. 2003).

For conservation efforts to have efficacy they must incorporate good taxonomy that aid in prioritizing regions in the most need of protection (Hall 1997, Wheeler 2004). The complex taxonomic history of *H. mirabilis* speaks to its morphological variation across the known range. At different times the species has been placed into five genera: *Chelifer*, *Chelodamus*, *Parachelifer*, *Pseudozaoana*, and finally *Hesperochernes* (Banks 1895, Chamberlin 1925, Beier 1932, Hoff 1949, Muchmore 1974). Its unusually wide geographic range has raised questions as to whether it is a cave-restricted species or actually comprises several distinct lineages in need of splitting into new species (Muchmore 1994, Niemiller et al. 2013). As presently defined, *H. mirabilis* may be the widest-ranging cave-adapted arthropod in North America (Niemiller et al. 2013). Through both our literature review and intensive surface collection efforts no evidence was found for *H. mirabilis* inhabiting surface or sub-surface habitat, such as the mesovoid substratum, upper soil profiles, sinkholes, or leaf litter. Further, *H. mirabilis* has clear adaptations for a troglobitic lifestyle: it does not have eyes, and has lengthened appendages relative to related species in the same genus (Muchmore 1974). The species also possesses a relatively thickened cuticle compared to other cave pseudoscorpions, which may serve to protect it against desiccation in the upper, non-riparian, drier areas of caves in which we collected specimens, in addition to more humid areas we found *Hesperochernes* such as near cave streams and in mounds of freshly deposited bat guano.

Our collection efforts included four days of sampling in southwestern Texas near El Paso, with surface-based collection, extraction of a large portion of a shallow ground-nesting kangaroo rat tunnel system, and a visual encounter survey and two-day baited trap in Panther Cave, a small cave that at the time was actively used by rodents. These efforts did not result in any collections of *Hesperochernes*, although we did recover syarinids and neobisiids. *Hesperochernes occidentalis* (reported as *Pseudozaona occidentalis*) was reported from two caves in Edwards County, Texas, which lies in the Balcones karst region, far west of the Ozarks karst region in which we sampled (Hoff and Clawson 1952, Muchmore 1992, Culver et al. 2003). In northeastern Mexico in San Luis Potasi and Tamaulipas (near to or bordering Texas), from eleven caves a series of chernetids were collected on bat guano (Reddell and Mitchell 1971). These chernetids were identified to family by W. B. Muchmore and not further due to his uncertainty in appropriate diagnostic characters for genera in this family; some may represent *Hesperochernes* (Reddell and Mitchell 1971). The

surface-adapted species *Hesperochernes molestus* has been reported from New Mexico in association with *Dipodomys*, *Neotoma*, *Perognathus*, and *Oncomys* rodents; in Texas, from one cave, in association with bats on guano piles in Val Verde County (Hoff 1956, Muchmore 1992). Similarly, the surface-adapted species *H. riograndensis* has been reported from New Mexico in a kangaroo rat nest, in four caves in Eddy County, and in one cave in Lincoln County; from Texas, in two caves in Iron and Terrell counties, respecitively. We did not include these species in our analysis, nor did we sample extensively from west of the Mississippi River. Given the extensive gene flow we recovered within *Hesperochernes* east of the Mississippi River and with populations in caves in the Ozarks karst region west of the Mississippi River, it is possible that gene flow is occurring between *H. mirabliis*, and these surface-adapted species or with potential subterranean *Hesperochernes* populations in Texas and northeastern Mexico. Within caves, the surface-adapted *H. utahensis* has been reported in association with the woodrat *Neotoma*, where it was consuming woodrat parasites (Knudsen 1956). The plasticity of the troglomorphic phenotype in *Hesperochernes* will be explored in future work.

Although we did not recover any from our collection efforts, surface-adapted species of *Hesperochernes* are known from west of the Mississippi River and from New York (Beier 1930, Nelson 1975). These epigean species have eyes and their appendages (especially the pedipalps) are relatively shorter with more developed musculature within segments. It is unknown how *H. mirabilis* may cross regions without subterranean habitat to gain access to new caves. There are several large geographic barriers to dispersal between known caves where *H. mirabilis* has been found. These include mountain ranges, rivers, and regions without karst (Fig. 1.2). One explanation for this remarkable distribution is phoresy, which is a non-parasitic association in which a smaller animal attaches to a larger animal for a given period of time and without notable expense of resources by the larger animal. Although phoresy on large insects is known in several pseudoscorpions (Lloyd and Muchmore 1975, Lira et al. 2014), it is not clear if *H. mirabilis* is capable of this behavior. Most collections of *Hesperochernes* species are from caves, but *H. laurae* has been collected from a wasp nest, *H. montanus* has been found in a bird nest, *H. tamiae* in the nests of ground squirrels and birds, *H. thomomysi* in ground squirrel nests, and both *H. canadensis* and *H. utahensis* are known from woodrat middens (Chamberlin 1935, Hoff 1948, Knudsen 1956, Nelson 1975, Cudmore 1986). We collected *H. mirabilis* in multiple instances in association with

woodrat nest material or bat guano from caves across our range of collection effort (Fig. 3.1); these associations have also been reported from caves in Illinois and Kentucky (Lewis et al. 2010). However, no reports exist of any species of *Hesperochernes* found directly on a bat or a woodrat. This includes research where the focus was trapping and examining these mammals (Graening et al. 2003, Francke and Villegas-Guzmán 2006). Although bats create a trophic link between caves and the surface, evidence to date appears to point against them transporting arthropods associated with guano communities between caves (Lewis et al. 2010). Other known associations of *Hesperochernes* are with true flies (Diptera) that are significantly larger in stature than pseudoscorpions. Of the two reported instances of a *Hesperochernes* clinging to a fly leg, one was likely a misidentification, and one interestingly was in a cave with a single pseudoscorpion specimen identified as *Pseudozaona* sp. and that can be safely assumed to have been *H. mirabilis* (Muchmore 1971b). This one instance of association with a fly was with *Amoebaleria defessa,* a common heleomyzid species found in southeastern karst caves, and occurred in the dark zone of Wrights Cave, Anderson Co., Tennessee (Barr 1961, Muchmore 1971a, Holsinger et al. 2013, Niemiller et al. 2013, Slay et al. 2016). It is unclear whether the Wrights Cave *H. mirabilis* was attacking the fly. Observations of thousands of heleomyzids in several hundred caves in the experience of the lead author while conducting fieldwork did not repeat this remarkable observation reported by Muchmore (1971b). Other large arthropods that may act as carriers for pseudoscorpions are rhaphidophorid camel crickets (*Ceuthophilus* spp.) and cave crickets (*Euhadenoecus* spp., *Hadenoecus* spp.) and overwintering erebidid moths (*Scoliopteryx libatrix*). No literature appears to have reported a pseudoscorpion clinging to cave crickets or to erebidid moths in a cave habitat. Direct observation of thousands of rhaphidophorid crickets and erebidid moths by CDRS in approximately 100 caves did not yield any instances of a pseudoscorpion attached to either of these large insects. Cave crickets in the Appalachian karst regions tend to have high degrees of genetic divergence (Caccone and Powell 1987), which suggests it is unlikely that these insects are migrating between caves along with pseudoscorpion passengers. In sum, a definitive case for phoresy by a cave pseudoscorpion on a larger animal has yet to be made. Nonetheless, if it is discovered that geographically separated populations are highly genetically connected, phoresy on wide-ranging larger animals such as mammals or large flying insects would be the most reasonable explanation for how this small arachnid came to be dispersed across large rivers and mountains.

SYSTEMATICS

Family Chernetidae Menge 1855

Subfamily Chernetinae Menge 1855

Tribe Chernetini Menge 1855

Hesperochernes Chamberlin 1924

urn:lsid:zoobank.org:act:D4A6B82B-AE1B-4B87-A653-C18A5C191A73

Hesperochernes Chamberlin 1924: 89–90; Beier 1932: 174–175; Beier 1933: 537–538; Hoff 1948: 341; Hoff 1949: 476; Hoff and Clawson 1952: 14; Hoff 1956: 31; Hoff 1958: 22, 48; Hoff 1963: 3; Muchmore 1974: 27–28; Harvey and Wynne 2014: 211.

Type species.—*Hesperochernes laurae* Chamberlin 1924, by original designation.

Remarks.—Following Chamberlin (1924) erecting this genus for the wasp-associated *Hesperochernes laurae*, diagnostic characters associated with its description were greatly expanded upon with morphometrics and qualitative descriptions by Beier (1932, 1933), Hoff (1948, 1949, 1956, 1958, 1963) and Hoff and Clawson (1952). Diagnostic characters were increasingly reduced in later emendations by Muchmore (1974, 1994), and even further reduced by Harvey and Wynne (2014). Currently, the singular reliable diagnostic feature for the genus that distinguishes it from other members of the subfamily Chernetinae is found in adult females. Females of this genus possess spermathecae characterized by tubules with a proximal opening in the genital operculum, that extend for varying lengths in varying degrees of convolution, and then terminate distally into a bulb in which sperm is presumed to be stored inside the female for an unknown duration. Given the great variation and evident gene flow among subterranean eastern Nearctic congeners, the reliability of species-level diagnostic characters of the 19 species placed in this genus may also be questionable, particularly if gene flow might be possible between presently defined species. A molecular approach used across all members of the genus would greatly aid in resolving this long-standing problem.

Hesperochernes mirabilis (Banks 1895)

[ZooBank ID registration currently in progress]

Chelifer mirabilis Banks 1895: 4, original description. Lectotype: USNM 4195, Indian Cave, Barren Co., Ky. July 24, 1881. H. G. Hubbard. [=Indian Cave, Barren Co., KY, USA; 24 July 1881; leg. HG Hubbard]. Paralectotopotype: Same data as lectotype. Paralectotypes: cave at Pennington Gap, Va. [=Gilley Cave, Lee Co., VA, USA; ca. 1860-1895; leg. unknown] (specimens not examined).

Chelodamus mirabilis Chamberlin 1925: 237, **genus transfer**.

Parachelifer mirabilis Beier 1932: 241, **genus transfer**; Roewer 1937: 313.

Pseudozaona mirabilis Hoff 1946: 201-203, **genus transfer.**

Hesperochernes mirabilis Muchmore 1974, **genus transfer.**

Pseudozaona occidentalis Hoff and Bolsterli 1956, **new junior synonym.**

Hesperochernes holsingeri Muchmore 1994, **new junior synonym.**

Types.—Lectotype male at United States National Museum, Smithsonian Institute, Washington, District of Columbia, United States (USNM), with label "Indian Cave, Barren Co., Ky. July 24, 1881. H. G. Hubbard. U.S.N.M. 4195", and in text (Banks 1895, 4) as "Indian Cave, Barren Co., Ky. June, (H. G. Hubbard)" [=Indian Cave, Baren Co., KY, USA]. We designate as paralectotypes the three specimens referred to in text (Banks 1895, 4) as collected from "Cave at Pennington Gap", which we infer as being Gilley Cave, Lee Co., Virginia, USA; these are also referenced by Beier (1932, 241), were considered lost by Hoff and Bolsterli (1956), and are apparently stored at Muséum d'histoire naturelle, Paris, France (MHNP). Paralectotype female of Banks (1895, 4) at USNM, from same locality as lectotype male. Paralectotype female of Hoff and Bolsterli (1956, 171–174) at Illinois Natural History Survey collection, Urbana, Illinois, USA (INHS); collected from Fincher Cave, Washington Co., Arkansas, USA. Paralectotype male of Hoff and Bolsterli (1956) at INHS; collected from Caroll Cave, Washington Co., AR, USA. Four female paratypes of Hoff and Bolsterli (1956, 174) at INHS; collected from Fincher Cave, Washington Co., AR, USA. One tritonymph paratype of Hoff and Bolsterli (1956, 174) at INHS.

Remarks.—We report most relevant morphometrics only and follow Chamberlin's (1931) guidelines for straight-line measurements; measurements of other parts are detailed elsewhere for

western populations as *Pseudozaona occidentalis* (Hoff and Bolsterli 1956); for eastern populations as *Hesperochernes holsingeri, Hesperochernes mirabilis,* and *Pseudozaona mirabilis* (Hoff 1946, Muchmore 1974, 1994). We confirm Muchmore's (1994) comments of the high degree of variation within this species: both within populations of specimens collected from a single cave or nearby caves, and also across its wide geographic range. This variation is slightly amplified with our considering *Pseudozaona occidentalis* and *Hesperochernes holsingeri* junior synonyms of *Hesperochernes mirabilis*. All measurements given in mm, with a mean value followed by a range and the number of specimens measured. All measurements from specimens either collected during this study or from loaned museum material.

Etymology.—*Hesperochernes* is a compound of the Latin *hespero-* indicating to the west, or western, and *-chernes*, of a laborer. In combination the genus can be inferred as "western laborer". The specific epithet *mirabilis* is from the Latin for excellent, good, or wonderful. An inferred common name from translating the species name is "Good Western Laborer". However, the common name Southeastern Cave Pseudoscorpion has appeared in print twice now and is appropriately descriptive, given the remarkable range of the species throughout caves of southeastern North America (Niemiller et al. 2013, Zigler et al. 2020).

Description.—Diagnostic characters matching those of family Chernetidae, subfamily Chernetinae, and tribe Chernetini (Menge 1855). Diagnostic characters matching those of genus *Hesperochernes* (Muchmore 1974, 28–30): "lack of an acuminate tactile seta on the tarsus of leg IV; cheliceral seta *b* and *sb* both denticulate terminally; spermathecae of female in form of long, thin tubules with conspicuous, ovoid terminal enlargements; trichobothrium *st* closer to *t* than to *sb*, and *ist* distinctly distad to *est*, which is near middle of finger." Muchmore (1974) considered the large size and attenuation of appendages (pedipalps and legs) modifications for subterranean habitat and not sufficient justification for creation of a new genus or placement into another genus, and without presenting a counter-argument disagreed with Hoff (1946) in placing *Chelifer mirabilis* and *Pseudozaona occidentalis* in *Pseudozaona*, and transferred these two subterranean species to *Hesperochernes*.

Diagnostic features of *H. holsingeri* (Muchmore 1994, 321−323): Large species with slender appendages; "palpal femur 1.30 mm and chela (without pedecil) 1.78 mm long. Palpal femur 4.05 and chela (without pedecil) 3.65 times as long as broad; femur + patella IV 5.8 and tibia 7.9 times as long as deep. Tergites with 13-18 clavodentate setae." Only female known. Error in Muchmore (1994) of material examined: female is holotype, not male, and a tritonymph is the paratype. Described from two specimens. Apparently deemed significantly divergent to be a new species on the basis of it being in Indiana, north of most known localities, and larger than other specimens collected from Indiana specimens ascribed to *H. mirabilis* (Muchmore 1994).

Morphometrics.—Body length 2.98 (2.00-3.86, n=51) for females, 2.50 (2.18-3.13, n=21) for males, 2.11 (1.65-2.67, n=8) for tritonymphs, 1.69 (1.34-2.04, n=4) for deutonymphs, 1.20 (1.00-1.37, n=3) for protonymphs.

Females

Carapace. Without eyes or eye spots; with two distinct transverse furrows; surface coarsely granulate; fungal hyphae or bacterial matts may be affixed to carapace integument. Carapace l/w 1.03 (n=93), carapace length 0.93 (0.64-1.11, n=97), carapace width 0.90 (0.55-1.09, n=98).

Pedipalps. Chela hand generally thickened, varies in robustness; chela hand and palp fingers attenuated relative to epigean congeners. Femur l/w 3.43 (n=88), femur length 0.96 (0.65-1.13, n=88), femur width 0.28 (0.22-0.35, n=88), patella l/w 2.87 (n=83), patella length 0.89 (0.62-1.09, n=83), patella width 0.31 (0.26-0.38, n=83), chela l/w 3.40 (n=155) or 3.60 with pedestal (n=116), chela length 1.46 (1.08-1.69, n=157), chela length with pedestal 1.55 (1.17-1.84, n=116), chela width 0.43 (0.34-0.52, n=155), movable finger length 0.76 (0.57-0.89, n=113).

Leg IV. Femur l/h 1.65 (n=62), femur length 0.28 (0.21-0.35, n=62), femur height 0.17 (0.14-0.20, n=62), patella l/h 3.50 (n=94), patella length 0.63 (0.49-0.76, n=94), patella height 0.18 (0.14-0.22, n=95), femur+patella length 0.76 (0.60-0.89, n=58), femur+patella 4.22 (n=58) times as long as greatest height along fused segments, tibia l/h 6.00 (n=87), tibia length 0.72 (0.56-0.87, n=87), tibia height 0.12 (0.09-0.17, n=87), tarsus l/h 5.78 (n=31), tarsus length 0.52 (0.44-64, n=31), tarsus height 0.09 (0.08-0.10, n=31).

Males

Carapace. Surface texture as with females. Carapace length 0.90 (0.77-1.05, n=52), carapace width 0.82 (0.73-0.92, n=51).

Pedipalps. Attenuated as with females. Femur width 0.27 (0.23-0.40, n=49), femur length 0.92 (0.70-1.05, n=50), patella width 0.30 (0.27-0.42, n=41), patella length 0.85 (0.67-1.00, n=40), chela width 0.42 (0.36-0.58, n=77), chela length 1.41 (1.15-1.57, n=77), chela length with pedestal 1.51 (1.24-1.71, n=57), movable finger length 0.75 (0.58-0.87, n=61).

Leg IV. Femur height 0.17 (0.10-0.21, n=31), femur length 0.26 (0.21-0.29, n=30), patella height 0.17 (0.11-0.23, n=58), patella length 0.60 (0.50-0.72, n=57), femur+patella length 0.73 (0.64-0.84, n=29), tibia height 0.12 (0.10-0.15, n=42), tibia length 0.68 (0.57-0.83, n=42), tarsus height 0.09 (0.08-0.10, n=13), tarsus length 0.52 (0.47-0.55, n=13).

Ecology and Habitat.—Limestone caves in karstic regions of the United States. No epigean records exist nor were recovered from surface sampling efforts in the present study. Within caves, the species is most frequently encountered in the dark zone, rarely in the transition zone, and almost never in the entrance zone. In transition and entrance zones we did not recover it from extensive in-cave leaf litter sampling that we did in all caves with this organic input; sampling this in-cave habitat has not been previously reported. Sampling leaf litter from sinkholes in southern Indiana did not recover *H. mirabilis* but on occasion turned up subterranean insects and pseudoscorpions thought to be trogloxenes or troglophiles, such as *Kleptochthonius griseomanus* (Lewis et al. 2020a, 2020b). Our field collection across the now expanded distribution range of *H. mirabilis* confirmed Muchmore's (1994) comments of a regular and predictable association with bat guano and rodent nests. Highest population numbers were found near or on bat guano, especially under recently or actively roosting bats, in large, occupied woodrat (*Neotoma* spp.) nests, and near recent deposits of scat of raccoon (*Procyon lotor*) or coyote (*Canis latrans*) that did exhibit extensive fungal fruiting bodies. Every cave visited that was observed to be actively used by bats or woodrats as confirmed by visual observations recovered *H. mirabilis*. Population densities were typically high from such caves, ranging from several hundred to a thousand individuals in caves with active roosting bats and recent guano deposits, and 100 individuals or more from caves with active woodrat (*Neotoma* spp.) middens in southern Indiana. In caves without observed guano piles or woodrat middens, we also regularly encountered larger populations of 25-50 individuals near

latrines used by raccoons and coyotes, and from dry decomposed bodies of animals that had died in the cave; in all cases plentiful prey in the form of springtails was observed near these organic inputs to the cave environment. Topotypic material was scant, likely due to past human activity driving out a previously significant Gray Bat (*Myotis grisescens*) population, and more recently, a cave gate that may be preventing bats from reestablishing in Indian Cave. However, we did recover topotypic specimens from *Neotoma* nests in which we visually confirmed the presence of a rodent and noted abundant numbers of external parasites that would be prey for these pseudoscorpions.

Type locality.—Indian Cave, Barren Co., Kentucky, USA, as implied by Banks (1895). We agree with Hoff's (1946) lectotype designation and associated type locality. This is justified by the higher population size encountered at Indian Cave compared to Gilley Cave, Lee Co., VA, which was also listed by Banks (1895) as an implied type locality, and the more centralized position of Indian Cave within the range of the species distribution. Indian Cave is the same type locality listed in Harvey's (1990, 2011, 2013) catalogs.

Distribution.—Known exclusively from limestone caves in karstic regions of the eastern United States. Superscripts: 1, specimen reported exclusively from our field collection; 2, specimen from previously unpublished museum material; 3, collection reported previously in unpublished reports to government or private agencies; 4, cave discovered during study not currently listed in local cave surveys (locality data available upon request); 5, specimen of field collection or museum collection origin from a previously published locality. An asterisk beside a state or county indicates a first published report for that administrative unit. Texas records were not seen or used in molecular analyses and may be questionable. We follow US standards for geographic features and have omitted all non-Latin characters from cave names (United States Board on Governing Names 1901, United States Geological Survey 2019).

ALABAMA. Blount Co.: Catfish Cave, Horse Cave. **Colbert Co.:** Elbow Cave[1], McCluskey Cave, McKinney Cave. **Dekalb Co.:** Cherokee Cave, Dunham Cave, Kelly Girls Cave[1]. **Jackson Co.:** Bucks Pocket Cave, Crossings Cave[1], Doug Green Cave, Dub Green Cave[1], Fern Cave[1], Geiger Cave[1], House of Happiness Cave[1], Pig Pen Cave, Reverb Rotunda[1], Sheldons Cave[1], Swaim Cave, Two Way Cave. **Jefferson Co.:** Cedar Pole Cave, Crystal Caverns, Krawcyzk

Caverns[1]. **Lauderdale Co.:** Basket Cave, Bone Cave, Colliers Cave, Key Cave[5], Slough Cave. **Madison Co.:** Adams Cave[1], ATF Pit[1,4], Blevins Gap Cave[1], Blue Balloon Cave[1], Burwell Cave, Cave Spring Cave[1], Copena Crawl[1], Cottrells Cave[1], Flintknapper Cave[1], Fox Den Cave[1], Hering Cave[1], Hurricane Cave, Matthews Cave[1], Spook Cave. **Marshall Co.:** Cave Mountain Cave, Dunham Cave[5], Merrill Cave, Painted Bluff Cave, Steves Cave, Warrenton Cave.

ARKANSAS. Benton Co.*: Logan Cave[1]. **Marion Co.:** Coon Cave, Flowstone Facade Cave, Square Cave[1], Summer Cave, Summit Cave. **Newton Co.:** Earls Cave, Fitton Spring Cave, Len House Cave, Tony Barnes Cave[1], Van Dyke Spring Cave, Walnut Cave. **Searcy Co.:** Crane Cave, Fallout Cave, In-D-Pendants Cave, Square Cave. **Washington Co.:** Caroll Cave, Fincher Cave, McNeeley Cave[1], Stevensons Cave.

GEORGIA. Catoosa Co.: Chickamauga Cave[5], Crane Cave[5]. **Chattaooga Co.:** Parker Cave[5], Scoggins II Cave[5]. **Dade Co.:** Howards Waterfall Cave[5], Johnsons Crook Cave No 2[5], Kirchmeyer Cave[5], Morrison Cave[5], Morrison Spring Cave[5], SSS Cave[5]. **Murray Co.:** Major Pullims Cave[5]. **Walker Co.:** Battlefield Cave Spring[5], Fricks Cave[5], Hickman Gulf Cave[5], Mountain Cove Farm Cave No. 1[5], Pigeon Cave[5].

ILLINOIS*. Monroe Co.*: Ski Pole Cave[1].

INDIANA. Crawford Co.*: Heron Cave[3], Salt Shake Cave[1]. **Harrison Co.:** Coon Cave[3], Debs Pit[3], Little Mouth Cave[1], Potato Run Cave. **Jefferson Co.:** Elmer Turner Cave[1], Wilsons Cave[5]. **Jennings Co.*:** Crosley Canyon Cave[1]. **Martin Co.*:** Daves Dig Cave[1], Redberry Cave[1]. **Monroe Co.*:** Fultz Saltpeter Cave[1]. **Orange Co.*:** Chris Continuous Crevice Cave[1], Diggers Delight Cave[1], M&M Cave[1], Q1B3 Cave[1]. **Washington Co.*:** Bear Den Cave[3].

KENTUCKY. Barren Co.: Cave Cave[1], Indian Cave[5]. **Bullitt Co.*:** Cave Hollow Cave[1]. **Christian Co.:** Chandler Cave. **Edmonson Co.*:** Little Beauty Cave[1], Whites Cave[1]. **Estill Co.:** Neon Possum Cave[1]. **Harlan Co.:** Saw Mill Cave. **Hart Co.:** Barnes Smith Cave. **Jefferson Co.*:** Hounz Lane Cave[1]. **Laurel Co.*:** Angel Hollow Cave[1]. **Pulaski Co.:** Cedar Creek Cave[1], Redbud Cave[1], Sinking Valley Cave System, Stab Cave[1]. **Warren Co.:** Balance Cave No. 2. **Unknown county:** Ranch Cave[1].

MISSOURI. Barry Co.: Sweet Potato Cave, Onyx Cave[1], Twin Cave[1]. **Camden Co.:** Gar Cave, Onyx Mine Cave. **Carter Co.:** Blue Spring Cave, Buzzard Cave, Crandle Hollow Cave, Cat Track Cave, Upper Camp Yarn Cave[1]. **Christian Co.:** Fitzpatrick Cave[1], Peter Hollow Cave. **Crawford Co.:** Moonshine Cave. **Dade Co.:** Maze Cave. **Dent Co.:** Bounds Branch Cave. **Franklin Co.:**

Hidden Room Cave. **Greene Co.*:** Junction Cave[1]. **Hickory Co.:** Siphon Cave. **Howell Co.:** Spring Creek Cave. **Madison Co.:** Marsh Creek Cave No. 2. **Oregon Co.:** Bat Cave, Bluehole Cave, Corbet Cave, Everett Chaney Cave, Three Entrance Cave. **Ozark Co.:** Bear Mountain Cave, Potato Cave. **Phelps Co.:** Apple Dumpling Cave, Garco Cave, Lane Cave, Phelps Cave, Rogers Cave, Zorumski Cave. **Pulaski Co.:** Campground Cave[1], Killman Cave, Little Cave, Wilson Cave No. 1. **Reynolds Co.:** Cooks Cave. **Shannon Co.:** Davis Cave. **Taney Co.:** Cane Blue Cave No. 2[1], Clayton Cave[1], Marholtz Cave, Zoo Cave. **Texas Co.:** FS Cave 130, FS Cave 135, Unnamed Cave No. 2, Unnamed Cave No. 11.

OHIO. Adams Co.: Cedar Fork Cave[1], Curly Cliff No. 2 Cave[5], Freelands Cave[5], Morrisons Cave[5]. **Highland Co.:** Pseudo Cave. **Ross Co.:** Buckskin Cave I, Skull Cave, Trimmers Cave. **Unknown county:** Merrell Cave.

OKLAHOMA*. Adair Co.*: AD-13[1], Adair Bat Cave[1], Charlie Owl Cave[1], Gallcatcher Cave[1]. **Delaware Co.*:** Twin Cave[1]. **Pontohoc Co.*:** Coal Creek Cave[1]. **Texas Co.*:** Featherhead Cave[1].

TENNESSEE. Anderson Co.: Blowing Springs Cave[1], Rieder Lost Creek Cave[1], Wrights Cave. **Bledsoe Co.*:** Aaron Tollets Cave[1]. **Campbell Co.*:** Panther Cave Nr1[1]. **Cannon Co.*:** Cane Sink Cave[1]. **Claiborne Co.*:** Obie Mill Cave[1], Powell Mountain Cave[1]. **Clay Co.*:** Big Hollow Spring Cave[1], JC Melton Cave[1], Kendall Cave[1]. **Cumberland Co.*:** Mill Cave*. **Davidson Co.*:** Bull Run Cave[1], Gillespie Cave[1], Newsom Branch Cave[1]. **DeKalb Co.*:** Chapman Cave[1], Christmas Cave[1], Cripps Mill Cave[1], Frazier Hollow Cave[1], Henry Rat Cave[1]. **Dickson Co.*:** Bowman Cave[1], Columbia Caverns[1]. **Fentress Co.*:** Cornstarch Cave*, Little Jack Creek Cave*, Reed Creek Cave*, Shane Cave*. **Franklin Co.:** Caney Hollow Cave*, Coons Labyrinth[1], Grapeville Cave, Grapevine Cave[1], Keith Cave[1], Miller Cave, Pennington Cave[1]. **Giles Co.*:** Hurricane Creek Cave[1], Thurstons Domain[1]. **Grundy Co.*:** Big Mouth Cave[1], Coppinger Cave*, Payne Saltpeter Cave*, Pennington Cave*. **Hamilton Co.*:** Tumbling Shoals Cave[1]. **Hickman Co.*:** House Cave[1], Walker Spring Cave[1]. **Jackson Co.:** Carter Cave[1], Carter Creek Cave[1], Duds Cave, Elliott Cave[1], Haile Cave, Flynn Creek Cave[1], Peter Cave[1], West Spivey Cave[1]. **Knox Co.*:** Blowing Hole Cave 1. **Lawrence Co.*:** Long Branch Cave[1]. **Lincoln Co.*:** Haley Cave[1], Kelso Saltpeter Cave[1]. **Loudon Co.*:** Phantom Insurgence Cave[1]. **Marion Co.*:** Clear Spring Cave[1], Excited Cows Cave*, Gilliam Dark Cave[1]. **Marshall Co.*:** Globe Cave[1], Petty Cave[1]. **Maury Co.*:** Billy Stone Cave[1], Darnells Cave[1], Rummage Cave[1]. **Meigs Co.*:** Blythe Ferry Cave[1]. **McMinn Co.*:** McCorckle Cave[1], Too Small Cave[1]. **Monroe Co.*:** Nobletts Cave[1].

Montgomery Co.: Coleman Cave. **Moore Co.:** Dance Cave. **Overton Co.*:** Marie Cave*, Mill Cave[1], Mill Hollow Cave*, Webb Cave[1]. **Perry Co.:** Alexander Cave. **Putnam Co.*:** Ament Cave*, Barr Cave[1], Bartlett Cave[1], Mine Lick Cave*. **Rhea Co.*:** Grassy Creek Cave[1], Piney River Cave[1]. **Rutherford Co.:** Herring Cave. **Smith Co.*:** Lancaster Cave[1], New Salem Cave Nr1[1]. **Sumner Co.*:** Mason Cave[1]. **Union Co.*:** Oaks Cave[1], Rogers Hollow Cave[1]. **Van Buren Co.*:** McElroy Cave*. **Warren Co.*:** Cumberland Caverns*, Dayton Cave[1], Joint Cave*, Little Bat Cave[1], Storage Cave*. **White Co.*:** Ghost River Cave*, Pollard Saltpeter Cave[2], Sparkman Cave*. **Wilson Co.*:** Buzzard Cave[1].

TEXAS: Coryell Co.: Goathead Cave. **Edwards Co.:** Dunbar Cave, Wyatt Cave.

VIRGINIA. Bath Co.: Cave Run Pit Cave. **Giles Co.:** Links Cave[1], Smokehole Cave. **Highland Co.:** Hennevars Cave[1], Vandevander Cave. **Lee Co.:** Gilley Cave[1], Robertson Cave No. 1[1], Pack Rat Cave[1], Secret Cave. **Montgomery Co.*:** Fred Bulls Cave[1], Kyle Cave[1], Salamander Cave[1]. **Roanoke Co.:** Goodwins Cave. **Rockingham Co.:** Church Mountain Cave[1], Eggleston Cave. **Russell Co.:** Boy Scout Cave, Ferguson Hollow Cave, Johnny Lester Riverside Caverns[1]. **Scott Co.:** Basil Duncan Cave, Big Spiders In A Little Maze Cave, Canyon To Nowhere Cave, Creek No. 1 Cave, Darty Cave, Duncan Mill Cave[1], Estes Playground Cave[1], Hillman Cave[1], Kerns Cave[1], McCulle Cave, WR Combs Cave. **Shenandoah Co.*:** Cueva Cellar[1,4], Onyx Ledge Cave[1,4]. **Smyth Co.*:** Beaver Creek Cave[1]. **Tazewell Co.*:** Little Gulley Cave[1]. **Washington Co.:** Davenport Cave, Sally Johnson Cave[1], Three Chambers Cave. **Wythe Co.*:** Early Cave[1].

Acknowledgements

Computing resources were provided by the Alabama Supercomputing Authority (ASC), Auburn University (Hopper), and CIPRES Science Gateway. CDRS was funded by the Cave Conservancy Foundation for both a significant PhD Fellowship and a travel fellowship to present part of this work at the International Society for Subterranean Biology meeting in 2018; by a Ralph Stone Graduate Fellowship from the National Speleological Society; by a Philip M. Smith Graduate Research Grant for Cave and Karst Research from the Cave Research Foundation; by a Meredith Birchfield grant from the Auburn University Museum of Natural History; by the Vincent Roth Fund for Systematics Research from the American Arachnological Society; and by an initial small research grant from Dogwood City Grotto, GA, that purchased initial caving gear used throughout

the extensive fieldwork of this project. Fieldwork would not have been possible without the extraordinary assistance of Matthew Niemiller, Pamela Hart, and Kirk Zigler throughout TAG; Julian J. Lewis in Kentucky, Indiana, and Ohio; Gerald Moni in Tennessee; Tom Malabad and Wil Orndorff in Virginia; Michael Slay in Arkansas; and Rickard Toomey in Kentucky. Many collecting trips were enriched, enabled, or resulted in specimens donated by Evan Carter, Kathy Lavoie, Golpar Garmestani, Naomi Taylor, and Christina Easterwood. Access to the tens of thousands of caves in the eastern USA would not be possible without the previous work of hundreds of cavers and speleologists that have come before us, who have contributed maps, location data, and established relationships with public and private landowners. We were privileged to gain access to these resources through connections and memberships in the National Speleological Society, Alabama Cave Survey, Georgia Speleological Survey, Indiana Cave Survey, Missouri Speleological Survey, Tennessee Cave Survey, and Virginia Speleological Survey. All collections were made with permits issued by state and federal bodies governing natural resources on federal lands and in Alabama, Arkansas, Georgia, Indiana, Kentucky, Missouri, Ohio, Oklahoma, Tennessee, and Virginia.

References

Banks N (1893) New Chernetidae from the United States. Canadian Entomologist 25: 64–67.

Banks N (1895) Notes on the Pseudoscorpionida. Journal of the New York Entomological Society 3: 1–13.

Banks N (1908) The pseudoscorpions of Texas. Bulletin of the Wisconsin Natural History Society 6: 39–42.

Barr TC Jr (1961) Caves of Tennessee. Bulletin 64. State of Tennessee, Department of Conservation and Commerce, Division of Geology, Nashville, TN, USA, 567 pp.

Barr TC Jr (1968) Cave ecology and the evolution of troglobites. Evolutionary Biology 2: 35–102.

Bayona-Vásquez NJ, Glenn TC, Kieran TJ, Pierson TW, Hoffberg SL, Scott PA, Bentley KE, Finger JW, Louha S, Troendle N, Díaz-Jaimes P, Mauricio R, Faircloth BC (2019) Adapterama III: Quadruple-indexed, double/triple-enzyme RADseq libraries (2RAD/3RAD). bioRxiv. https://doi.org/10.1101/205799

Beier M (1930) Die Pseudoskorpione des Wiener Naturhistorischen Museums. III. Annalen des Naturhistorischen Museums in Wien 44: 199–222.

Beier M (1932) Pseudoscorpionidea II. Subord. C. Cheliferinea. Das Tierreich 58: i–xxi, 1–294.

Beier M (1933) Pseudoskorpione aus Mexiko. Zoologischer Anzeiger 104: 91–101.

Beier M (1976) Pseudoscorpione von der Dominicanischen Republik (Insel Haiti). Revue Suisse De Zoologie 83: 45–58.

Berlese A (1904) Apparecchio per raccogliere presto ed in gran numero piccoli arthropodi. Redia 2: 85–89.

Caccone A, Powell JR (1987) Molecular evolutionary divergence among North American cave crickets. II. DNA-DNA hybridization. Evolution 41: 1215–1238.

Campbell JW, Woods M, Ball HL, Pirkle RS, Carey V, Ray CH (2011) Terrestrial macroinvertebrates captured with a baited ramp-pitfall trap from five limestone caves in North Alabama and Georgia (USA) and their association with soil organic matter. Journal of Natural History 45: 2645–2659. https://doi.org/10.1080/00222933.2011.597884

Cardoso RC, Ferreira RL, Souza-Silva M (2021) Priorities for cave fauna conservation in the Iuiú karst landscape, northeastern Brazil: a threatened spot of troglobitic species diversity. Biodiversity and Conservation 30: 1433–1455. https://doi.org/10.1007/s10531-021-02151-5

Chamberlin JC (1924) *Hesperochernes laurae*, a new species of false scorpion from California inhabiting the nest of Vespa. Pan-Pacific Entomologist 5: 89–92.

Chamberlin JC (1931) The arachnid order Chelonethida. Stanford University Publications, Biological Sciences 7: 1–284.

Chamberlin JC (1935) A new species of false scorpion (*Hesperochernes*) from a bird's nest in Montana. The Pan-Pacific Entomologist 11: 37–39.

Chamberlin JC (1952) New and little-known false scorpions (Arachnida, Chelonethida) from Monterey County, California. Bulletin of the American Museum of Natural History 99: 259–312.

Chamberlin RV (1925) Diagnoses of new American Arachnida. Bulletin of the Museum of Comparative Zoology 67: 209–248.

Cokendolpher JC (2009) New troglobitic *Tyrannochthonius* from Fort Hood, Texas (Pseudoscorpionida: Chthoniidae) [Un nuevo *Tyrannochthonius* troglobio de Fort Hood, Texas (Pseudoscorpionida: Chthoniidae)]. Texas Memorial Museum Speleological Monographs 7: 67–78.

Cudmore WW (1986) Nest associates and ectoparasites of the eastern wood rat, *Neotoma floridana*, in Indiana. Canadian Journal of Zoology 64: 353–357.

Culver DC, Christman MC, Elliott WR, Hobbs III HH, Reddell JR (2003) The North American obligate cave fauna: regional patterns. Biodiversity & Conservation 12: 441–468. https://doi.org/10.1023/A:1022425908017

Danecek P, Auton A, Abecasis G, Albers CA, Banks E, DePristo MA, Handsaker RE, Lunter G, Marth GT, Sherry ST, McVean G, Durbin R, 1000 Genomes Project Analysis Group (2011) The variant call format and VCFtools. Bioinformatics 27: 2156–2158. https://doi.org/10.1093/bioinformatics/btr330

Darwin C (1872) The origin of species by means of natural selection, or the preservation of favoured races in the struggle for life. 6th ed. John Murray, London, United Kingdom, 458 pp.

Dixon GB, Zigler KS (2011) Cave-obligate biodiversity on the campus of Sewanee: The University of the South, Franklin County, Tennessee. Southeastern Naturalist 10: 251–266. https://doi.org/10.1656/058.010.0206

Eaton DAR, Overcast I (2020) ipyrad: Interactive assembly and analysis of RADseq datasets. Bioinformatics 36: 2592–2594. https://doi.org/10.1093/bioinformatics/btz966

Ellingsen E (1910) Die Pseudoskorpione des Berliner Museums. Mitteilung aus dem Zoologischen Museum in Berlin 4: 357–423.

Engel AS, Niemiller ML, Zigler KS, Stephen CDR, Carter ET, Paterson AT, Keenan SW, Taylor SJ (2017) Invertebrate and vertebrate cave fauna records for the Appalachian Valley and Ridge. In: Moore K, White S (Eds), Proceedings of the 17th International Congress of Speleology (Ed. 2), July 23–29, Sydney, NSW Australia, Volume 1. Australian Speleological Federation Inc., Sydney, Australia, 82–86. Available from: http://www.uis-speleo.org/index.php?option=com_content&view=article&id=92&Itemid=417.

Finlayson G, Madani G, Dennis G, Harvey M (2015) First reported observation of phoresy of pseudoscorpions on an endemic New Zealand mammal, the lesser short-tailed bat, *Mystacina tuberculata*. New Zealand Journal of Zoology 42: 298–301. https://doi.org/10.1080/03014223.2015.1063517

Francke OF, Villegas-Guzmán GA (2006) Symbiotic relationships between pseudoscorpions (Arachnida) and packrats (Rodentia). Journal of Arachnology 34: 289–298.

Gardner JE (1986) Invertebrate Fauna from Missouri Caves and Springs. Conservation Commission of the State of Missouri, Jefferson City, MO, 72pp.

Garnett WB, Foote BA (1966) Notes on the biology of certain heleomyzid flies of eastern North America (Diptera: Heleomyzidae). Journal of the Kansas Entomological Society 39: 552–555.

Garnett WB, Foote BA (1967) Biology and immature stages of *Pseudoleria crassata* (Diptera: Heleomyzidae). Annals of the Entomological Society of America 60: 126–134.

Gill GD (1962) The heleomyzid flies of America north of Mexico (Diptera: Heleomyzidae). Proceedings of the United States National Museum 113: 495–603.

Gill GD, Peterson BV (1987) Heleomyzidae. In: McAlpine JF (Ed.), Manual of Nearctic Diptera. Volume 2. Biosystematics Research Centre, Ottawa, Ontario, Canada, 309–316.

Glenn TC, Bayona-Vasquez NJ, Kieran TJ, Pierson TW, Hoffberg SL, Scott PA, Bentley KE, Finger JW, Watson PR, Louha S, Troendle N, Diaz-Jaimes P, Mauricio R, Faircloth BC (2017) Adapterama III: Quadruple-indexed, triple-enzyme RADseq libraries for about $1USD per Sample (3RAD). https://doi.org/10.1101/205799

Graening GO, Slay ME, Tinkle KK (2003) Subterranean biodiversity of Arkansas, part 1: Bioinventory and bioassessment of caves in the Sylamore Ranger District, Ozark National Forest, Arkansas. Journal of the Arkansas Academy of Science 57. Available from: http://www.ozarksubterranea.com/GraeningSlayTinkle2004.pdf (July 18, 2013).

Graening GO, Slay ME, Bitting C (2006) Cave fauna of the Buffalo National River. Journal of Cave and Karst Studies 68: 153–163.

Hagen H (1879) Hoehlen-Chelifer in Nord-America. Zoologischer Anzeiger 2: 399–400.

Hall CN (1997) Protection of karst lands by The Nature Conservancy. In: Special Publication 3. Conservation and Protection of the Biota of Karst. Extended Abstracts and Field-Trip Guide for the symposium held February 13 through 16, 1997 Nashville, Tennessee. Karst Waters Institute, Charles Town, WV, USA, 20–22.

Harker Jr. DF, Barr Jr. TC (1980) Western Kentucky coal field: preliminary investigations of natural features and cultural resources. Volume II. Caves and associated fauna of the western Kentucky coal field. Kentucky Nature Preserves Commission, Frankfort, KY, USA. Technical Report, 114pp.

Harvey MS (1989) Two new cavernicolous chthoniids from Australia, with notes on the generic placement of the south-western Pacific species attributed to the genera *Paraliochthonius* Beier and *Morikawia* Chamberlin (Pseudoscorpionida: Chthoniidae). Bulletin of the British Arachnological Society 8: 21–29.

Harvey MS (1990) Catalogue of the Pseudoscorpionida. Manchester University Press, Manchester, United Kingdom, 726 pp.

Harvey MS (2011) Pseudoscorpions of the World, version 2.0. Western Australian Museum, Perth. Available from: http://www.museum.wa.gov.au/catalogues/pseudoscorpions (February 24, 2015).

Harvey MS (2013) Pseudoscorpions of the World, version 3.0. Western Australian Museum, Perth. Available from: http://museum.wa.gov.au/catalogues-beta/pseudoscorpions (June 23, 2019).

Harvey MS, Wynne JJ (2014) Troglomorphic pseudoscorpions (Arachnida: Pseudoscorpiones) of northern Arizona, with the description of two new short-range endemic species. Journal of Arachnology 42: 205–219. https://doi.org/10.1636/K14-34.1

Hobbs HH III, Flynn MF (1981) The cave fauna of Ohio. Pholeos 1: 7–14.

Hobbs HH III, Hazelton EA (2010) A pictorial preliminary assessment of the cave fauna of Ohio. Pholeos 28: 4–32.

Hobbs HH III, Hazelton EA (2011) An assessment of the biodiversity of the caves and rock shelters of Ohio. Grant Final Report. Ohio Cave Survey, 120pp.

Hoff CC (1945) *Hesperochernes canadensis*, a new chernetid pseudoscorpion from Canada. American Museum Novitates 1273: 1–4.

Hoff CC (1946) A study of the type collections of some pseudoscorpions originally described by Nathan Banks. Journal of the Washington Academy of Sciences 36: 195–205.

Hoff CC (1948) *Hesperochernes thomomysi*, a new species of chernetid pseudoscorpion from California. Journal of the Washington Academy of Sciences 38: 340–345.

Hoff CC (1949) The pseudoscorpions of Illinois. State of Illinois Department of Registration and Education Natural History Survey Division Bulletin 24: 411–499.

Hoff CC (1956) Pseudoscorpions of the family Chernetidae from New Mexico. American Museum Novitates 1800: 1–66.

Hoff CC (1958) List of the pseudoscorpions of North America north of Mexico. American Museum Novitates 1875: 1–50.

Hoff CC (1963) Pseudoscorpions from the Black Hills of South Dakota. American Museum Novitates 2134: 1–10.

Hoff CC, Clawson DL (1952) Pseudoscorpions from rodent nests. American Museum Novitates 1585: 1–38.

Hoff CC, Bolsterli JE (1956) Pseudoscorpions of the Mississippi River drainage basin area. Transactions of the American Microscopical Society 75: 155–179.

Holsinger JR (1963) Annotated checklist of the macroscopic troglobites of Virginia with notes on their geographic distribution. Bulletin of the National Speleological Society 25: 23–36.

Holsinger JR, Culver DC (1988) The invertebrate cave fauna of Virginia and a part of eastern Tennessee: zoogeography and ecology. Brimleyana: 1–162.

Holsinger JR, Culver DC, Hubbard Jr. DA, Orndorff WA, Hobson CS (2013) The invertebrate cave fauna of Virginia. Banisteria 42: 9–56.

Knudsen JW (1956) Pseudoscorpions, a natural control of Siphonaptera in *Neotoma* nests. Bulletin of the Southern Californian Academy of Sciences 55: 1–6.

Lewis J, Milne M, Lewis S, Stephen C, Dunlap K, Dourson D (2020a) Sinkholes – biodiversity hotspots of epigean terrestrial karst ecosystems on the Hoosier National Forest. In: Orndorff WD, Lewis JJ, Kosič Ficco K, Weberg MH, Orndorff ZW (Eds), 2019 National Cave and Karst Management Symposium Proceedings, 7-11 October 2019, Bristol, Virginia. National Speleological Society, Huntsville, AL, USA, 86–88. Available from: http://nckms.org/proceedings.

Lewis JJ (1983) The obligatory subterranean invertebrates of glaciated southeastern Indiana. Bulletin of the National Speleological Society 45: 34–40.

Lewis JJ (1998) The subterranean fauna of the Blue River area. Species at Risk Program, U.S. Geological Survey; The Nature Conservancy; Natural Heritage Program, Indiana DNR, Division of Nature Preserves, Washington, District of Columbia, 241pp.

Lewis JJ (2005) Bioinventory of caves of the Cumberland Escarpment area of Tennessee. Technical report. Tennessee Chapter of The Nature Conservancy, Nashville, Tennessee, 158pp.

Lewis JJ, Lewis SL (2005a) Cave fauna study for the Interstate 66 EIS (Somerset to London, Kentucky). In: Proceedings of the 2005 National Cave and Karst Management Symposium: NCKMS Steering Committee. , 15–20. Available from: http://www.nckms.org/2005/pdf/Papers/lewis%20I-66.pdf (February 14, 2014).

Lewis JJ, Lewis SL (2005b) Inventory of the subterranean fauna of Tims Ford State Park, Franklin County, Tennessee. Lewis & Associates LLC. Cave, Karst, and Groundwater Consulting, Borden, IN

Lewis JJ, Lewis SL (2007) A biological reconnaissance of selected caves in the Highland Rim area of central Tennessee. Final Report. The Nature Conservancy Tennessee Chapter Cave Program, 42pp.

Lewis JJ, Pursell FA, Huffman H (1997) The biological inventory of caves of the Blue River Bioreserve. In: Special Publication 3. Conservation and Protection of the Biota of Karst. Extended Abstracts and Field-Trip Guide for the symposium held February 13 through 16, 1997. Nashville, Tennessee. Karst Waters Institute, Charles Town, WV, USA, 37–41.

Lewis JJ, Whitaker JO Jr, Krantz GW (2010) A biological reconnaissance of the invertebrate fauna of twelve Tennessee caves with notes on the guanophilic mites of the genus *Macrocheles*. Journal of the Tennessee Academy of Science 85: 53–61.

Lewis JJ, Moss P, Tecic D, Nelson ME (2003) A conservation focused inventory of subterranean invertebrates of the southwestern Illinois karst. Journal of Cave and Karst Studies 65: 9–21.

Lewis JJ, Milne MA, Stephen CDR, Dourson DC (2020b) Karst sinkholes as foci of biodiversity in the Hoosier National Forest. Journal of Cave and Karst Studies 82: 169–182. https://doi.org/10.4311/2020LSC0103

Lira AFA, Tizo-Pedroso E, Albuquerque CMR (2014) Phoresy by *Americhernes* aff. *incertus* (Pseudoscorpiones: Chernetidae) on a tropical fly *Fannia canicularis* (Diptera: Fanniidae) in a fragment of the Atlantic Forest, Brazil. Entomological News 124: 24–28. https://doi.org/10.3157/021.124.0103

Lloyd JE, Muchmore WB (1975) Pseudoscorpions phoretic on fireflies II. The Florida Entomologist 58: 241–242.

Macfadyen A (1953) Notes on methods for the extraction of small soil arthropods. Journal of Animal Ecology 22: 65–77. https://doi.org/10.2307/1691

Maher SP, Kramer AM, Pulliam JT, Zokan MA, Bowden SE, Barton HD, Magori K, Drake JM (2012) Spread of White-Nose Syndrome on a network regulated by geography and climate. Nature Communications: 1306. https://doi.org/10.1038/ncomms2301

McDaniel VR, Paige KN, Tumlinson CR (1979) Cave fauna of Arkansas: Additional invertebrate and vertebrate records. Journal of the Arkansas Academy of Science 33: 84–85.

Menge A (1855) Ueber die Scheerenspinnen. Neueste Schriften der naturforschenden Gesselschaft, Danzig 5: 513–525.

Miller MA, Pfeiffer W, Schwartz T (2011) The CIPRES Science Gateway: A community resource for phylogenetic analyses. In: Proceedings of the 2011 TeraGrid Conference: Extreme Digital Discovery. New York, NY. Available from: http://dl.acm.org/citation.cfm?id=872857 (July 9, 2013).

Minh BQ, Schmidt HA, Chernomor O, Schrempf D, Woodhams MD, von Haeseler A, Lanfear R (2020) IQ-TREE 2: new models and efficient methods for phylogenetic inference in the genomic era. Teeling E (Ed.). Molecular Biology and Evolution 37: 1530–1534. https://doi.org/10.1093/molbev/msaa015

Moles ML (1914) A pseudoscorpion from poplar trees. Journal of Entomology and Zoology 6: 81–83.

Muchmore WB (1971a) On phoresy in pseudoscorpions. Bulletin of the British Arachnological Society 2: 38.

Muchmore WB (1971b) Phoresy by North and Central American pseudoscorpions. Proceedings of the Rochester Academy of Science 12: 79–97.

Muchmore WB (1974) Clarification of the genera *Hesperochernes* and *Dinocheirus* (Pseudoscorpionida, Chernetidae). Journal of Arachnology 2: 25–36.

Muchmore WB (1990) Pseudoscorpionida. In: Dindal DL (Ed.), Soil Biology Guide. John Wiley and Sons, New York, New York, United States, 503–527.

Muchmore WB (1992) Cavernicolous pseudoscorpions from Texas and New Mexico (Arachnida: Pseudoscorpionida). Texas Memorial Museum, Speleological Monographs 3: 127–153.

Muchmore WB (1994) Some pseudoscorpions (Arachnida: Pseudoscorpionida) from caves in Ohio and Indiana, U.S.A. Transactions of the American Microscopical Society 113: 316–324.

Murienne J, Harvey MS, Giribet G (2008) First molecular phylogeny of the major clades of Pseudoscorpiones (Arthropoda: Chelicerata). Molecular Phylogenetics and Evolution 49: 170–84.

Nelson S Jr (1975) A systematic study of Michigan Pseudoscorpionida. American Midland Naturalist 93: 257–301.

Niemiller ML, Zigler KS (2013) Patterns of cave biodiversity and endemism in the Appalachians and Interior Plateau of Tennessee, USA. PLoS ONE 8: e64177. https://doi.org/10.1371/journal.pone.0064177

Niemiller ML, Zigler KS, Fenolio DB (2013) Cave Life of TAG. Biology Section of the National Speleological Society, Huntsville, AL, US, 45 pp.

Niemiller ML, Zigler KS, Stephen CDR, Carter ET, Paterson AT, Taylor SJ, Engel AS (2016) Vertebrate fauna in caves of eastern Tennessee within the Appalachians karst region, USA. Journal of Cave and Karst Studies 78: 1–24.

Packard AS (1888) The cave fauna of North America, with remarks on the anatomy of the brain and origin of the blind species. Memoirs of the National Academy of Sciences 4: 3–156, 15 pls.

Packard AS (1894) On the origin of the subterranean fauna of North America. The American Naturalist 28: 727–751.

Peck SB (1989) The cave fauna of Alabama: Part I. The terrestrial invertebrates (excluding insects). Bulletin of the National Speleological Society 51: 11–33.

Perez-Gelabert DE (2008) Arthropods of Hispaniola (Dominican Republic and Haiti): a checklist and bibliography. Zootaxa 1831: 1–530.

Reddell JR, Mitchell RW (1971) A checklist of the cave fauna of Mexico. I. Sierra de el Abra, Tamaulipas and San Luis Potosi. In: Association for Mexican Cave Studies. Bulletin 4. Speleo Press, Austin, Texas, United States, 137–180.

Reeves WK (2001) Invertebrate and slime mold cavernicoles of Santee Cave, South Carolina, U.S.A. Proceedings of the Academy of Natural Sciences of Philadelphia 151: 81–85. https://doi.org/10.1635/0097-3157(2001)151[0081:IASMCO]2.0.CO;2

Reeves WK, Jensen JB, Ozier JC (2000) New faunal and fungal records from caves in Georgia, USA. Journal of Cave and Karst Studies 62: 169–179.

Salvidio S, Oneto F, Ottonello D, Costa A, Romano A (2014) Trophic specialisation at the individual level in a terrestrial generalist salamander. Canadian Journal of Zoology: 141117143819004. https://doi.org/10.1139/cjz-2014-0204

Samoray S (2011) 2011 White-Nose SSyndrome monitoring and bat population survey of hibernacula in Tennessee. Tennessee Chapter of The Nature Conservancy, Nashville, Tennessee, 29pp.

Sato H (1983) *Hesperochernes shinjoensis*, a new pseudoscorpion (Chernetidae) from Japan. Bulletin of the Biogeographical Society of Japan 38: 31–34.

Slay ME, Niemiller ML, Sutton M, Taylor SJ (2016) Cave life of the Ozarks. Biology Section of the National Speleological Society, Huntsville, AL, US, 45 pp.

Snider RJ, Nelson SO (1991) Michigan Pseudoscorpionida, a checklist. Michigan Academician 24: 259–263.

Stamatakis A (2014) RAxML version 8: a tool for phylogenetic analysis and post-analysis of large phylogenies. Bioinformatics. https://doi.org/10.1093/bioinformatics/btu033

Stephen CDR (2012) Alabama Rhinotermitidae: Nomenclature, Identification, Survey, and Phenology. Masters. Auburn University

Stephen CDR, Harvey MS (2018) William B. Muchmore (1920-2017): his taxonomic contributions and a complete bibliography. Journal of Cave and Karst Studies 80: 39–48. https://doi.org/10.4311/1700036R1

Tullgren A (1918) Ein sehr einfacher Ausleseapparat für terricole Tierformen. Zeitschrift für Angewandte Entomologie 4: 149–150. https://doi.org/10.1111/j.1439-0418.1918.tb00820.x

United States Board on Governing Names (1901) Second report of the United States Board on Geographic Names 1890-1899. United States Board on Governing Names, Washington, DC, US, 150pp.

United States Geological Survey (2019) U.S. Board on Geographic Names, Domestic Names. Available from: https://www.usgs.gov/core-science-systems/ngp/board-on-geographic-names/domestic-names.

Viana ACM, Ferreira RL (2021) A new troglobitic species of *Allochthonius* (subgenus *Urochthonius*) (Pseudoscorpiones, Pseudotyrannochthoniidae) from Japan. Subterranean Biology 37: 43–55. https://doi.org/10.3897/subtbiol.37.58580

Weary DJ, Doctor DH (2014) Karst in the United States: a digital map collection and database. U.S. Geological Survey Open-File Report 2014-1156. U.S. Geological Survey, Washington, District of Columbia, 23pp. Available from: http://dx.doi.org/10.3133/ofr20141156.

Wheeler QD (2004) Taxonomic triage and the poverty of phylogeny. Philosophical Transactions of the Royal Society of London. Series B: Biological Sciences 359: 571–583.

Wickham H, Chang W, Henry L, Pedersen TL, Takahashi K, Wilke C, Woo K, Yutani H, RStudio (2019) ggplot2: Create elegant data visualisations using the grammar of graphics. Available from: https://cran.r-project.org/package=ggplot2.

WNS Decontamination Team (2012) National White-Nose Syndrome decontamination protocol - version 06.25.2012. 5pp.

Zigler KS, Niemiller ML, Stephen CDR, Ayala BN, Milne MA, Gladstone NS, Engel AS, Jensen JB, Camp CD, Ozier JC, Cressler A (2020) Biodiversity from caves and other subterranean habitats of Georgia, USA. Journal of Cave and Karst Studies 82: 125–167. https://doi.org/10.4311/2019LSC0125

Zukal J, Bandouchova H, Bartonicka T, Berkova H, Brack V, Brichta J, Dolinay M, Jaron KS, Kovacova V, Kovarik M, Martínková N, Ondracek K, Rehak Z, Turner GG, Pikula J (2014) White-Nose Syndrome fungus: a generalist pathogen of hibernating bats. Boyles JG (Ed.). PLoS ONE 9: e97224. https://doi.org/10.1371/journal.pone.0097224

Fig. 3.1. Map of cave collection effort: (a) east of Mississippi River; (b) west of Mississippi River. In both maps, red circles indicate collection with CDRS directly involved; blue squares indicate cave collection efforts with collaborators who donated pseudoscorpions identified by CDRS. Grey regions indicate karst (Weary and Doctor 2014).

(a)

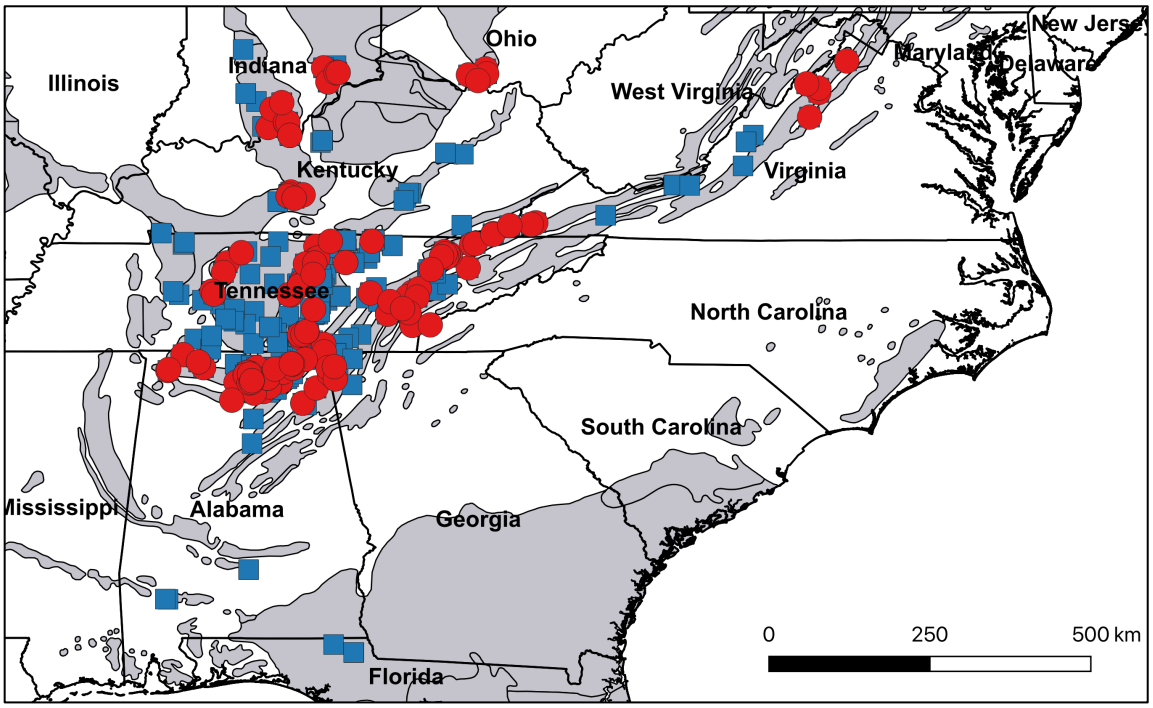

(b)

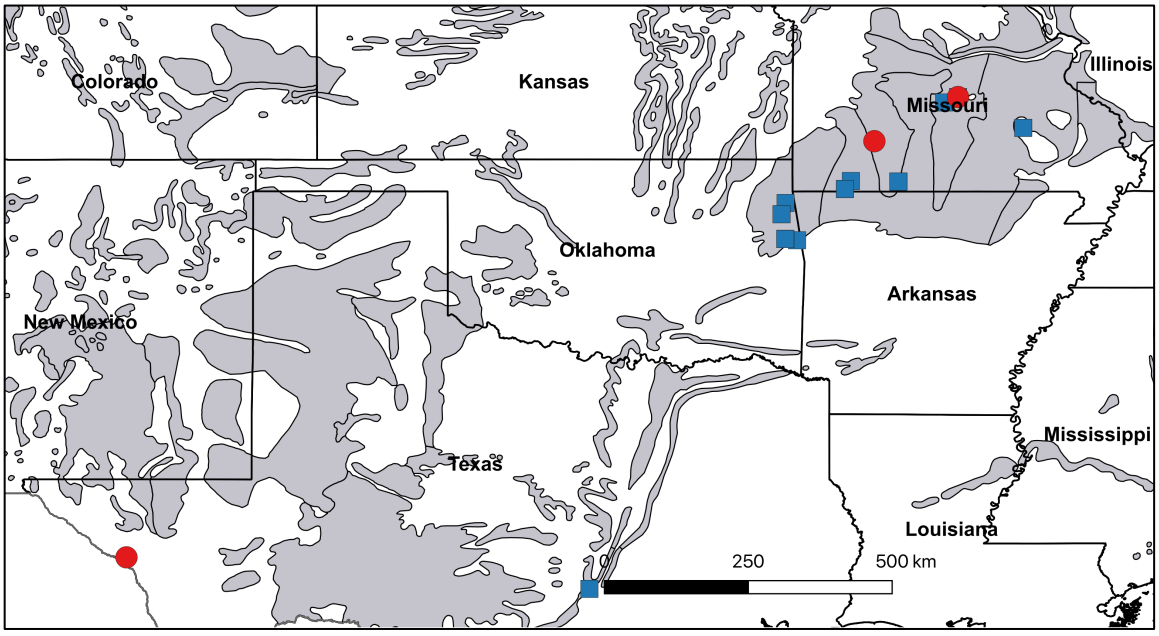

Fig. 3.2. Map of surface collection effort by bulk sampling of leaf litter. Karstic regions indicated in grey. This sampling method was highly successful in collecting pseudoscorpions but did not recover *Hesperochernes*. Grey regions indicate karst (Weary and Doctor 2014).

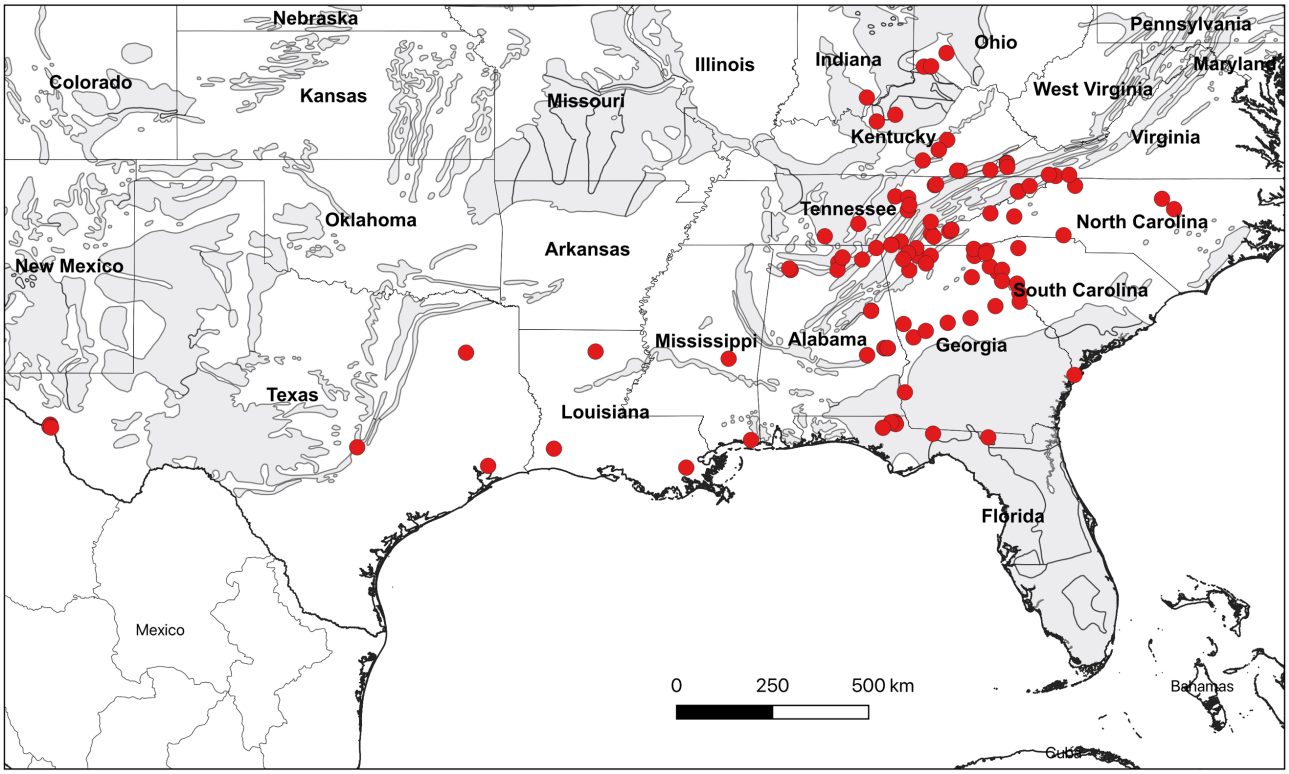

Fig. 3.3. Maps of surface collection effort by sticky trap sampling programs: (a) in red, subterranean termite sticky traps in place from 2010-2011 years in triplicate at each locality and replaced weekly; (b) *Lymantria dispar* sticky traps in place May through August in only 2010 (green), 2010 and 2011 (orange) or only 2011 (red). All traps were checked and this sampling method did occasionally result in a collection of a pseudoscorpion associated with a flying insect but did not recover *Hesperochernes*. Grey regions indicate karst (Weary and Doctor 2014).

(a)

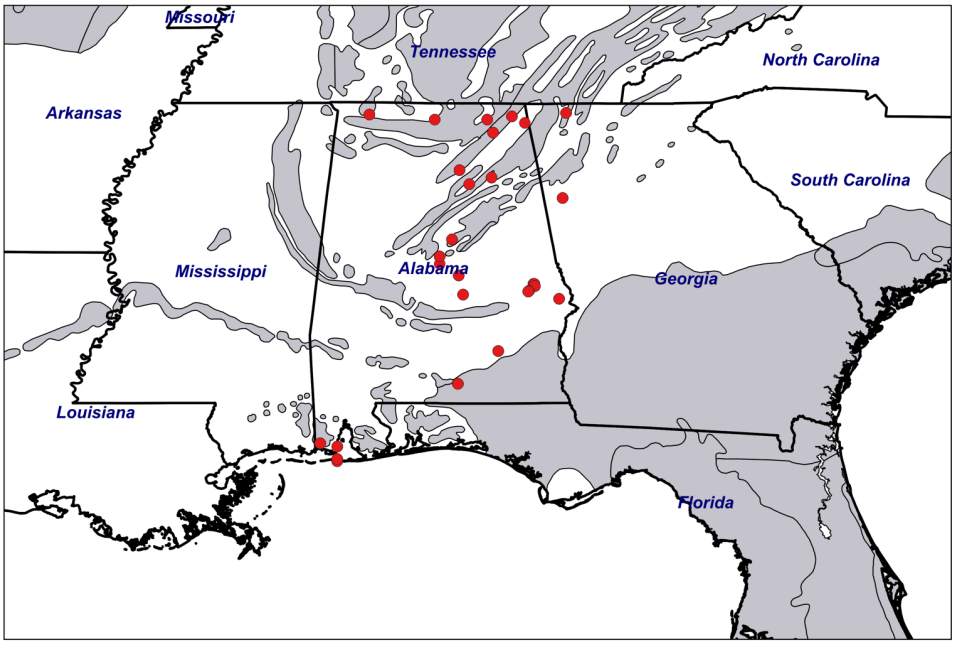

(b)

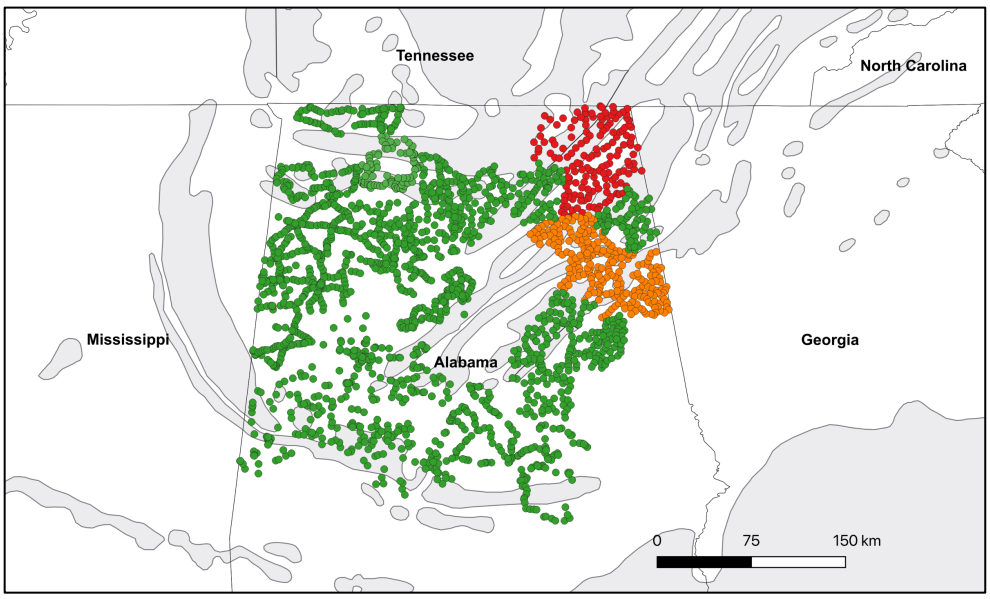

Fig. 3.4. Map of pilot study region. Yellow diamonds represent cave localities in Oklahoma and Tennessee where *Hesperochernes* were sampled, usable DNA extracted, and COI successfully amplified. Grey regions indicate karst (Weary and Doctor 2014).

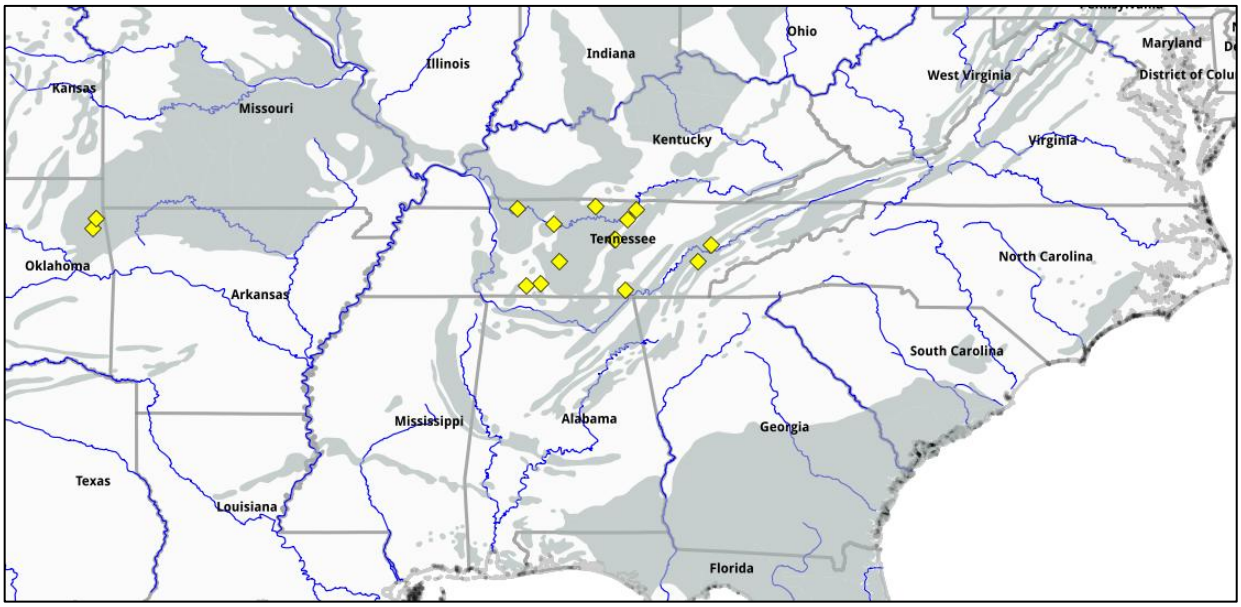

Fig. 3.5 Bayesian tree from pilot study: generated tree of aligned COI sequences with both forward and reverse sequences on same tree. Numbers on nodes indicate posterior support probabilities. Samples coded beginning with a T indicate Tennessee localities; those starting with O indicate Oklahoma localities. Outgroups are specimens of families Chthoniidae and Neobisiidae collected and identified by CDRS.

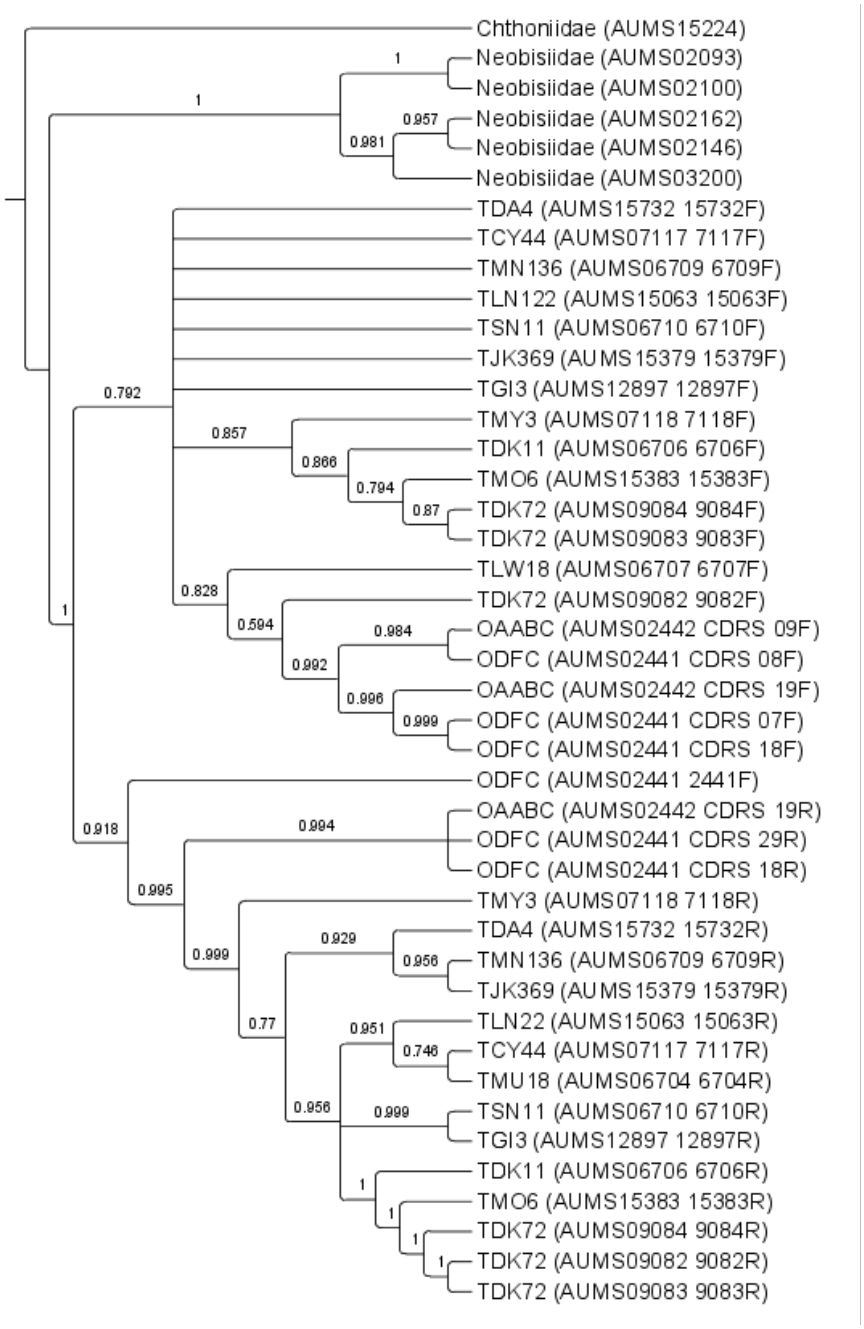

Fig. 3.6 Genital region of female *Hesperochernes holsingeri*. Specimen catalog number CS821.3, collected by CDRS and J.J. Lewis from type locality in Jefferson County, Indiana and accessioned at AUMNH. Specimen cleared in lactic acid, oriented ventrally, mounted in glycerol, and drawn from slide at 200x magnification.

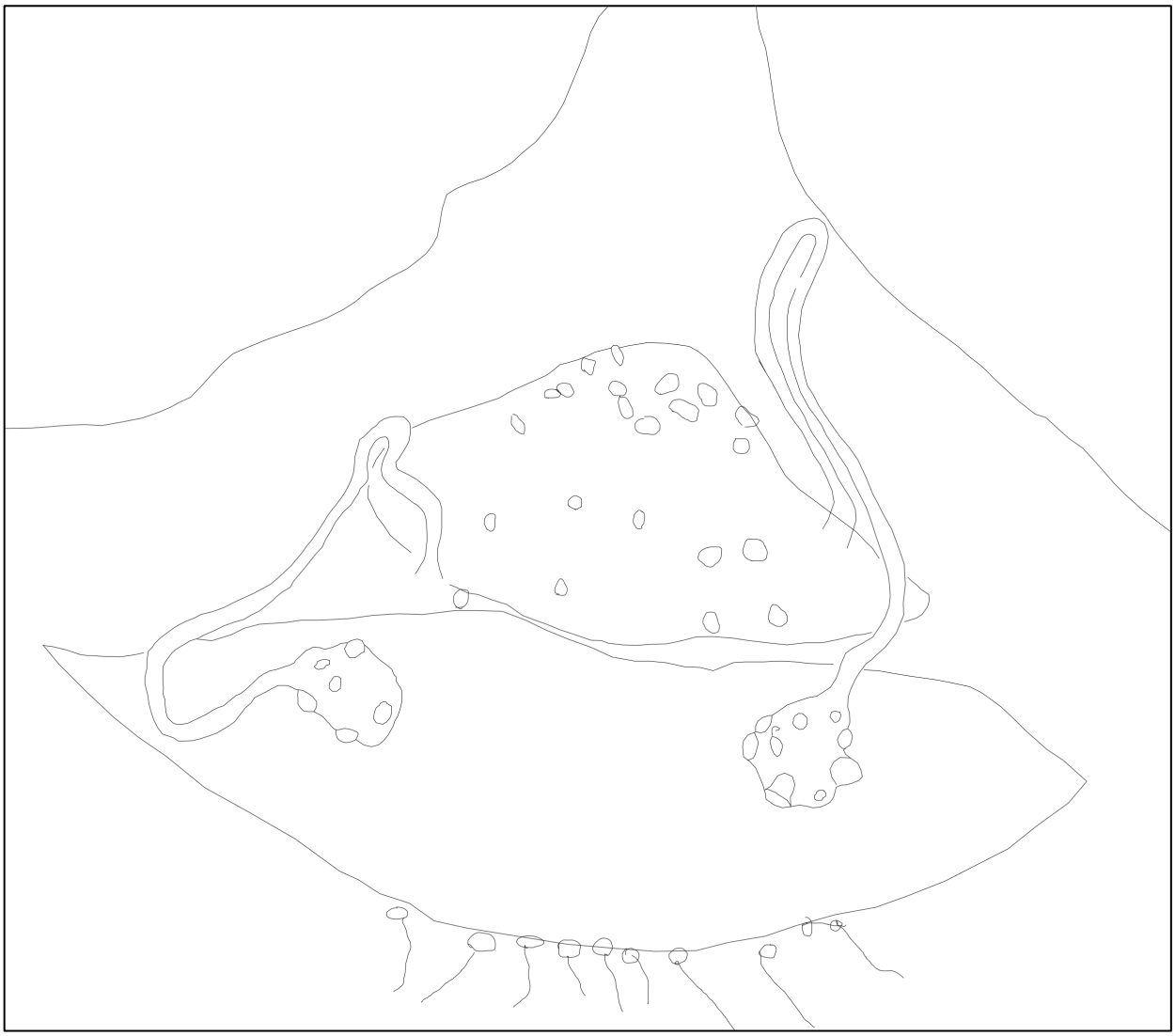

Fig. 3.7 Genital region of female *Hesperochernes mirabilis.* Specimen catalog number CS803.4, from type locality in Lee County, Virginia, collected by CDRS and accessioned at AUMNH. Specimen cleared in lactic acid, oriented ventrally, mounted in glycerol, and drawn from slide at 200x magnification.

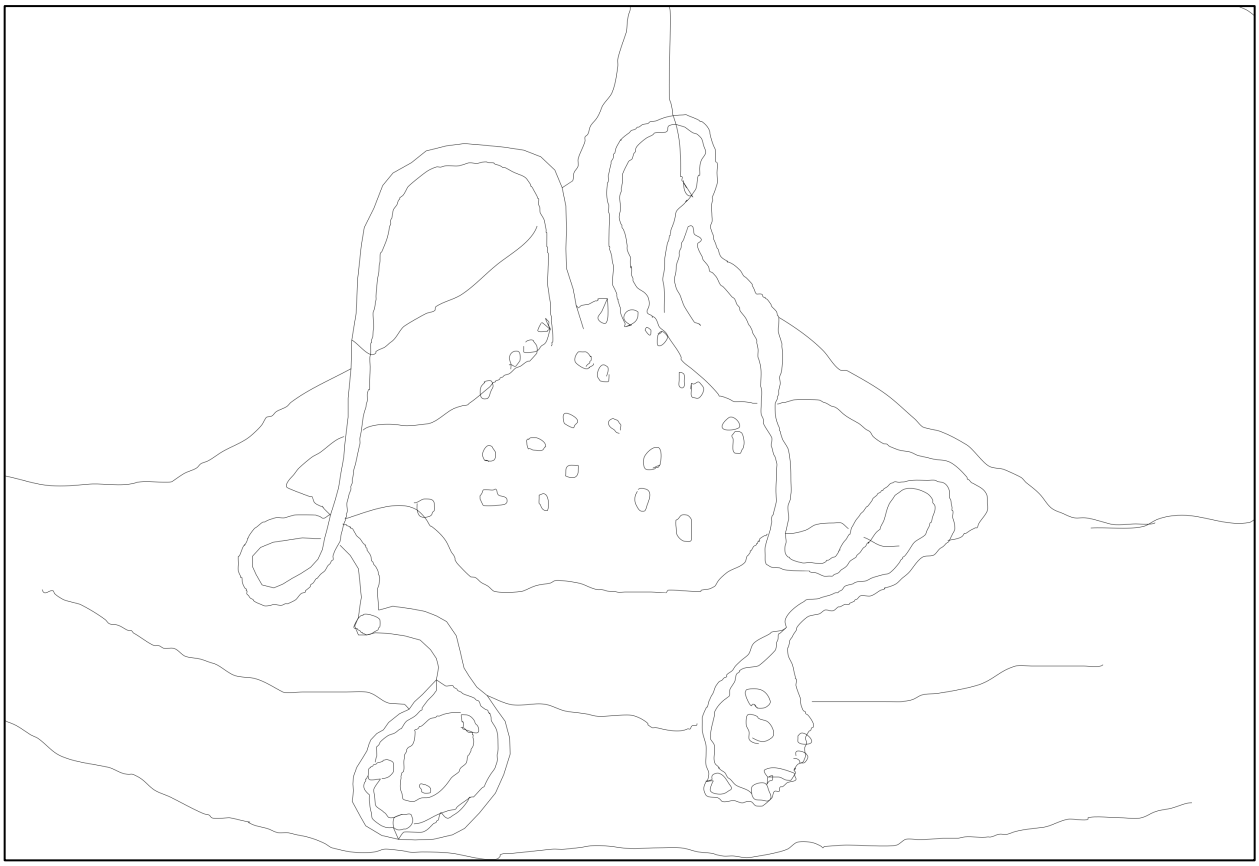

Fig. 3.8 Genital region of female *Hesperochernes occidentalis*. Specimen catalog number CS803.4, near-topotypic material collected in same county as cave of holotype and cave of paratypes, collected by M. Slay and accessioned at AUMNH. Specimen cleared in lactic acid, oriented ventrally, mounted in glycerol, and drawn from slide at 200x magnification.

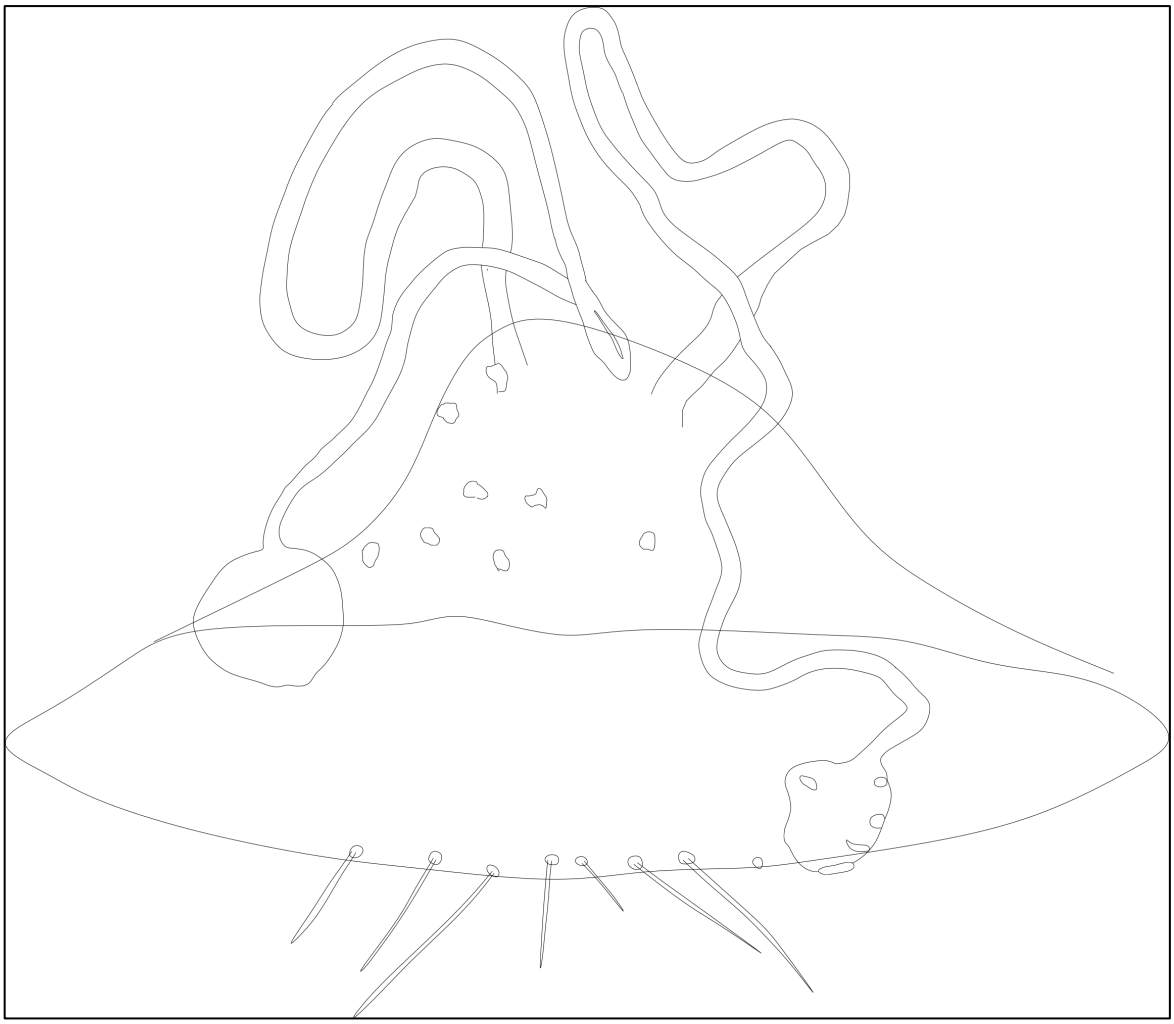

Fig. 3.9 Genital region of female *Hesperochernes tamiae.* Specimen catalog number CS873.2, paratype from type locality matching that of holotype, on loan from ZMB. Specimen cleared in lactic acid, oriented ventrally, mounted in glycerol, and drawn from slide at 200x magnification.

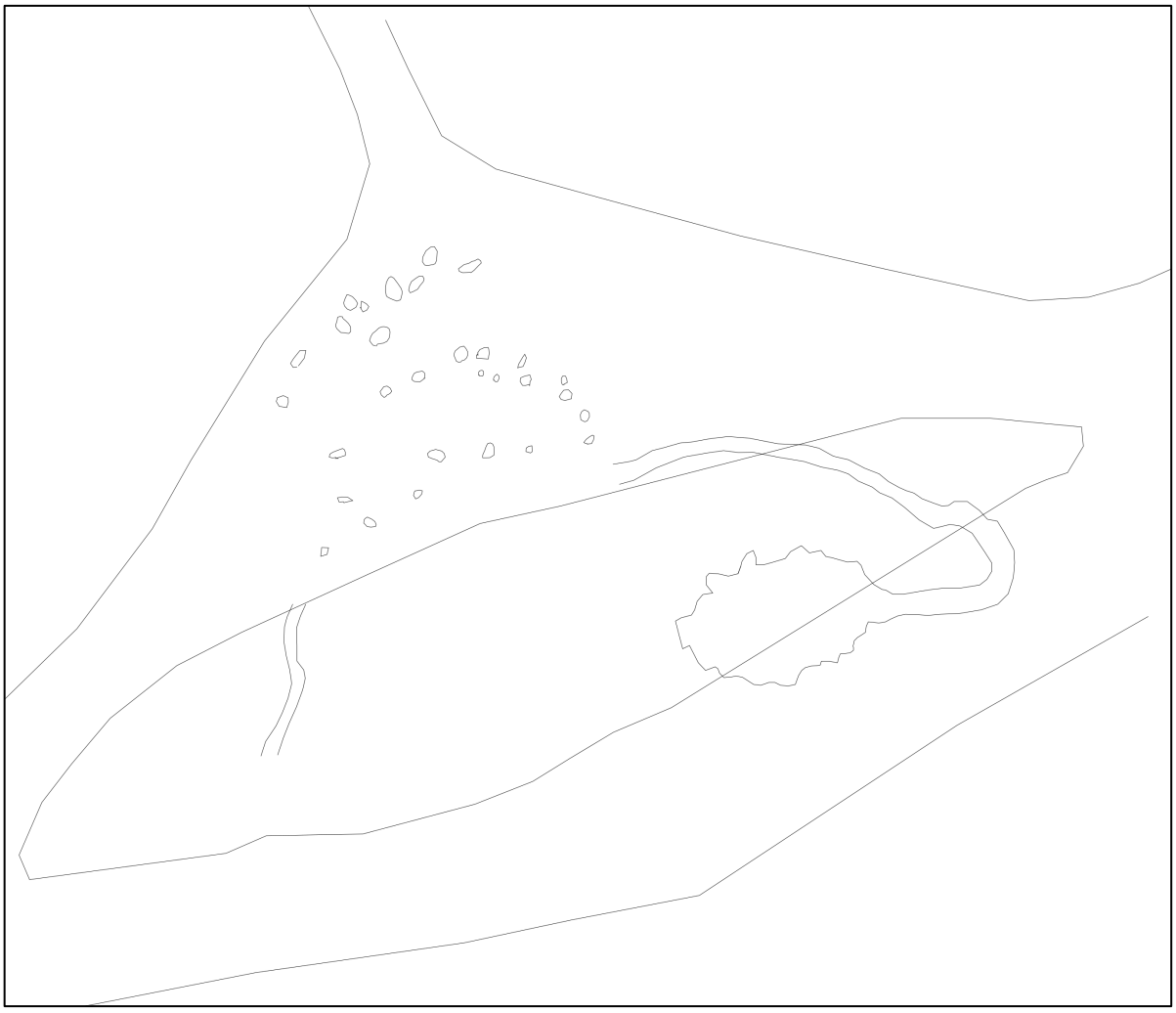

Fig. 3.10 Genital region of male *Hesperochernes holsingeri*. Specimen catalog number CS82.12, collected by CDRS and J.J. Lewis from type locality in Jefferson County, Indiana and accessioned at AUMNH.. Specimen cleared in lactic acid, oriented ventrally, mounted in glycerol, and drawn from slide at 200x magnification.

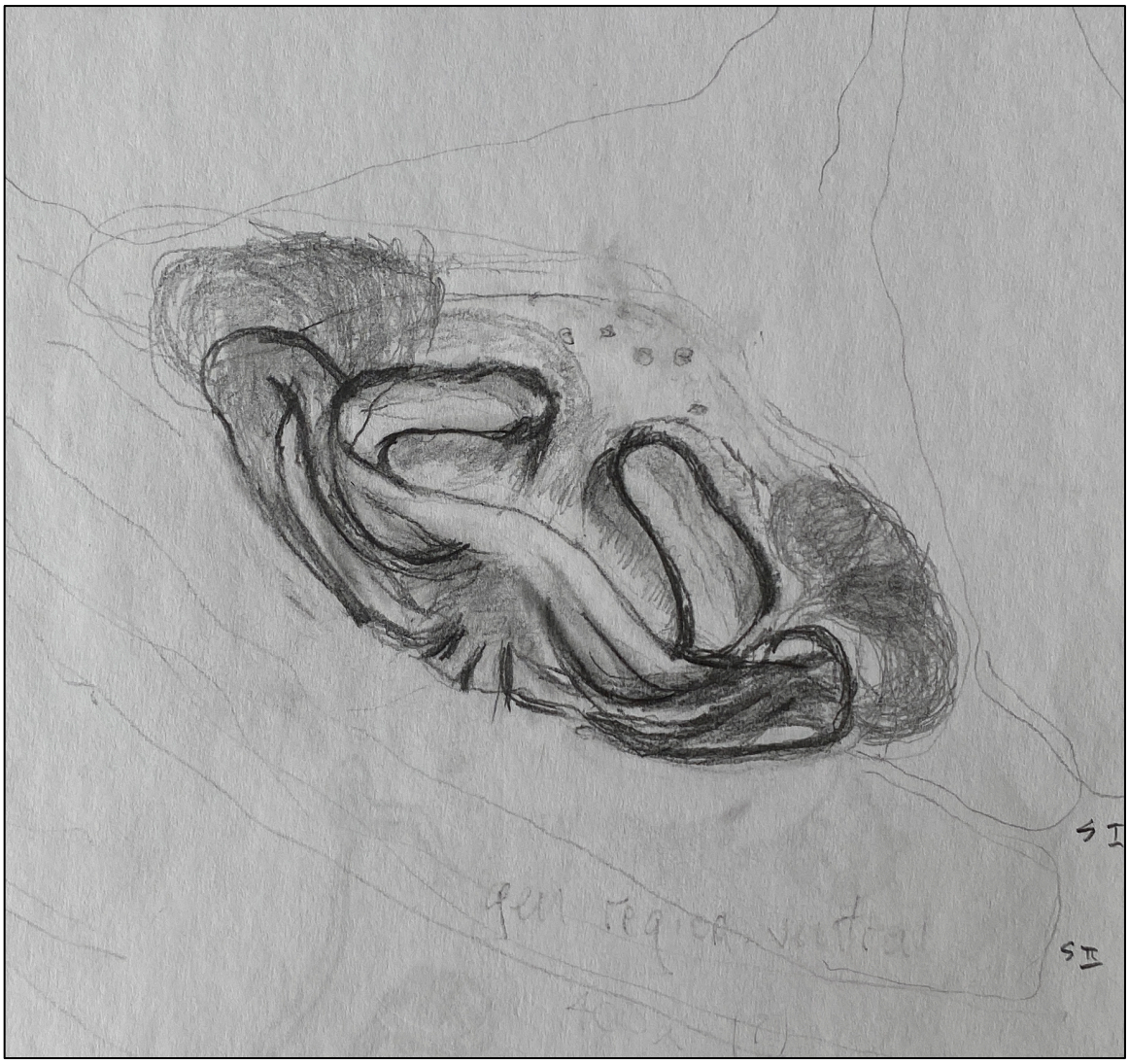

Fig. 3.11 Genital region of male *Hesperochernes mirabilis*. Specimen catalog number C415.3, collected by CDRS and J.J. Lewis from western type locality of Indian Cave, Barren County, Kentucky and accessioned at AUMNH.. Specimen cleared in lactic acid, oriented ventrally, mounted in glycerol, and drawn from slide at 200x magnification.

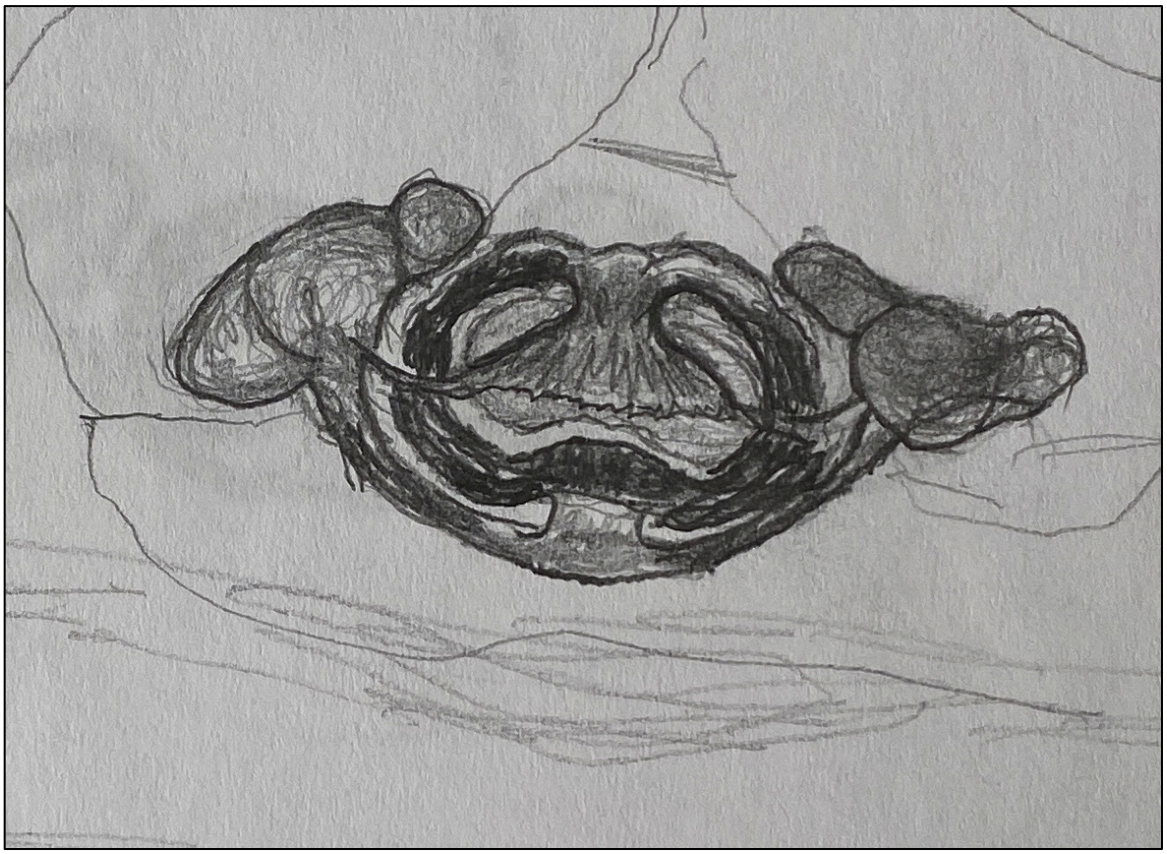

Fig. 3.12 Genital region of male *Hesperochernes occidentalis*. Specimen catalog number CS803.3, collected by M. Slay and P. Ardiapole from near type locality in McNeely Cave, Washington County, Arkansas and accessioned at AUMNH.. Specimen cleared in lactic acid, oriented ventrally, mounted in glycerol, and drawn from slide at 200x magnification.

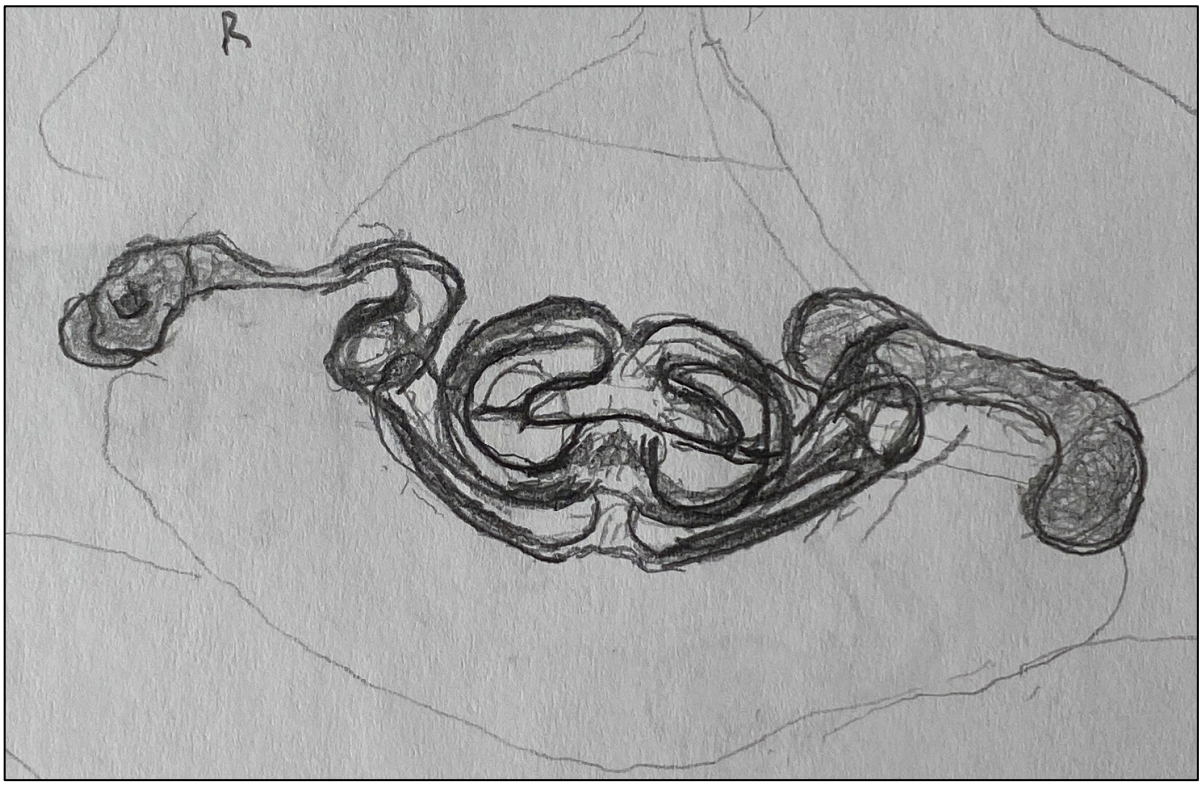

Fig. 3.13 Genital region of male *Hesperochernes tamiae*, paratype. Specimen catalog number CS873.1, collected from a ground squirrel nest (*Tamias* sp.), leg. Babij and Allen, February 1925, at type locality in Ithaca, Tomkins County, New York; on loan from ZMB, ZMB catalog number 31988 (original verbatim label: "Ithaca, New-York aus Nest von Erdhörnchen (Tamias sp.) Frühjahr 1925, Babij u. Allen leg. 2020."). Specimen cleared in lactic acid, oriented ventrally, mounted in glycerol, and drawn from slide at 200x magnification.

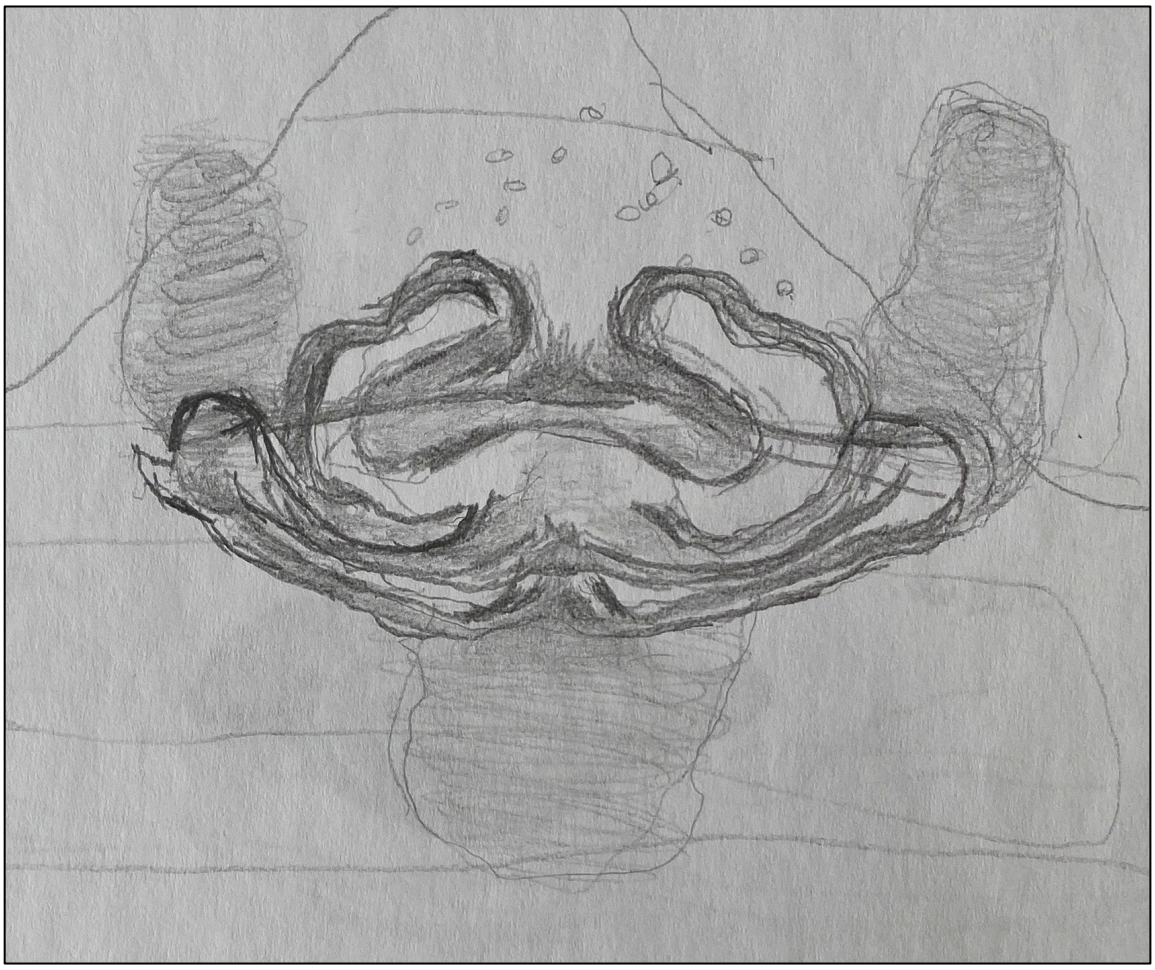

Fig. 3.14 Straight-line measurement analysis. PCA of five straight-line measurement characters from the four subterranean *Hesperochernes* species considered here (*H. holsingeri*, red circles; *H. mirabilis*, green triangles; and *H. occidentalis*, blue squares) and one epigean *Hesperochernes* species (*H. tamiae*, grey cross).

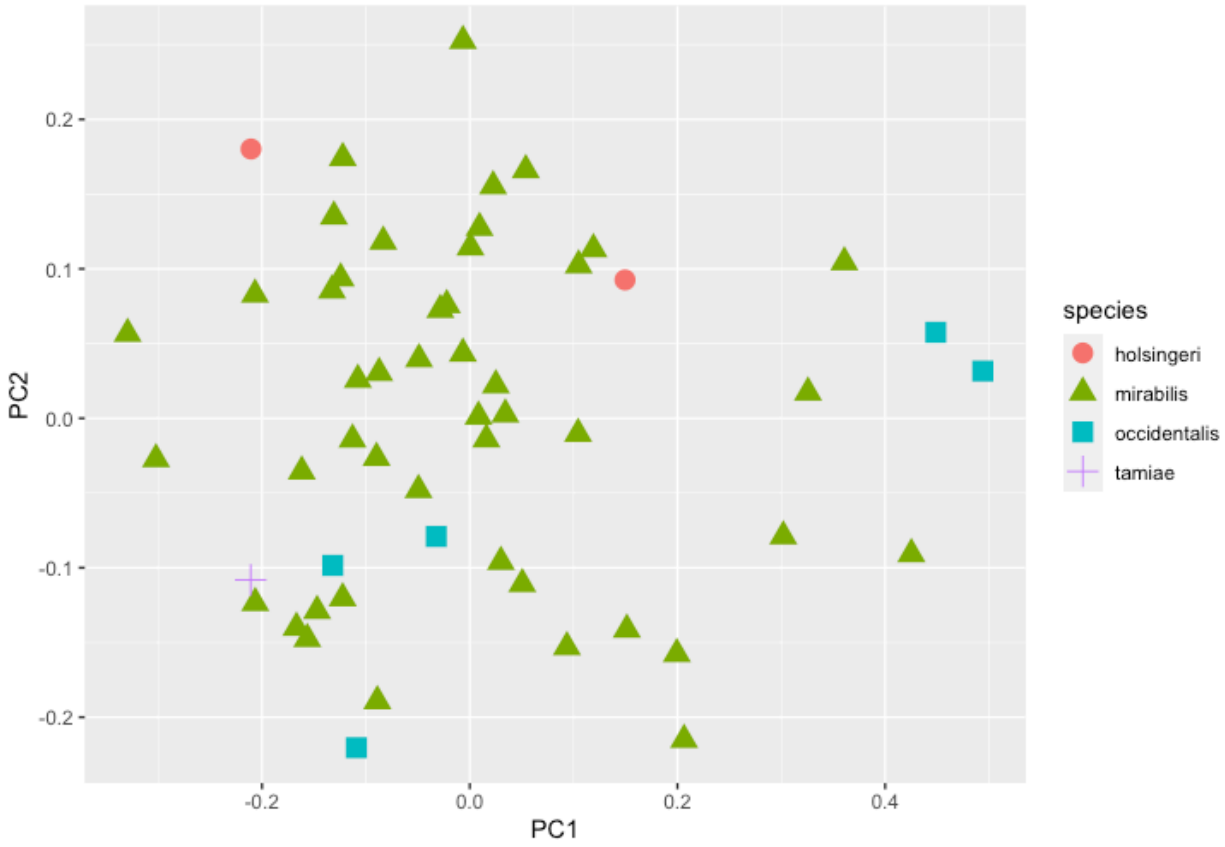

Fig. 3.15 PCAs from geometric morphometric analyses: (a) PCA of eastern vs. western cave localities; (b) PCA of northern vs. southern cave localities.

(a)

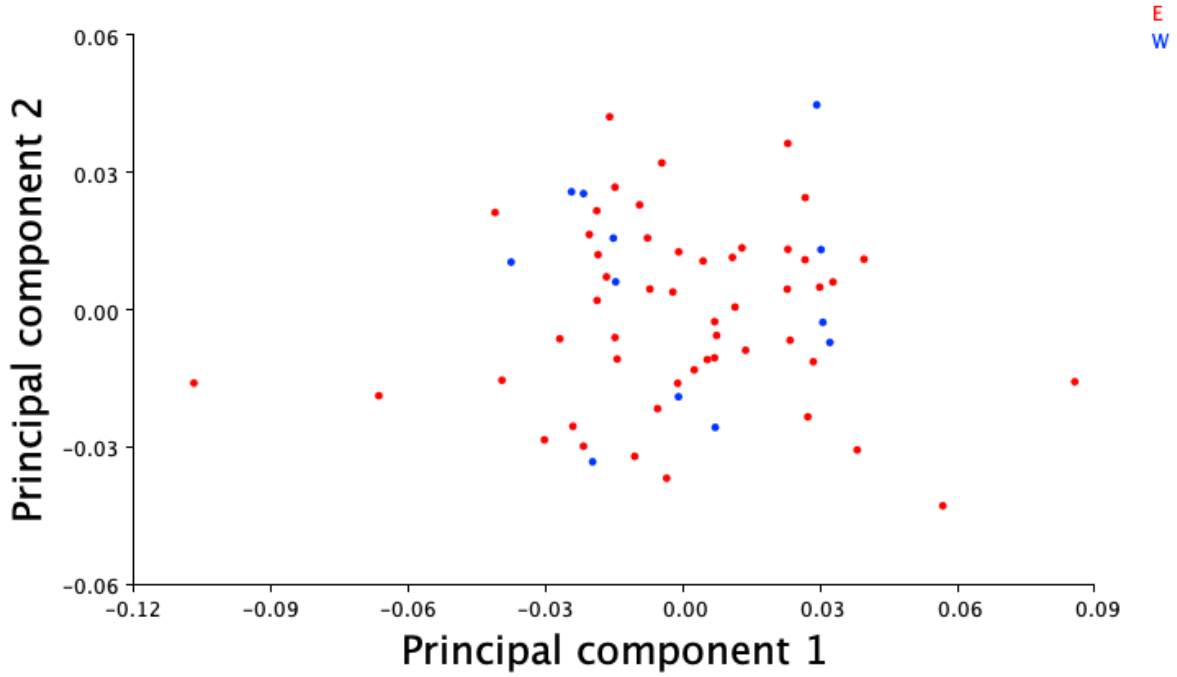

(b)

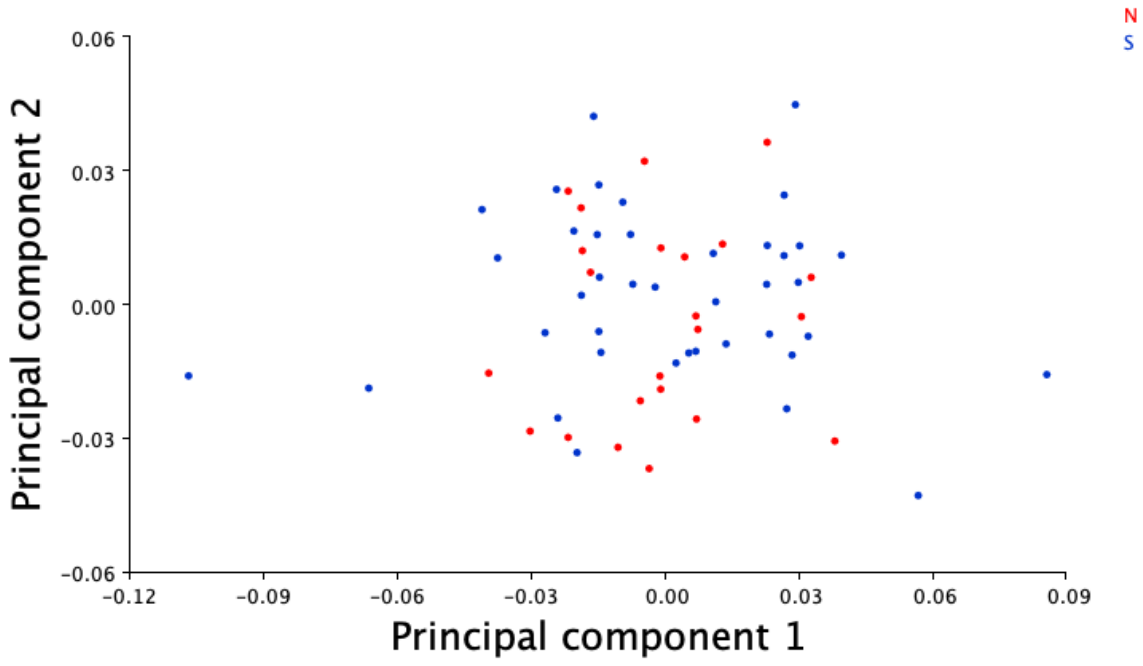

Fig. 3.16 CVAs from geometric morphometric analyses: (a) CVA of eastern vs. western cave localities; (b) CVA of northern vs. southern cave localities.

(a)

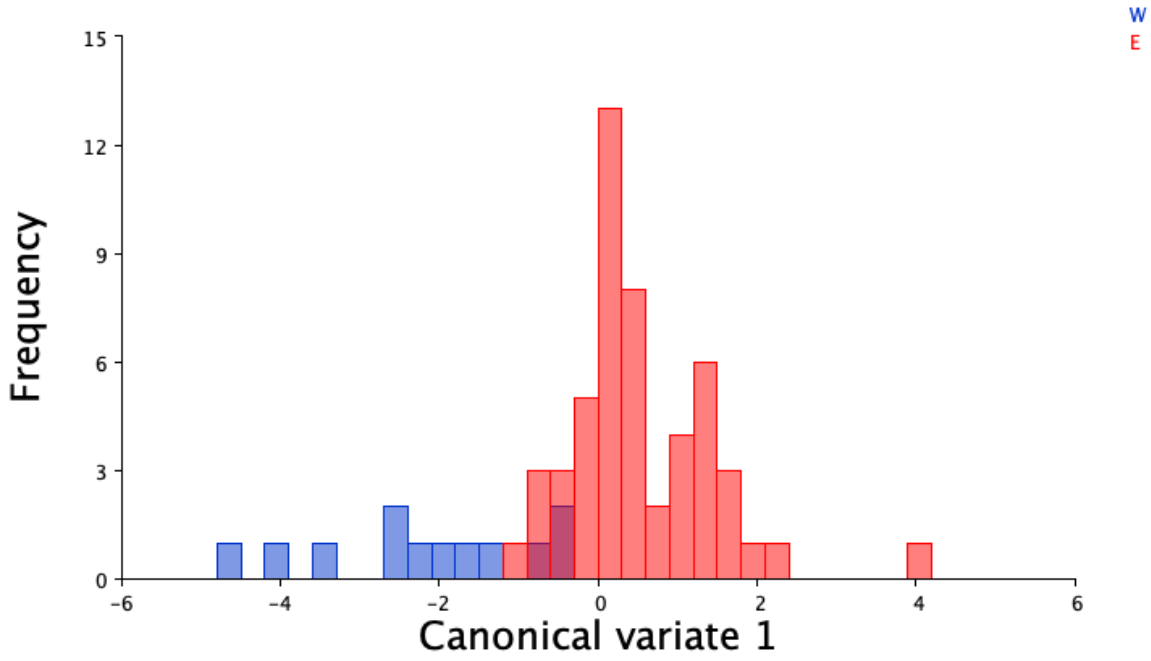

(b)

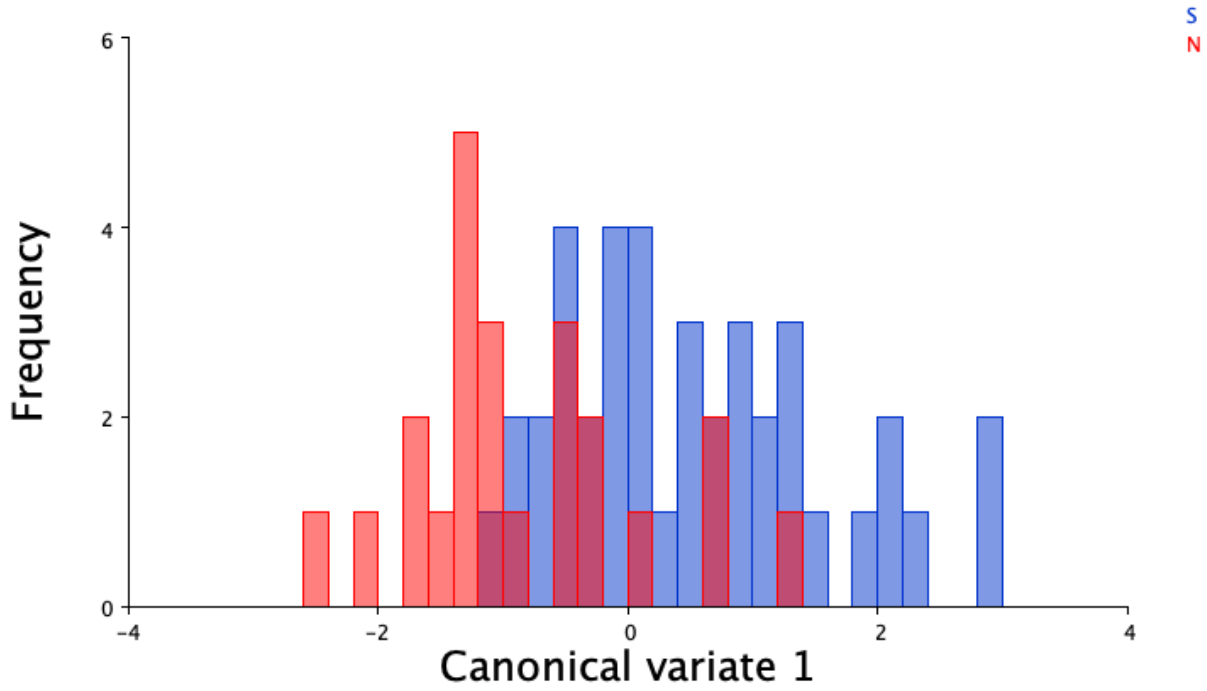

Fig. 3.17 Map of Nearctic and Neotropical *Hesperochernes* type localities east of the Great Plains: (a) blue circles, type localities of surface species; (b) black triangles, type localities of cave-adapted species. The alternate type locality for *Hesperochernes mirabilis* as conceived by Banks (1895) in western Virginia is also given.